Magnetoencephalography to characterize cortical effects of conditioned pain modulation in patients treated with spinal cord stimulation

MSc thesis Technical Medicine – Sensing and Stimulation
L.J. (Laurien) Reinders
December 2022

Universiteit Leiden
The Netherlands

TUDelft Delft University of Technology

Erasmus University Rotterdam
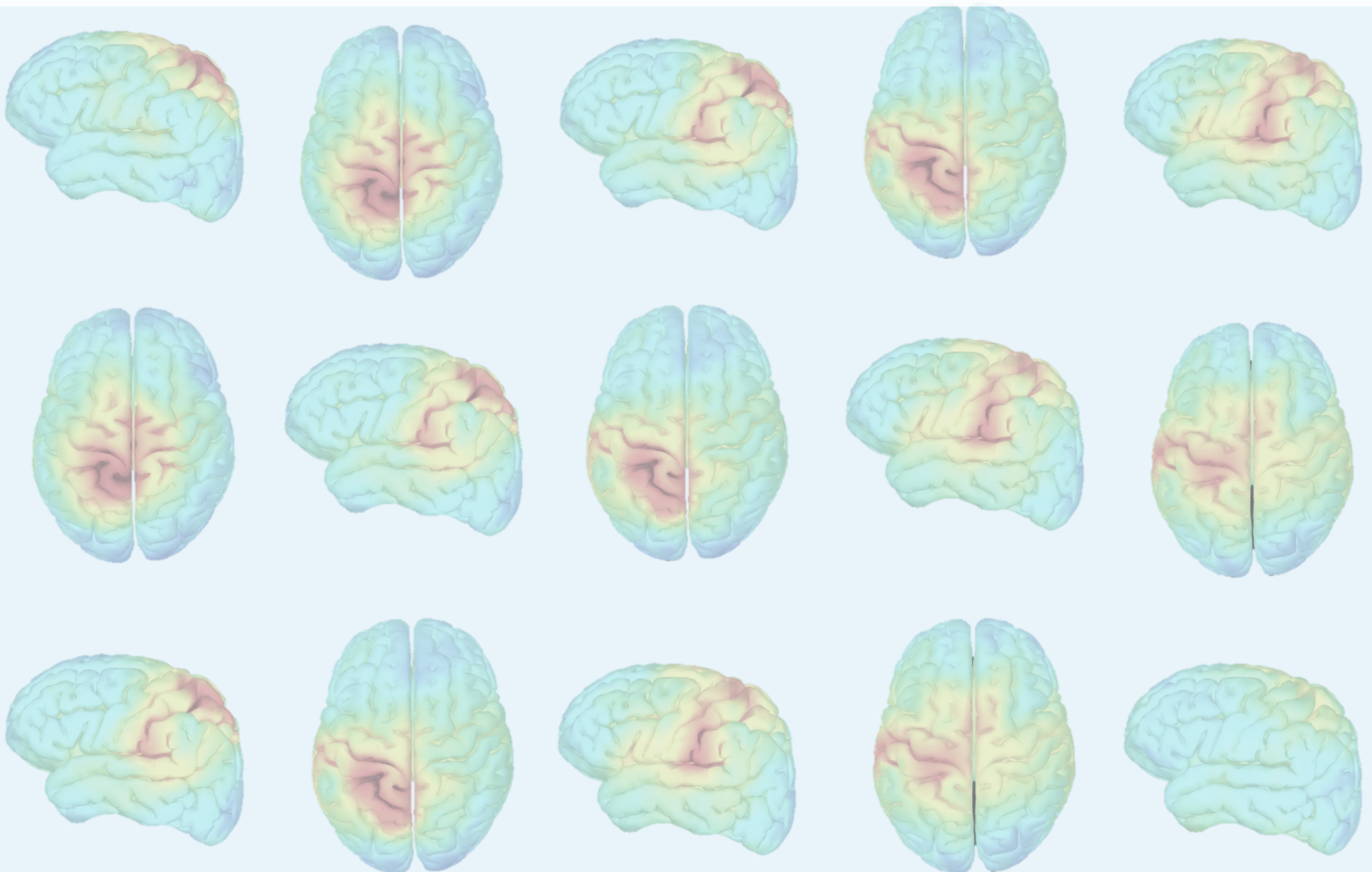
This page was intentionally left blank.

.

Magnetoencephalography to characterize cortical effects of conditioned pain modulation in patients treated with spinal cord stimulation

Laurien Reinders

Student number : 4472306

16 December 2022

Thesis in partial fulfilment of the requirements for the joint degree of Master of Science in

Technical Medicine

Leiden University ; Delft University of Technology ; Erasmus University Rotterdam

Master thesis project (TM30004 ; 35 ECTS)

Dept. of Biomechanical Engineering, TU Delft

March 2022 – December 2022

Supervisors:

Dr. ir. Cecile de Vos

Dr. Sander Frankema

Prof. dr. ir. Alfred Schouten

Thesis committee members:

Prof. dr. ir. Alfred Schouten, TU Delft (chair)

Dr. Sander Frankema, EMC

Dr. ir. Cecile de Vos, EMC

Dr. Monique van Velzen, LUMC

Dr. ir. Patrick Forbes, EMC

An electronic version of this thesis is available at http://repository.tudelft.nl/.

Universiteit Leiden
The Netherlands

TUDelft
Delft University of Technology

Erasmus University Rotterdam

This page was intentionally left blank.

Summary

Introduction: Spinal Cord Stimulation (SCS) is a successful last-resort treatment for chronic pain patients, although its exact mechanisms of action (MOAs) still need to be unraveled. The MOAs of SCS partly rely on spinal mechanisms (gate control theory) and supraspinal mechanisms likely play a role as well. Pain processing involves a complex network of cortical structures and can be modulated. Conditioned pain modulation (CPM) is a measure to describe the modulation of pain perception. CPM relies on the 'pain inhibits pain' theory, where a nociceptive test stimulus (TS) is modulated by applying a nociceptive conditioning stimulus (CS). CPM is often less efficient in chronic pain patients, but this might be improved by effective SCS.

Objective: The aim of this thesis is to assess how effective SCS affects the supraspinal mechanisms of pain modulation in chronic pain patients. The supraspinal mechanisms are evaluated using magnetoencephalography (MEG) to assess the cortical response to TS *before, during* and *after* CPM in chronic pain patients treated with SCS.

Methods: Chronic pain patients treated with SCS underwent MEG sessions after receiving tonic and burst SCS for one week. Each session consisted of three CPM blocks: *before, during* and *after* CPM. During each CPM block 22 TS were administered accompanied by CS *during* CPM, after each block the subject reported a subjective pain rating of TS (and CS). The cortical response to TS, measured using MEG, was analyzed in the time and time-frequency (TF) domain using *Brainstorm* and *Matlab* software. TF decomposition was computed in several pain related regions of interest using complex Morlet wavelets. We examined how CPM affected event related spectral perturbations, induced by TS, in the alpha (8-12 Hz) and beta (13-30 Hz) frequency ranges. The average cortical response during tonic and burst SCS was evaluated in all subjects, and separately in the five clearest SCS responders (effective) and the five clearest SCS non-responders (non-effective).

Results: 17 subjects were included. On average a decrease in subjective pain ratings of TS was observed *during* CPM. In the time domain, TS evoked activity in areas related to the sensory-discriminative aspect of pain. In the TF domain, TS induced event related desynchronization (ERD) followed by event related synchronization (ERS) in the alpha and beta frequency ranges in the bilateral sensorimotor cortices. *During* CPM the power of beta ERS was significantly decreased during burst SCS. A trend was observed towards a decrease in power of beta ERS for the effective burst SCS group, whereas no decrease was observed for the non-effective burst, effective tonic and non-effective tonic SCS groups.

Conclusion: The results suggest that on average, effective burst SCS decreases the power of beta ERS *during* CPM, this decrease indicates successful modulation of pain. Therefore, I suggest that effective burst SCS is capable of improving the supraspinal mechanisms of pain modulation, whereas effective tonic SCS is not capable of doing so. This suggestion indicates a partially different MOA for tonic and burst SCS. Future studies containing larger group sizes should validate these findings.

Preface

This master thesis concludes my six years of study at the Technical University Delft, Erasmus University Rotterdam and University Leiden. During the bachelor Clinical Technology and Technical Medicine I developed myself on both the clinical and technical aspects of medicine. The brain has always fascinated me: how we move, feel and act is all determined by neurons firing in the brain. Researching the brain is challenging yet this makes it an interesting topic. I found the perfect combination of a challenging, clinical-technical integrated and brain-related subject for my thesis at the department of pain medicine at the Erasmus MC. The last couple of months I learned a lot about the brain, pain and signal analysis. I enjoyed working on this thesis and I am looking forward to perform further research in the field of neuromodulation.

Many thanks to my main supervisor Cecile de Vos, who helped me a lot throughout the journey of my thesis project. We had many meetings to discuss the challenging analysis of the magnetoencephalography data and interpretation of the results. Your enthusiasm always kept me motivated. Next, I would like to thank Alfred Schouten for his critical thinking and feedback on the signal analysis, it prevented that Cecile and I got trapped in a tunnel vision regarding the signal analysis. Furthermore, I would like to thank Sander Frankema for his critical thinking and feedback on the clinical aspects of spinal cord stimulation and conditioned pain modulation, it kept me sharp on the clinical interpretation of the results. I would like to thank my friends for our fun times outside the hours I spent on my thesis. Finally, I would like to thank my family and Jhorie for always believing in me and your unconditional support.

Laurien Reinders
Rotterdam, December 2022

Contents

List of abbreviations

ACC   anterior cingulate cortex

BPI   brief pain inventory

CPM   conditioned pain modulation

CRPS   complex Regional Pain Syndrome

CS   conditioning stimulus

DLPFC   dorsolateral prefrontal cortex

DNIC   diffuse noxious inhibitory control

DNP   diabetic neuropathy

ECG   electrocardiogram

EEG   electroencephalography

ERD   event related desynchronization

ERS   event related synchronization

ERSP   event related spectral perturbation

FBSS   failed back surgery syndrome

HEOG   horizontal electro-oculogram

IPG   implantable pulse generator

M1   primary motor cortex

MCC   middle cingulate cortex

MEG   magnetoencehpalography

MN   minimum norm

MOA   mechanism of action

MRI   magnetic resonance imaging

NRS   numeric rating scale

OFC   orbito frontal cortex

PAG   periaqueductal gray

PCC   posterior cingulate cortex

PCS   pain catastrophizing score

PSD   power spectral density

PVAQ pain vigilance and awareness questionnaire

ROI   region of interest

S1   primary somatosensory cortex

S2   secondary somatosensory cortex

SCS   spinal cord stimulation

SMA   supplementary motor area

SSP   signal space projection

TF   time frequency

TS   test stimulus

VEOG vertical electro-oculogram

VPL   ventral posterolateral

1.   Introduction

1.1   Chronic pain

Pain is defined as 'an unpleasant sensory and emotional experience associated with, or resembling that associated with, actual or potential tissue damage' by the International Association for the Study of Pain (IASP) [1]. Pain often occurs as a symptom warning of a medical condition or injury. When the cause is treated pain usually resolves. However, in some cases the underlying cause of pain cannot be treated or pain persists despite successful treatment, leading to chronic pain. The IASP defines chronic pain as pain that recurs or lasts longer than three months [2]. Chronic pain has a high prevalence, affecting an estimated 20% of the people worldwide [3], and is associated with a high disease and disability burden [3,4]. Given the high global prevalence and burden of chronic pain, it is important to achieve an effective treatment for chronic pain patients.

Pain is a complex and limited understood concept, however some important structures in the processing of pain are identified. A nociceptive signal usually starts when a peripheral nerve is stimulated by a painful stimulus. From the peripheral nerve the nociceptive signal travels through the spinal cord towards the brainstem and brain. A complex network of multiple supraspinal structures is involved in the further processing of the nociceptive signal, such as the somatosensory cortices, the thalamus, insula, anterior cingulate cortex (ACC) and prefrontal cortex. Figure 1 displays an overview of involved structures and how they are connected [5].
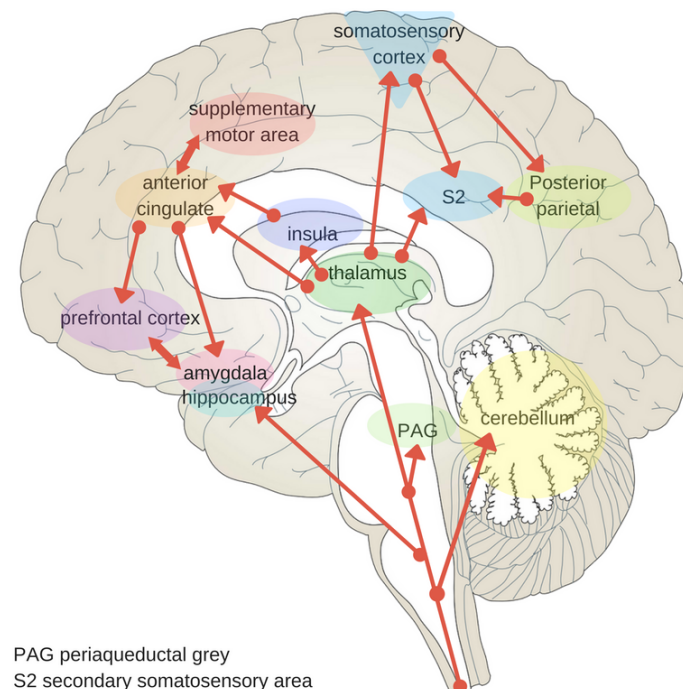
Figure 1: *A selection of involved supraspinal structures in the processing of pain. Figure from Bright Brain Centre [5].*

There are three important pathways involved in pain processing: the ascending lateral pathway, the ascending medial pathway and the descending pain inhibitory pathway [6–8]. The ascending lateral pathway is responsible for the sensory-discriminative component of pain and is activated by C-, Aδ- and Aβ-fibers. This pathway reaches the somatosensory and parietal cortex via the ventral posterolateral (VPL) nuclei of the thalamus [6]. The ascending medial pathway is responsible for the motivational-affective component of pain and is activated by C-fibers. This pathway reaches among other structures the anterior cingulate cortex (ACC) and insula via the mediodorsal and VPL nuclei of the thalamus [9]. The descending pathway suppresses ongoing pain and involves supraspinal structures such as the ACC and periaqueductal gray (PAG). The exact interactions in pain have to be unraveled, so far studies show connections between the somatosensory cortices, cingulate cortex, insula, amygdala, thalamus and frontal cortex [7, 8, 10].

The nociceptive signals can be modulated to either draw attention to the pain stimulus (intensified) or to allow for attention to other activities (inhibition). The endogenous pain modulation relies on bottom-up and top-down pain modulatory systems. The bottom-up pain modulatory system consists of the influences that are stimulus driven (e.g. stimulus intensity), whereas top-down modulation relies on the supraspinal mechanisms that are subject-driven (e.g. attention) [11]. The modulation of pain is possibly disturbed in chronic pain patients [12].

1.2   Spinal cord stimulation

Spinal Cord Stimulation (SCS), an implantable neurostimulation modality, is a successful last-resort treatment for chronic pain patients. A SCS system consists of an implantable pulse generator (IPG), placed in a subcutaneous pocket. The IPG is connected to one or two electrode leads and placed in the dorsal epidural space. The Aβ-fibers of the dorsal column are electrically stimulated by the leads [13]. SCS has shown to be effective for the majority of patients suffering from one of the following conditions: complex regional pain syndrome (CRPS), failed back surgery syndrome (FBSS), angina pectoris and peripheral ischemia [14]. SCS has a long-term success rate of $47 - 74\%$, where success is defined as pain relief of $>50\%$ [15–17]. Despite SCS being successful for many chronic pain patients, there remains a group, suffering from one of the indicated conditions, that does not benefit from SCS.

To understand why treatment is not successful for all chronic pain patients, it is crucial to further unravel the mechanisms of action (MOAs) of SCS. Traditionally the MOA of SCS relies on the gate control theory as proposed by Melzack and Wall in 1965 [18]. The gate control theory states that the nociceptive signals, carried by the nociceptive C- and Aδ-fibers, are inhibited by stimulating the non-nociceptive Aβ-fibers. The inhibition occurs at the common nerve synapse location in the substantia gelatinosa of the dorsal horn of the spinal cord [14]. However, more MOAs are thought to be involved in SCS with interactions at the spinal and supraspinal levels. These interactions include activation of the descending pain inhibitory pathways and activation of supraspinal structures [14, 19, 20]. Hence the MOAs of SCS partly rely on spinal mechanisms (gate control theory), but probably also supraspinal mechanisms play a role which are explored in this thesis.

Different SCS programming modes are available. The conventional SCS mode consists of a tonic waveform, which is associated with paresthesia (Figure 2a). The burst SCS is a novel paresthesia-free mode, which consists of trains of stimulation pulses mimicking physiological thalamo-cortical firing patterns [21–23] (Figure 2b). Some studies showed a larger pain inhibiting effect of burst SCS over tonic SCS and therefore it is suggested that the MOA of burst SCS might partly differ from the MOA of tonic SCS [24–28]. A small sample EEG study (5 subjects) by de Ridder et al. [24] suggested that tonic and burst SCS both affect the sensory-discriminative component of pain (ascending lateral pathway) and the descending pain pathway, and that burst SCS has additional effects by affecting the motivational-affective component of pain (ascending medial pathway). The study by Niso et al. [29] supported this hypothesis by reporting that burst SCS seems to reduce cortical attention to somatosensory stimuli.

(a) *Tonic SCS*
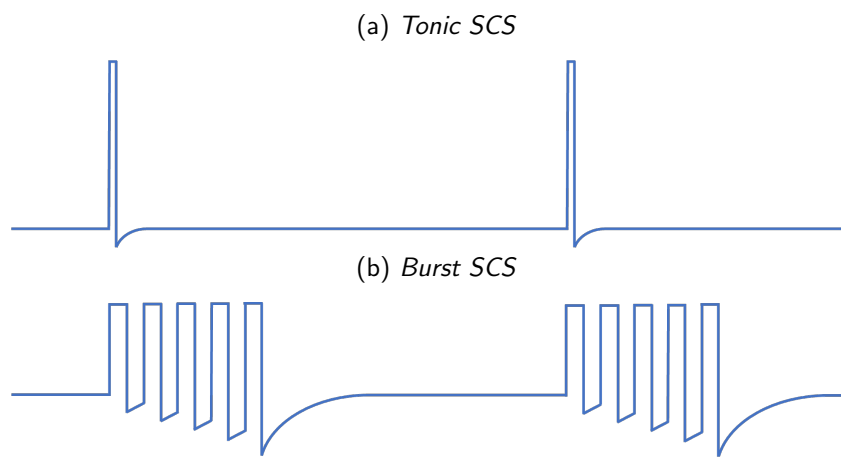
(b) *Burst SCS*

Figure 2: *Waveforms associated with tonic (conventional) and burst SCS mode.*

1.3 Conditioned pain modulation

Conditioned pain modulation (CPM) is a centrally processed measure of the net effect of the descending pain pathway [30]. CPM relies on the 'pain inhibits pain' theory, where a first painful stimulus (test stimulus, TS) is inhibited by applying a second painful stimulus (conditioning stimulus, CS) [31, 32]. There are two bottom-up inputs during CPM (TS and CS) and top-down modulation through supraspinal mechanisms plays a role.

CPM is based on mechanisms first described in 1979 in rats by Le Bars et al. [14]. They showed an inhibiting effect on the TS by applying a CS. The phenomenon was described as diffuse noxious inhibitory control (DNIC). The DNIC mechanisms rely on the spino-bulbo-spinal loop. The CS produces nociceptive ascending signals that project to the brainstem and the brainstem sends descending signals back to the spinal dorsal horn. In the spinal dorsal horn, the receptors of the wide dynamic range neurons are modulated, which has an inhibiting effect on the incoming ascending TS signals. To standardize the terminology, in 2010 it was recommended by a panel of experts [33] to use the term CPM to describe the observed pain inhibiting effect in humans by a CS on a TS. The MOAs of CPM are not fully understood yet: part of CPM relies on the spino-bulbo-spinal loop and supraspinal mechanisms also play a role [30, 34, 35].

In the clinic, CPM is used to evaluate the endogenous pain inhibitory capacity of patients. The endogenous pain modulation capacity is often disturbed in chronic pain patients, which is observed as a less efficient CPM (decreased pain inhibitory effect of CS on TS). It is important to note that also a healthy subject may express a less efficient CPM and that a chronic pain patient may express an efficient CPM. However, on a group-level, an efficient CPM is observed for healthy subjects and a less efficient CPM for chronic pain patients. There is an ongoing debate about whether the less efficient CPM in chronic pain patients is the cause or the effect of chronic pain. Further research is required to unravel this 'chicken and egg' problem [30, 31, 36, 37].

The effect of CPM is usually described as the difference in perceived pain intensity of the TS between before and during application of the CS. Another way to evaluate the effect of CPM is to measure the brain response to the TS before and during application of the CS. The direct brain responses to the TS can be measured using electroencephalography (EEG) or magnetoencephalography (MEG). In this study, we evaluated the direct brain response during CPM which can give insights into the supraspinal processing of a nociceptive signal and how the nociceptive signals are affected during CPM in chronic pain patients treated with SCS.

1.4 Magnetoencephalography

Magnetoencephalography (MEG) was used in this study to measure the direct brain response during CPM. MEG is a non-invasive brain imaging technique that detects changes in the magnetic fields associated with neuronal activity in the brain. The magnetic fields result from the intracellular ionic current produced by neurons, the magnetic field is perpendicular to the direction of the current (figure 3) [38]. The magnetic fields are measured by placing the subjects' head inside a MEG helmet. A state-of-the-art MEG helmet includes around 300 superconducting quantum interference device (SQUID) sensors to detect neuronal magnetic fields. The small neuronal magnetic fields are measured in a magnetically shielded room, to shield out the earth's relatively stronger magnetic fields [38, 39].

MEG has a very high temporal resolution (millisecond range) [38, 40, 41] and a relatively good spatial resolution (2-3 mm) at the cortical surface [38, 42]. The spatial resolution is better using MEG compared to the more well-known brain imaging technique electroencephalography (EEG) that measures the neuronal electrical fields. The magnetic fields are not distorted by the tissue conductivity of the skull and cerebrospinal fluid, whereas electrical fields are sensitive to this resulting in a better source localization for MEG [38, 41]. MEG has an advantage over EEG in pain research due to its better source localization, however it should be kept in mind that MEG is less affordable, accessible and mobile [40, 41].

1.5 Pain and neural oscillations

The brain response to a nociceptive stimulus can be studied in the time and time-frequency domain. In the time domain, the brain response is evaluated is by averaging the response to multiple nociceptive stimuli, resulting in an averaged evoked response. The evoked response is characterized by
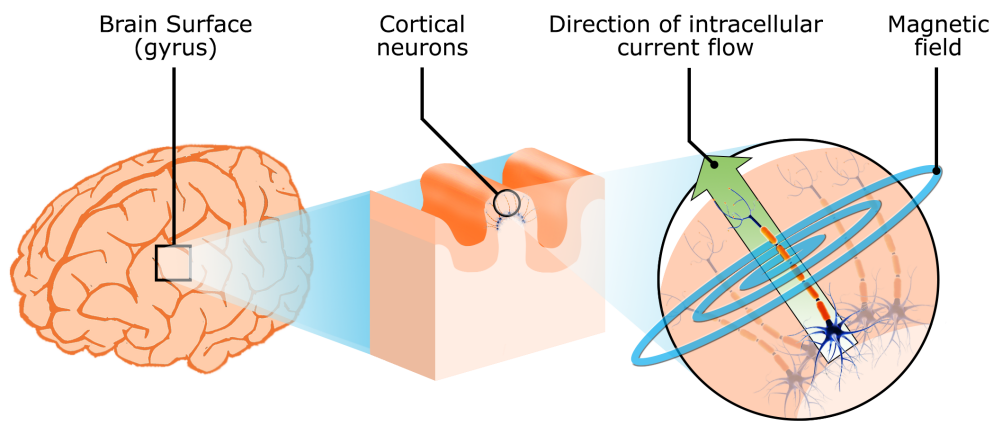
Figure 3: *Magnetic fields produced by the intracellular ionic currents of cortical neurons. The neuronal magnetic fields can be measured using magnetoencephalography (MEG). Figure from N. Vukovic [43].*

a waveform that is phase-locked to the stimulus. The response is generated by groups of neurons firing at the same time [44].

The brain response to a nociceptive stimulus can also be analyzed in the time-frequency (TF) domain to study the oscillatory activity that is not phase-locked to the stimulus [44]. The stimulus can lead to event related spectral perturbations (ERSPs), which are changes in the ongoing brain oscillations. The stimulus can either lead to desynchronization of the firing neurons, this is called event related desynchronization (ERD). On the other hand, it can lead to synchronization of the firing neurons, this is called event related synchronization (ERS). ERD and ERS are expressed by a respectively lower or higher power of the signal within a certain frequency range relative to the baseline before stimulation [45].

Oscillations display the dynamic behavior and show characteristic spatiotemporal patterns during sensory tasks [46]. ERS, observed as a higher power of the (synchronized) oscillatory activity, is thought to reflect an idling state. Whereas ERD, observed as a lower power of the oscillatory activity, is thought to reflect (non-synchronized) activation and an increased excitability level of cortical neurons [45, 47]. Resulting in a counterintuitive concept that ERD, represented by a lower power of the signal, is associated with increased activity of neurons. Whereas ERS, represented by a higher power of the signal, is associated with decreased activity of neurons.

After a nociceptive stimulus, ERD can be observed in the alpha (8-12 Hz) and beta (13-30 Hz) frequency bands in the sensorimotor cortices, which is associated with an increased excitability level of cortical neurons. The ERD often is followed by ERS in the same frequency bands, which is associated with deactivation of the sensorimotor cortices and may represent inhibition of a cortical network [46]. Diers et al. [48] observed increased beta-ERS in the contralateral S1 when the attention of a subject was attended to the nociceptive stimulus, therefore they propose that beta-ERS might reflect top-down modulation of painful stimuli.

1.6   Cortical response during CPM in chronic pain patients

Jin [49] examined in her thesis project how event related spectral perturbations (ERSPs) induced by a nociceptive stimulus were altered during CPM in healthy controls and chronic pain patients. She observed a lower power of beta ERS after a nociceptive stimulus in chronic pain patients in comparison to healthy controls. She suggests that lower beta-ERS in chronic pain patients might be caused by a chronic CPM state due to the chronic pain functioning as an ongoing CS. She also suggests that due to the chronic CPM state these patients may experience a flooring effect on the experimental CPM. This was in line with the fact that she did not find a decrease in power of beta ERS during CPM, whereas she did find a significant decrease in power of beta ERS during CPM for the healthy controls. Another cause of not finding a significant decrease of beta ERS in chronic pain patients might be that chronic pain patients have a distributed top-down modulation of pain, resulting in a weaker inhibitory effect of CPM on the cortical response to a nociceptive stimulus. Possibly, effective SCS improves the chronic pain state and the supraspinal mechanisms of modulation of pain of chronic pain patients and thereby also the inhibitory effect of CPM on the cortical response to a nociceptive stimulus.

1.7   Thesis objective

The main objective of this thesis is to assess how effective spinal cord stimulation (SCS) affects the supraspinal mechanisms of pain modulation in chronic pain patients. The supraspinal mechanisms are evaluated using magnetoencephalography (MEG) to assess the cortical response to a nociceptive test stimulus *before*, *during* and *after* conditioned pain modulation in chronic pain patients receiving spinal cord stimulation. The cortical responses are compared between 1) effective and non-effective spinal cord stimulation, 2) tonic and burst spinal cord stimulation, 3) effective tonic and effective burst spinal cord stimulation and 4) non-effective tonic and non-effective burst spinal cord stimulation.

1.8   Hypotheses

For all groups, I expect that after a nociceptive stimulus alpha and beta ERD is induced in the sensorimotor cortices, which represents activation of these cortical areas. I expect that the ERD is followed by alpha and beta ERS, which represents the deactivation of the same cortical areas. I hypothesize that *during* CPM, on a group-level, modulation takes place by the CS on the TS. Which is seen as a decreased power of alpha- and beta-ERD and alpha- and beta-ERS.

1.8.1   Effective and non-effective SCS

I expect that when a chronic patient receives effective SCS treatment that their chronic pain state shifts towards a state where they experience less pain. Resulting in a reduced ongoing CPM state. Therefore, I expect that the flooring effect on CPM as described by Jin [49] is not or is less applicable. In other words, I hypothesize that CPM in the effective SCS group, on a group-level, resembles the CPM response in healthy individuals observed as an efficient inhibitory effect of CPM on the cortical response.

The group that experiences no effect of SCS treatment still has an ongoing chronic pain state. Therefore, I hypothesize that the group with non-effective SCS, on a group-level, shows a CPM response that is comparable to the CPM response in chronic pain patients observed as an inefficient inhibitory effect of CPM on the cortical response.

1.8.2   Tonic and burst SCS

During tonic SCS subjects experience paresthesias, meaning that they have a continuous stimulation of the somatosensory system. Therefore, I expect that during tonic SCS the subjects have a higher baseline of cortical activity in the sensorimotor cortices. Since ERSPs are expressed as the relative difference in power with regard to the baseline, the power of the ERSP depends on the cortical activity on the baseline. If the baseline of cortical activity is higher and the amount of desynchronization and synchronization does not change, the relative difference of the ERSP is lower. I hypothesize that during tonic SCS subjects have a higher baseline of cortical activity in the sensorimotor cortices and that therefore the power of the ERSPs is lower.

1.8.3   Effective and non-effective SCS per stimulation mode

Some studies showed a greater pain inhibiting effect by burst SCS in comparison to tonic SCS [24–28] and therefore I hypothesize that burst SCS has a partly different MOA than tonic SCS. Possibly the MOA of burst SCS includes improvement of the top-down modulation of pain, whereas tonic SCS does not improve the top-down modulation. Therefore, I expect that when burst SCS is effective a greater inhibitory effect by CPM on the cortical response is observed in comparison with effective tonic SCS.

When tonic and burst SCS are not effective I expect that only a limited inhibitory effect by CPM on the cortical response is observed.

2. Methods

2.1 Data acquisition

Measurements were performed at two institutions: the Montreal Neurological Institute (MNI) in Canada and the Donders Institute Nijmegen in The Netherlands. In both institutes data was acquired with a 275-channel whole-head CTF MEG scanner in a magnetically shielded room with a sampling rate of 2400 Hz. The study was approved by the Institutional Review Board of the Montreal Neurological Institute and the CMO region Arnhem-Nijmegen. All subjects provided informed written consent.

2.2 Study design

Each subject came to the clinic four times on four separate days with a one-week interval between the visits. During the first visit, the subjects had their default SCS setting, this visit was used to let the subjects get used to the MEG measurements and perform baseline measurements. At the end of the first visit, the SCS setting was changed to tonic SCS, burst SCS or sham SCS and this new stimulation mode was applied for a one-week period. After one week the subjects returned for the first MEG session. After the session, the stimulation mode was changed to another mode (burst, tonic or sham) and this mode was again applied for one week followed by a MEG session. This process was repeated for the last stimulation mode (Figure 4). Before each session (same day or one day before the session) patients were asked to fill out three questionnaires: the Brief Pain Inventory (BPI), the Hospital Anxiety and Depression Scale (HADS) and the Pain Catastrophizing Scale (PCS). Besides, at the start of each session we asked the current pain (NRS 0-10) they experience due to their chronic pain condition. The order in which the different stimulation modes were applied was counterbalanced among the subjects. Furthermore, the subjects were blinded to the applied SCS programming mode, although they could sense the difference between tonic (paresthesias) and burst/sham (paresthesia-free) SCS. Sham SCS consisted of low-intensity burst SCS, it is unclear to what extent low-intensity burst SCS has a therapeutic effect, therefore this thesis focuses on the tonic and burst SCS stimulation modes.

During each session the subjects underwent MEG recordings with a total duration of approximately 40 minutes. The MEG recordings were performed under the following conditions: resting state measurements (2x 5 min), median nerve stimulation (2x 4 min), tibial nerve stimulation (2x 4 min) and the CPM test (1x 9 min). The CPM test consisted of three blocks: *before*, *during* and *after* application of CS (3x 3 min). In this thesis the three CPM blocks are analyzed. Next to the subjects' MEG recordings, on each day of a session a two-minute empty room MEG recording was collected to capture the noise of the empty room which was used later in the processing of the MEG recordings.

Alongside the MEG recordings, other parameters were also collected during each session. We collected the subjects' digitized head points to represent the individual head shape using a Polhemus tracking device. For registration of the head inside the MEG helmet, fiducial reference points were

taken at the nasion and left and right pre-auricular points. Furthermore, we collected cardiac activity using electrodes that measured the electrocardiogram (ECG) and we collected ocular movement using electrodes that measured the vertical electro-oculogram (VEOG) and the horizontal electro-oculogram (HEOG).
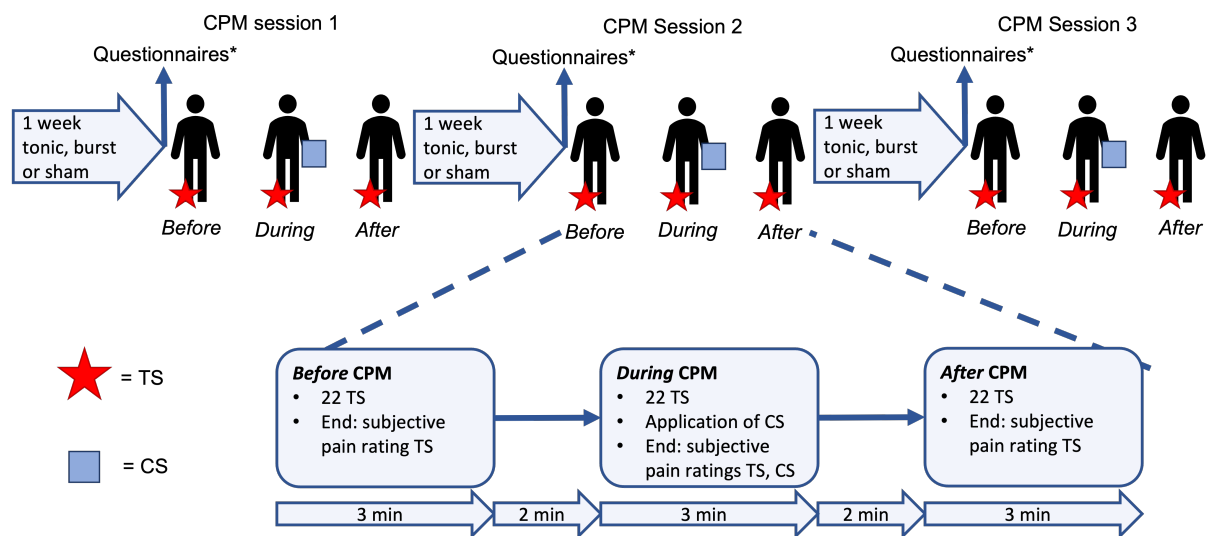
Figure 4: *Study design consisting of three CPM sessions after a one-week period of a stimulation mode (tonic, burst, sham). Each session consisted of three CPM blocks: before, during and after CPM. It is unclear to what extent sham (low-intensity burst) SCS has a therapeutic effect, therefore this thesis focuses on tonic and burst SCS. TS = test stimuli, CS = conditioning stimulus, NRS = numeric ratings scale [0-10]. *Questionnaires consisted of the brief pain inventory (BPI), the hospital anxiety and depression scale (HADS), the pain catastrophizing scale (PCS) and the current pain (NRS 0-10) due to their chronic pain condition.*

2.3 Conditioned pain modulation protocol

Each CPM block (*before, during, after*) consisted of the application of 22 TS, accompanied by a CS in the *during* CPM block (Figure 4). Each block lasted approximately three minutes and the between-block interval was approximately two minutes. Directly after each block, the subjects were asked to rate the pain intensity of TS on a 0 to 10 numeric rating scale (NRS) with 0 representing no pain and 10 the worst pain imaginable. After the *during* CPM block the subjects were also asked to rate the pain intensity of CS on the NRS.

A constant current stimulator (DS7A, Digitimer Ltd) produced brief transcutaneous electrical stimuli that were used as TS. The TS was applied at the right sural nerve. To obtain a low contact source impedance at the site of the TS application, the subject's skin was prepared by applying a skin prep gel and wiping the excess gel with alcohol swabs. Two silver/silver-chloride electrodes were placed at a distance of 2.5 cm on the right ankle using a conductive paste. One TS had a duration of 21 ms and consisted of five 1-ms electrical pulses with a 4 ms inter-pulse interval. The inter-TS interval was randomized between 6 and 10 seconds to minimize stimulus predictability and adaptation. The amplitude of the TS was adjusted for each subject during each session prior to the recordings. The average stimulation intensity was 16 mA for the FBSS patients, 35 mA for the CRPS patient and

38 mA for the DNP patient. Between sessions the stimulation intensity applied within a subject minimally differed (0-3 mA). We aimed for a stimulus amplitude that caused a pain intensity score of 5 on a 0 to 10 pain intensity scale.

The CS consisted of placing a commercial ice pack on the left forearm. The ice pack had a dimension of 9.5 x 28 cm containing 0.5 L gel and was stored in a freezer at a temperature of -18 °C. Approximately five minutes before applying the CS the ice pack was taken out of the freezer. The ice pack was wrapped in thin fabric to prevent skin damage on the forearm, leading to an approximate temperature of -10 °C.

2.4 Data analysis

Data analysis was performed with *Brainstorm* (version 3 2022) [50], which is documented and freely available for download online under the GNU general public license (http://neuroimage.usc.edu/brainstorm). *Matlab* (version R2022a) was used to perform additional analysis steps that could not be performed in *Brainstorm*.

2.4.1 Data pre-processing

The raw MEG data was pre-processed by one person, see Appendix A for a flow diagram containing all pre-processing steps. First, the recordings were manually inspected to identify bad segments which were excluded. After that, it was detected whether a stimulus artifact was present in the recordings and, if present, the duration of the artifact was measured. The stimulus artifact was present in 15 of the 17 subjects and the duration varied between the subjects and sessions (mean 33 ms, range 25-70 ms post stimulus). The stimulus artifact was removed using linear interpolation between 5 ms before stimulus and the duration of the stimulus artifact. A bandpass filter (1-200 Hz) was applied and notch filters were used to remove the contamination from the power line and the harmonics of the power line (50, 100, 150, 200 Hz for the recordings collected at the Donders Institute; 60, 120, 180 Hz for the recordings at the MNI). Power spectral densities (PSDs) using Welch's method were computed for each recording, including the noise recording. The PSDs, signal traces and 2D sensor topographies were evaluated to identify and exclude bad channels. The HEOG and VEOG channels were used to detect eye blinks, upon which signal space projections (SSPs) were used to remove the artifacts caused by eye blinks. The PSDs and signal traces were evaluated to detect whether cardiac activity caused artifacts in the recordings. If so, the ECG channels were used to detect the cardiac activity, upon which SSPs were used to remove the artifacts caused by cardiac activity. Next, the PSDs were evaluated to detect whether the stimulation frequency of the active SCS device caused artifacts in the MEG measurements. If so, notch filters were applied to remove the (harmonics of the) stimulation frequency from the signal. Lastly, PSDs were created of the pre-processed data and one final manual inspection was performed of the PSDs and signal traces. If a part of the recording still contained too much noise, this part was marked as a bad segment leading to the final pre-processed data files.

The pre-processed continuous data files were split up in epochs per TS trial, with 3 seconds pre-stimulus baseline till 6 seconds post-stimulus ([-3, 6]). A trial was rejected when it contained a

bad segment despite the pre-processing, e.g. when the trial contained a lot of muscle activity. The pre-processed accepted trials were used for further analysis.

2.4.2 Head model and source estimation

A head model is required to estimate the brain sources of the signals recorded by the MEG sensors. A head model explains how the neural electric currents (source space) produce magnetic fields at the sensors (sensor space) taking into account the different head tissues the magnetic fields pass [51]. As no individual MRIs were available, we used the default MRI *ICBM125* and warped the MRI using the digitized head points. To generate the head model an overlapping spheres approach was used. The head model consisted of the cortex surface of 15.000 vertices and was used to assess the activity of the cortical sources.

The brain activity at a lot of brain locations (i.e. 15.000 vertices), determined by the head model, is estimated from much fewer sensor locations: an ill-posed inverse problem. The problem is overcome by using a minimum norm (MN) imaging approach with unconstrained sources (three dipole orientations). This approach results in three time series, displaying the activity for each vertex in three orientations.

2.5 Regions of interest

Several regions of interest (ROIs) were selected to evaluate the cortical response to the TS in the time and time-frequency (TF) domain during the three conditions: *before*, *during* and *after* CPM. The ROIs were defined based on the lateral ascending pathway (sensory-discriminative component) and the medial ascending pathway (affective-motivational component) of pain. The ROIs associated with the sensory-discriminative aspect of pain were: the primary somatosensory cortex (S1) area related to the foot (TS given at ankle), the primary motor cortex (M1), the secondary somatosensory cortex (S2), the supplementary motor area (SMA) and the superior parietal lobule. All ROIs were created for the left and right hemispheres.

The ROIs associated with the affective-motivational component of pain were: the insula, anterior cingulate cortex (ACC), middle cingulate cortex (MCC), posterior cingulate cortex (PCC), dorsolateral prefrontal cortex (DLPFC) and the orbitofrontal cortex (OFC). Again, all scouts were created for both hemispheres. The left and right ROIs were combined for the cingulate cortices since the left and right cingulate cortices are anatomically very close to each other.

Jin [49] evaluated the spatial pattern of beta ERS by computing the magnitude at every vertex in the beta frequency range between 610 and 3680 ms post stimulus. She observed that the beta-ERS was mainly expressed in the bilateral sensorimotor cortices (S1, M1, SMA) (Figure 5). Due to computational limitations, it was not possible to reproduce the spatial pattern of beta ERS for this data, however I expect that also for the chronic pain patients treated with a SCS the response of beta ERS is most expressed in the bilateral sensorimotor cortices. Due to this reason and to make the results of this study comparable to the study of Jin [49], I created a ROI representing the bilateral sensorimotor cortices (consisting of the S1 area related to the foot, M1 and SMA), see Figure 6. See Appendix B for an overview of all other ROIs projected on the source map.

The ROIs of S1, M1, SMA, superior parietal lobule and S2 were created based on the observed averaged response in the time domain, displayed on a source map, after a nociceptive stimulus. All other ROIs were defined using the predefined ROIs of the Destrieux atlas [52].
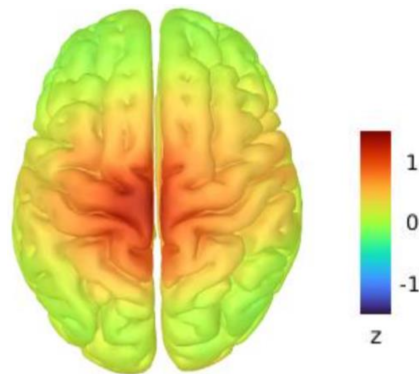
Figure 5: *Source map showing the average magnitude of beta ERS between 610-3680 ms post stimulus. Averaged over healthy controls and chronic pain subjects. Beta ERS was localized mainly in the bilateral sensorimotor cortices. Figure from Jin [49].*
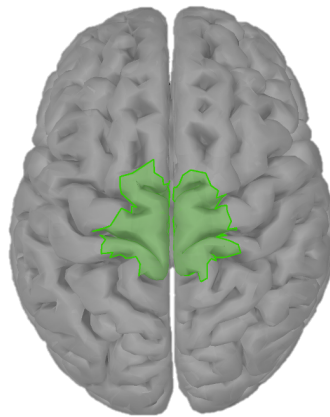
Figure 6: *The ROI of the bilateral sensorimotor cortices projected on the source map, consisting of the S1 area related to the foot, M1 and SMA of both hemispheres.*

2.6 Cortical response in the time domain

The norm of the three time series (three orientations) is projected on the brain resulting in source maps using current density as outcome measure. The source maps were created for all CPM conditions and stimulation modes per subject. The source maps were averaged over all subjects and stimulation modes for each condition, which resulted in source maps displaying the cortical activation pattern evoked by TS in the time domain *before, during* and *after* CPM. Subsequently, the source maps of the three CPM conditions were averaged, which resulted in an average cortical activation pattern evoked by a nociceptive stimulus in the time domain. The time series (norm of the three orientations) is extracted for each ROI, resulting in an averaged (all subjects, all stimulation modes) time series for each CPM condition per ROI.

2.7 Cortical response in the time-frequency domain

To evaluate the response in each ROI in the time-frequency domain to TS a time-frequency decomposition was computed using complex Morlet wavelets resulting in TF maps with as measure the power (square of the magnitude of the coefficients). The Morlet wavelets are scaled and shifted versions of the mother wavelet, which had a central frequency of 1 Hz and a full width half maximum value of 3 seconds (number of cycles: 6). The TF maps were created from 1 till 60 Hz, with linear steps of 1 Hz. To prevent the signals that are not phase-locked to TS from canceling out, I computed the TF maps for each trial separately. Subsequently, I computed the average TF map of all trials, resulting in a trial-averaged TF map per subject per condition. The trial-averaged TF maps were then z-scored with respect to baseline [-2, -0.5 s] to make them comparable between subjects. The z-scored trial-averaged TF maps were then averaged between subjects, resulting in an averaged TF map per ROI per condition.

The TF maps were further analyzed by evaluating the power of the ERSPs (ERD and ERS) in the alpha (8 - 12 Hz) and beta (13 - 30 Hz) frequency bands. The power of each ERSP was calculated by extracting the average power in the defined frequency range and in a defined time range. The time range of the ERSPs was defined for each ROI separately. First, the time series for both frequency bands were computed for the averaged TF maps per ROI per condition. Secondly, the time series were averaged for both frequency bands over all conditions, leading to an average time series of each ROI for both frequency bands. The averaged time series were then used to determine the time range of each ERSP: the time range of the ERD was marked when the z-score was smaller than 0.4; the time range of the ERS was marked when the z-score was larger than 0.4 (Appendix D). Finally, the power of each ERSP was calculated in the defined frequency range and time range.

2.8 Comparisons

2.8.1 Effective and non-effective SCS

First, the cortical responses in the TF domain are compared between subjects experiencing effective SCS and non-effective SCS. The effective SCS group was defined as the five subjects that were the clearest responders to SCS. All subjects had to rate the pain (NRS 0-10) they experience due to their chronic pain condition several times. They rated the average pain during the week with the SCS mode (BPI), current pain during filling out the BPI (BPI) and current pain at the start of each session. Whether a subject was a responder was based on 3 measures: 1) the mean of the given pain scores, 2) the consistency (standard deviation) of the given pain scores and 3) how well they were capable of rating their pain based on an expert opinion. The mean pain score had to be ≤ 4 for responders and ≥ 5 for non-responders. All responders and non-responders needed to have a standard deviation of the given pain scores ≤ 1.5 and they had to be capable of rating their pain.

The effective and non-effective groups consisted of subjects that were respectively the five clearest responders and five clearest non-responders to both tonic and burst SCS, so a responder was part of the effective SCS group with two MEG sessions (tonic, burst) and a non-responder was part of the non-effective SCS group with two MEG sessions (tonic, burst). Resulting in group sizes of 10

for both groups.

2.8.2 Tonic and burst SCS

The second comparison is between tonic and burst stimulation. Each subject received tonic and burst stimulation, so each subject belonged to both groups.

2.8.3 Effective and non-effective SCS per stimulation mode

The third comparison is between effective tonic and effective burst SCS. The five subjects that belonged to the effective SCS group received both tonic and burst SCS. For the third comparison the effective SCS group was split into: 1) effective tonic SCS (n=5) and 2) effective burst SCS (n=5). Both groups consisted of the same five subjects.

Lastly, the fourth comparison is between non-effective tonic and non-effective burst SCS. The five subjects that belonged to the non-effective SCS group received both tonic and burst SCS. For the fourth comparison the non-effective SCS group was split into two groups: 1) non-effective tonic SCS (n=5) and 2) non-effective burst SCS (n=5). Both groups consisted of the same five subjects.

2.9 Statistical analysis

Statistical analysis was performed using *SPSS* (version 28) software. To compare the subjective pain ratings and the power of the ERSPs across the three CPM conditions (*before*, *during* and *after* CPM) I used a repeated measures ANOVA. Mauchly's test of sphericity was used to test whether the assumption of sphericity of the data was met for the repeated measures ANOVA. When the repeated measures ANOVA revealed statically significant differences, a post-hoc analysis was performed.

The subjective pain ratings and power of ERSPs were compared between groups between the same CPM condition (e.g. pain rating *before* CPM of the effective SCS group vs. pain rating *before* CPM of the non-effective SCS group). I used a paired samples two-sided t-test for the comparisons where each subject was in both groups (tonic and burst SCS, effective tonic and effective burst SCS, non-effective tonic and non-effective burst SCS). I used an independent samples two-sided t-test for the comparison where the groups consisted of different subjects (effective and non-effective SCS). Levene's test was used to test whether the assumption of equal variances was met for the independent samples t-test.

A difference in pain rating or power of ERSP was regarded statistically significant when the p-value was below 0.05. No correction was performed for the multiple comparisons made (section 4.5.4).

3. Results

3.1 Subject characteristics

26 subjects were enrolled in this study and underwent MEG sessions. 9 subjects were excluded for further analysis due to various reasons: completed only the first MEG session (1); data contamination caused by dental implants (4); data contamination caused by an insulin pump (1); missing burst session (1) and data contamination during burst session by an unknown cause (2). This resulted in 17 included subjects for the tonic and burst SCS groups. Figure 7 displays an overview of all groups.

The general subject characteristics are summarized in Table 1 and the session specific characteristics are summarized in Table 2.
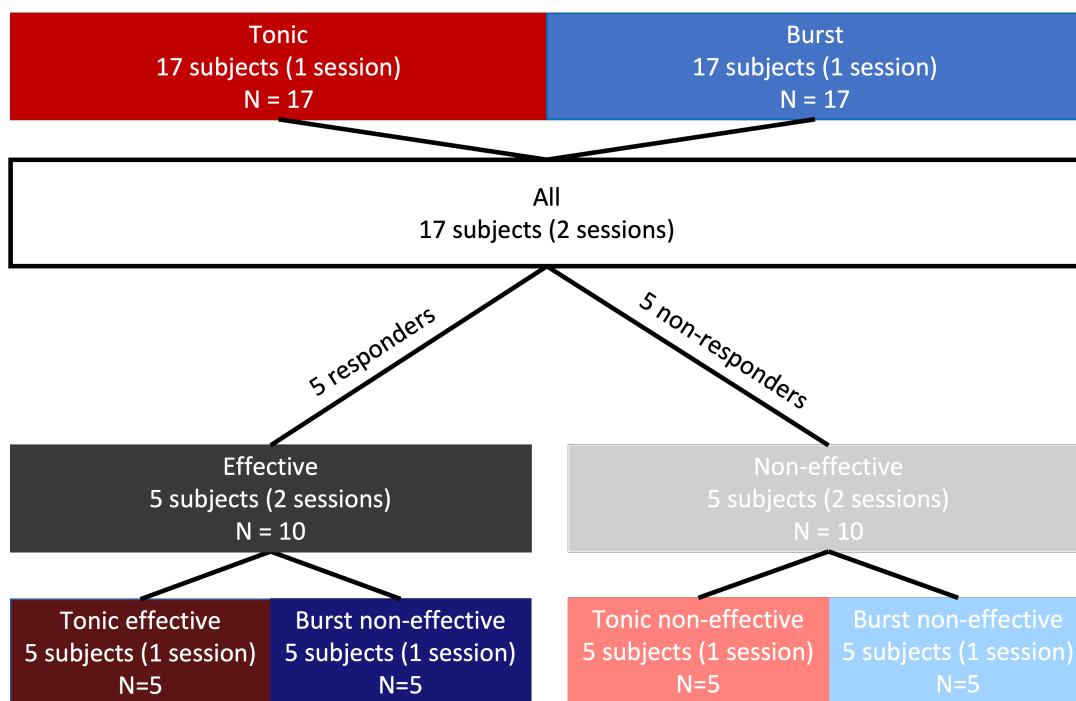
Figure 7: *Overview of all evaluated groups. Each subject underwent tonic and burst SCS. Only the five clearest responders and five clearest non-responders were included in the effective and non-effective SCS groups, resulting in smaller group sizes for these groups. The N in 'N =' represents the number of MEG sessions.*

3.2 Effect of CPM on pain ratings

The subjective pain ratings to TS on a NRS scale (0-10) *before*, *during* and *after* CPM are summarized in Table 3. The pain ratings to TS significantly decreased *during* CPM (Figure 8), except for the group subjects with non-effective burst SCS. The pain ratings remained significantly decreased *after* CPM for subjects with non-effective SCS, where the pain ratings significantly increased again *after* removing the CS for subjects with effective SCS (Figure 8a). The pain ratings remained significantly decreased *after* CPM for subjects receiving tonic stimulation (Figure 8b).

Characteristic	All subjects	Effective SCS	Non-effective SCS
Number of subjects	17	5	5
Age [yrs ± std]	53 ± 9	48 ± 7	58 ± 10
Sex [M/F]	8 / 9	1 / 4	2 / 3
Years lived with chronic pain [yrs ± std]	19 ± 13	22 ± 8	18 ± 22
Pain location			
Back	10/17	3/5	2/5
Right hip/leg/foot	7/17	3/5	2/5
Left hip/leg/foot	7/17	1/5	2/5
Pain condition			
FBSS	15/17	5/5	4/5
CRPS	1/17	0/5	1/5
DNP	1/17	0/5	0/5

Table 1: *General subject characteristics. FBSS = failed back surgery syndrome, CPRS = complex regional pain syndrome, DNP = diabetic neuropatic pain*

Characteristic	Tonic	Burst	Effective	Non-effective	Tonic effective	Burst effective	Non-effective tonic	Non-effective burst
Number of sessions	17	17	10*	10*	5	5	5	5
BPI average pain [NRS (0-10) ± std]	4.2 ± 2.2	4.1 ± 2.5	2.8 ± 1.1	6.6 ± 1.1	3.2 ± 1.3	2.4 ± 0.9	6.4 ± 1.1	6.8 ± 1.1
PVAQ score [mean ± std]	37 ± 13	37 ± 11	30 ± 12	38 ± 13	30 ± 14	29 ± 12	38 ± 15	38 ± 12
PCS [mean ± std]	12 ± 8	13 ± 11	4 ± 4	12 ± 5	5 ± 4	3 ± 3	13 ± 6	11 ± 5
Pain rating CS [mean NRS (0-10) ± std]	5.9 ± 2.2	4.9 ± 2	5.3 ± 2.1	5.2 ± 2.2	6.4 ± 1.3	4.1 ± 2.1	6.1 ± 2.5	4.4 ± 1.9

Table 2: *Session specific subject characteristics. PVAQ = Pain Vigilance and Awareness Questionnaire, PCS = Pain Catastrophizing Score. * 5 subjects that each underwent a tonic and burst session.*

Although we adjusted the TS amplitude prior to each session and aimed for a TS amplitude that caused a pain intensity score of 5 on a 0 to 10 NRS scale, this was not achieved in every subject during each session. The subjective pain ratings were higher in the non-effective SCS group in comparison to the effective SCS group *before* CPM (difference of 1.6, p = 0.017) and *during* CPM (difference of 1.6, p = 0.016). The subjective pain ratings were also higher for the effective group during burst SCS in comparison with tonic SCS *before* CPM (difference of 0.9, p = 0.037) and a trend was observed for a higher pain rating *during* CPM (difference of 1.3, p = 0.073) and *after* CPM (difference of 1.4, p = 0.052).

Although a decrease in pain ratings *during* CPM was observed on a group level, not every individual had a pain inhibitory effect by CPM. During tonic stimulation 12 out of 17 subjects presented an inhibitory effect of CPM on pain, 3 subjects experienced no difference in pain between the *before* and *during* CPM condition and 2 subjects experienced more pain *during* CPM compared to the *before* CPM condition. During burst stimulation 12 out of 17 subjects experienced an inhibitory effect of

CPM on pain and 5 subjects experienced no difference in pain between the *before* and *during* CPM condition.

Group	TS pain rating [mean NRS (0-10) ± SE]			Difference [mean NRS (0-10) ± SE]
	Before	*During*	*After*	*During* vs. *Before*
Effective (n=10)	4.7 ± 0.4	3.5 ± 0.5	4.3 ± 0.5	-1.2 ± 0.2 (p = 0.001)
Non-effective (n=10)	6.2 ± 0.5	5.1 ± 0.4	5.6 ± 0.6	-1.2 ± 0.2 (p = 0.002)
Tonic (n=17)	5.0 ± 0.5	4.1 ± 0.4	4.6 ± 0.5	-0.9 ± 0.3 (p = 0.001)
Burst (n=17)	5.1 ± 0.4	4.1 ± 0.3	4.7 ± 0.3	-1.0 ± 0.3 (p < 0.001)
Tonic effective (n=5)	4.2 ± 0.5	2.8 ± 0.6	3.6 ± 0.7	-1.4 ± 0.5 (p = 0.045)
Burst effective (n=5)	5.1 ± 0.5	4.1 ± 0.7	5.0 ± 0.7	-1.0 ± 0.4 (p = 0.011)
Tonic non-effective (n=5)	6.6 ± 0.8	5.4 ± 0.6	6.3 ± 1.1	-1.2 ± 0.4 (p = 0.057)
Burst non-effective (n=5)	5.9 ± 0.5	4.6 ± 0.3	5.1 ± 0.5	-1.3 ± 0.2 (p = 0.041)

Table 3: *Mean and standard error (SE) of pain ratings to TS on a NRS scale [0-10] before, during and after CPM for the different groups. n is the number of MEG sessions.*
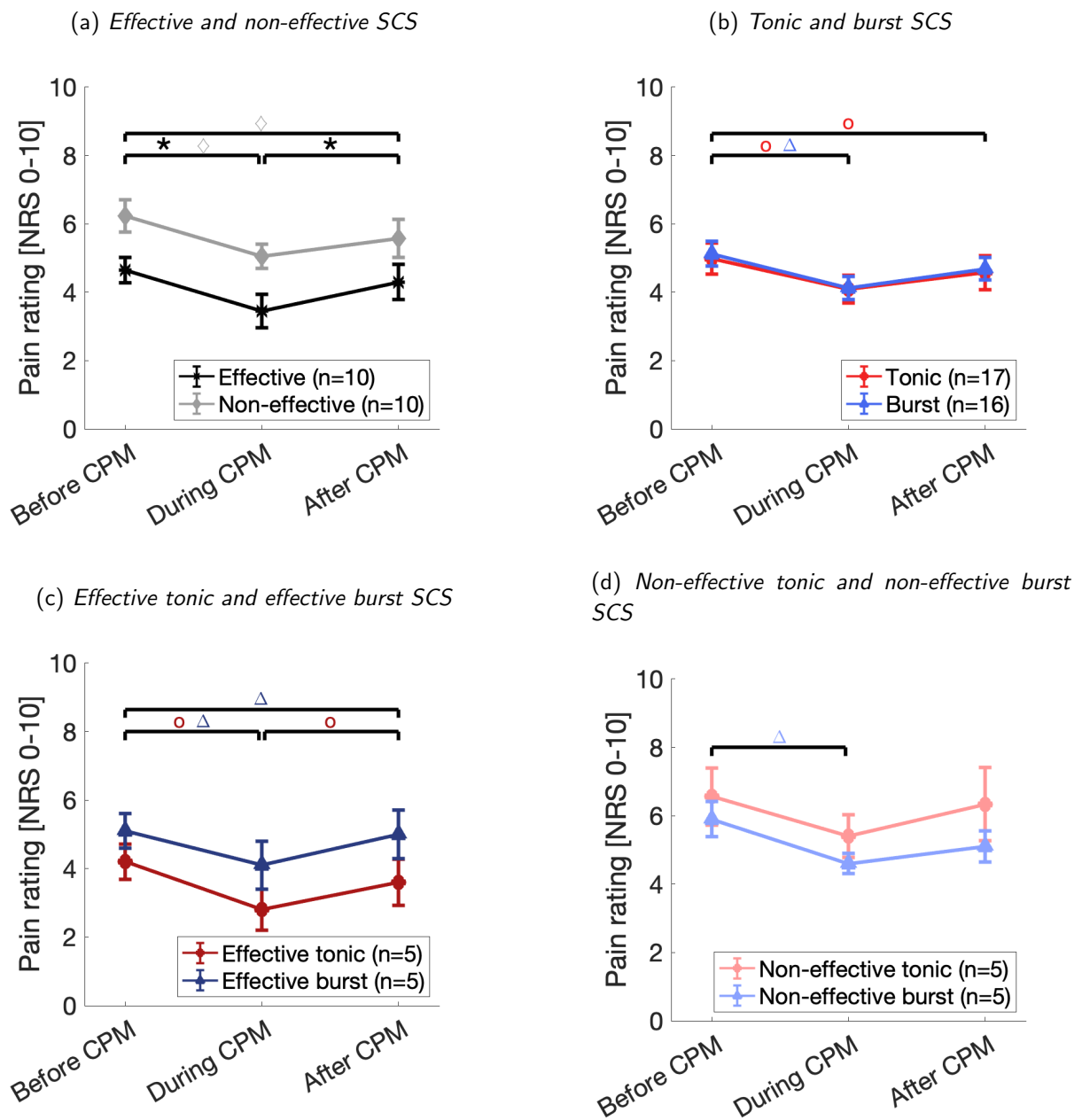
Figure 8: *Mean and standard error of subjective pain ratings to TS on the NRS scale (0-10) before, during and after CPM. Difference in pain rating between CPM conditions with a p-value<0.05 for effective (⋆), non-effective (◇), tonic (○), effective tonic (○), non-effective tonic (○), burst (△), effective burst (△) or non-effective burst SCS (△). n is the number of MEG sessions.*

3.3 Cortical response in the time domain

Figure 9 displays the averaged (all subjects, all conditions) cortical activation pattern evoked by TS displayed on a source map. First, activity is observed mainly in the bilateral sensorimotor cortices. Around 120 ms post stimulus activity is observed in the S2. Note that these source maps are different from the source map displayed in Figure 5. The source maps of Figure 9 display the activity (expressed in z-scores) at different points in time, whereas the source map of Figure 5 shows the sources of beta ERS.

Appendix C.1 displays the cortical activation pattern evoked by TS on source maps *before, during* and *after* CPM. Appendix C.2 displays the extracted time series for the bilateral sensorimotor cortices, left S2, bilateral ACC and right insula.
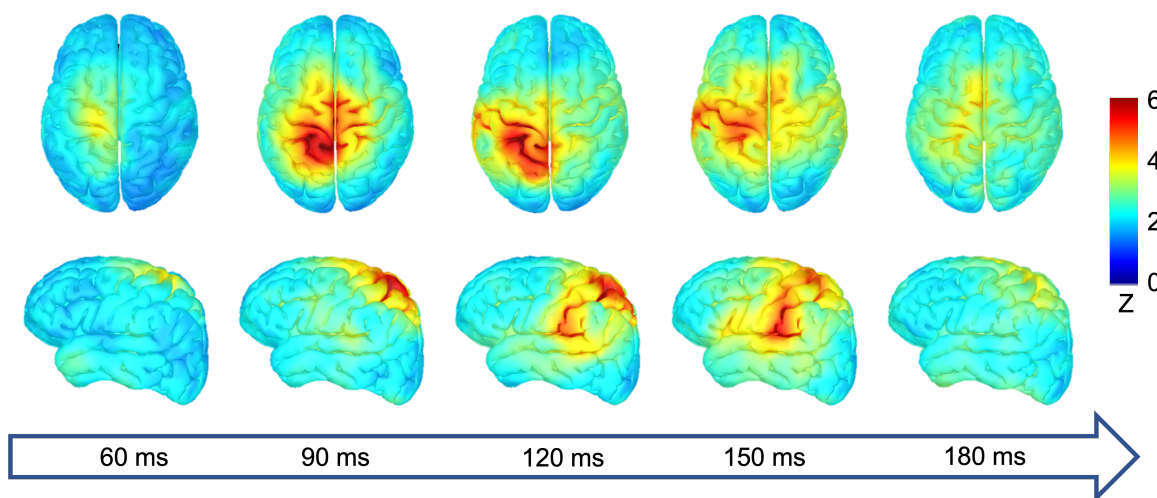
Figure 9: *Source map showing the average cortical response in the time domain to a nociceptive stimulus (TS) applied at the right sural nerve, expressed in z-scores relative to the baseline. The response is averaged over all subjects, stimulation modes and CPM conditions. At t = 0 TS is applied, the primary and secondary somatosensory cortices (S1, S2), primary motor cortex (M1) and supplementary motor area (SMA) show increased activity between 60 till 180 ms post stimulus. View from above and view on the left hemisphere. Note that these source maps show activity over time and are thus different from the source map in Figure 5 which shows the sources of beta-ERS*

3.4 Cortical response in the time-frequency domain

In the following subsections, the results are shown for the ROI consisting of the S1, M1 and SMA of both hemispheres (bilateral sensorimotor cortices), since the response was the clearest in this area and it is expected that this area is the main source of beta ERS (Figure 5). The TF response was averaged over all subjects and conditions (Figure 10) to determine the start and end times for each ERSP. Appendix D displays the start and end of beta ERS in the bilateral sensorimotor cortices determined by the averaged time series. Appendix E shows the start and end time for each ERSP per ROI. The duration of the stimulus artifact varied between the subjects and was especially present within the alpha frequency range. Besides, the start and end times of the ERD strongly varied between the subjects. Beta ERS is the ERSP that is the least influenced by the stimulus artifact and is less susceptible to subject variability in the start en and times, therefore the following sections display the results of the average power of beta ERS in the bilateral sensorimotor cortices. See Appendix F for the results of all ERSPs of each ROI.

In the bilateral sensorimotor cortices alpha ERD 345 till 660 ms post stimulus was observed after a nociceptive stimulus, followed by alpha ERS 893 till 5020 ms post stimulus. Beta ERD was observed 190 till 470 ms post stimulus, followed by beta ERS 554 till 2963 ms post stimulus. Table 4 summarizes the average power of beta ERS in this time range for each evaluated group and condition.

Group	Power beta ERS [mean z-score ± SE]			Difference [mean z-score ± SE]
	Before	*During*	*After*	*During* vs. *Before*
Effective (n=10)	0.60 ± 0.14	0.28 ± 0.08	0.56 ± 0.17	-0.32 ± 0.16 (p = 0.076)
Non-effective (n=10)	1.08 ± 0.49	0.86 ± 0.31	0.92 ± 0.38	-0.21 ± 0.21 (p = 0.348)
Tonic (n=17)	0.65 ± 0.25	0.63 ± 0.19	0.84 ± 0.21	-0.02 ± 0.12 (p = 0.852)
Burst (n=17)	0.95 ± 0.23	0.44 ± 0.14	0.71 ± 0.19	-0.51 ± 0.19 (p = 0.017)
Tonic effective (n=5)	0.42 ± 0.12	0.36 ± 0.12	0.83 ± 0.18	-0.07 ± 0.17 (p = 0.719)
Burst effective (n=5)	0.77 ± 0.18	0.20 ± 0.10	0.29 ± 0.26	-0.57 ± 0.23 (p = 0.066)
Tonic non-effective (n=5)	1.09 ± 0.77	0.90 ± 0.50	0.81 ± 0.53	-0.20 ± 0.34 (p = 0.590)
Burst non-effective (n=5)	1.06 ± 0.70	0.83 ± 0.44	1.02 ± 0.59	-0.23 ± 0.31 (p = 0.498)

Table 4: *Mean and standard error (SE) of average power [z-score] of beta (13-30 Hz) event related synchronization (ERS) induced by TS before, during and after CPM for the different groups in the bilateral sensorimotor cortices.*

3.4.1 Effective and non-effective SCS

The averaged TF maps for the effective and non-effective SCS groups are displayed in Figure 11. For both effective and non-effective SCS the power of beta ERS seems to decrease *during* CPM (11b, 11e) when compared to the TF map *before* CPM (11a, 11d). When the CS is removed, the power of beta ERS seems to increase again (11c, 11f). Figure 12a shows the extracted power of beta ERS for both groups. The effective SCS group showed a trend towards a decrease in power of beta ERS *during* CPM of 0.32 (p = 0.08), a relative decrease with the *before* CPM condition of
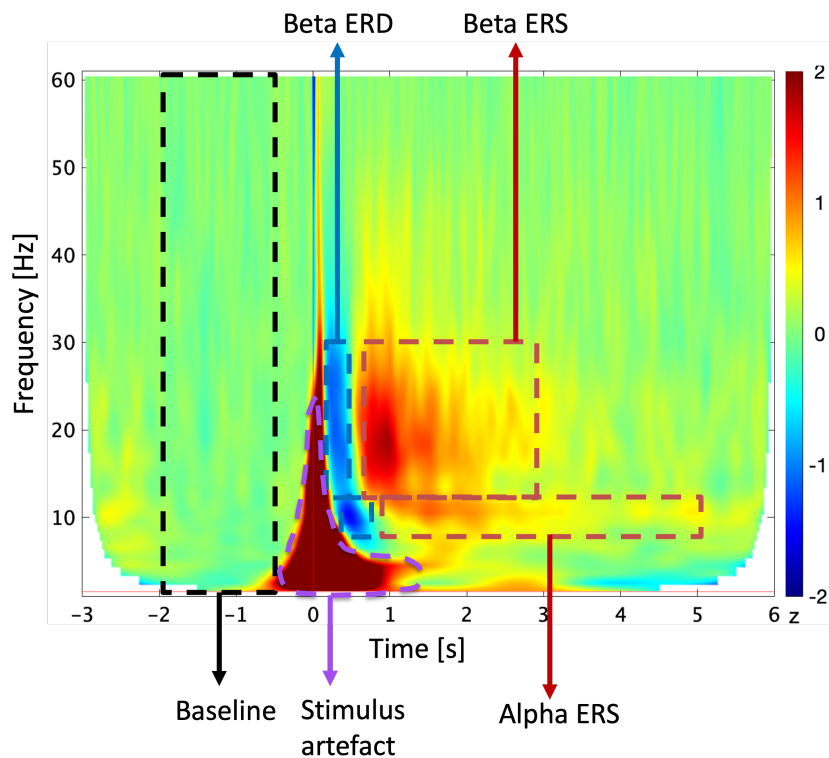
Figure 10: *Averaged time frequency response over all subjects and conditions in the bilateral senso- rimotor cortices. At t = 0 the nociceptive test stimulus (TS) is applied. The event related spectral perturbations (ERSPs) are expressed as relative power with respect to the baseline. First event related desynchronization (ERD) is observed for the alpha (8-12 Hz) and beta (13-30 Hz) frequency ranges, followed by event related synchronization (ERS). Alongside the measured neuronal activity, TS also caused a stimulus artifact measured in the data.*

53%. For non-effective SCS no statistically significant decrease in power of beta ERS *during* CPM was observed.

3.4.2 Tonic and burst SCS

The average power of beta ERS for tonic and burst SCS are displayed in Figure 12b. For burst SCS the power of beta ERS *during* CPM decreased significantly with 0.51 (p = 0.02), a relative decrease of 54%. *After* removing the CS the power significantly increased with 0.27 (p = 0.04), a relative increase of 61%. For tonic SCS no differences were observed between the three CPM conditions. The power of beta ERS *before* CPM was higher for burst SCS in comparison with tonic SCS (difference of 0.32, p = 0.045).

3.4.3 Effective and non-effective SCS per stimulation mode

The average power of beta ERS for effective tonic and effective burst SCS are displayed in Figure 12c. For the effective burst SCS group, a trend was observed towards a decrease in power of beta ERS of 0.57 (p = 0.07), a relative decrease of 74%. For effective tonic SCS the power of beta ERS seems to remain equal between the *before* and *during* CPM condition, however *after* CPM the power increases. In comparison with the *before* CPM condition, the power of beta ERS increased significantly with 0.40 (p = 0.02), a relative increase of 130%.
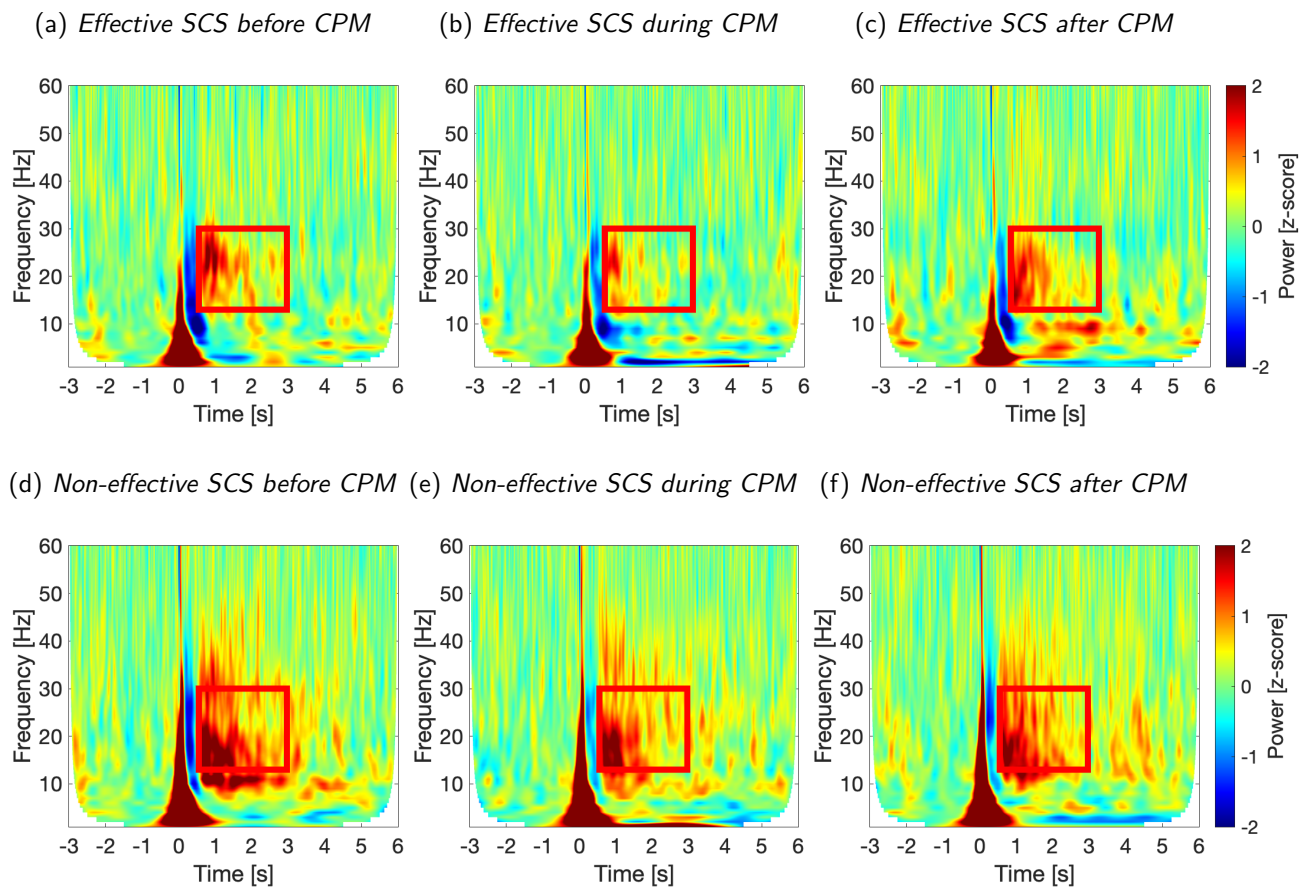
Figure 11: *Averaged time-frequency maps (TF) maps, z-scored with respect to baseline, for effective and non-effective SCS per CPM condition for the bilateral sensorimotor cortices. At t = 0 the nociceptive test stimulus (TS) is applied. First event related desynchronization (ERD) is observed for the alpha (8-12 Hz) and beta (13-30 Hz) frequency ranges, followed by event related synchronization (ERS). The average power of beta-ERS is extracted for each condition in the time and frequency ranges defined by the red box.*

During non-effective tonic and burst SCS (Figure 12d) no statistically significant differences were observed between the CPM conditions.

(a) *Effective and non-effective SCS*

(b) *Tonic and burst SCS*

(c) *Effective tonic and effective burst SCS*

(d) *Non-effective tonic and non-effective burst SCS*
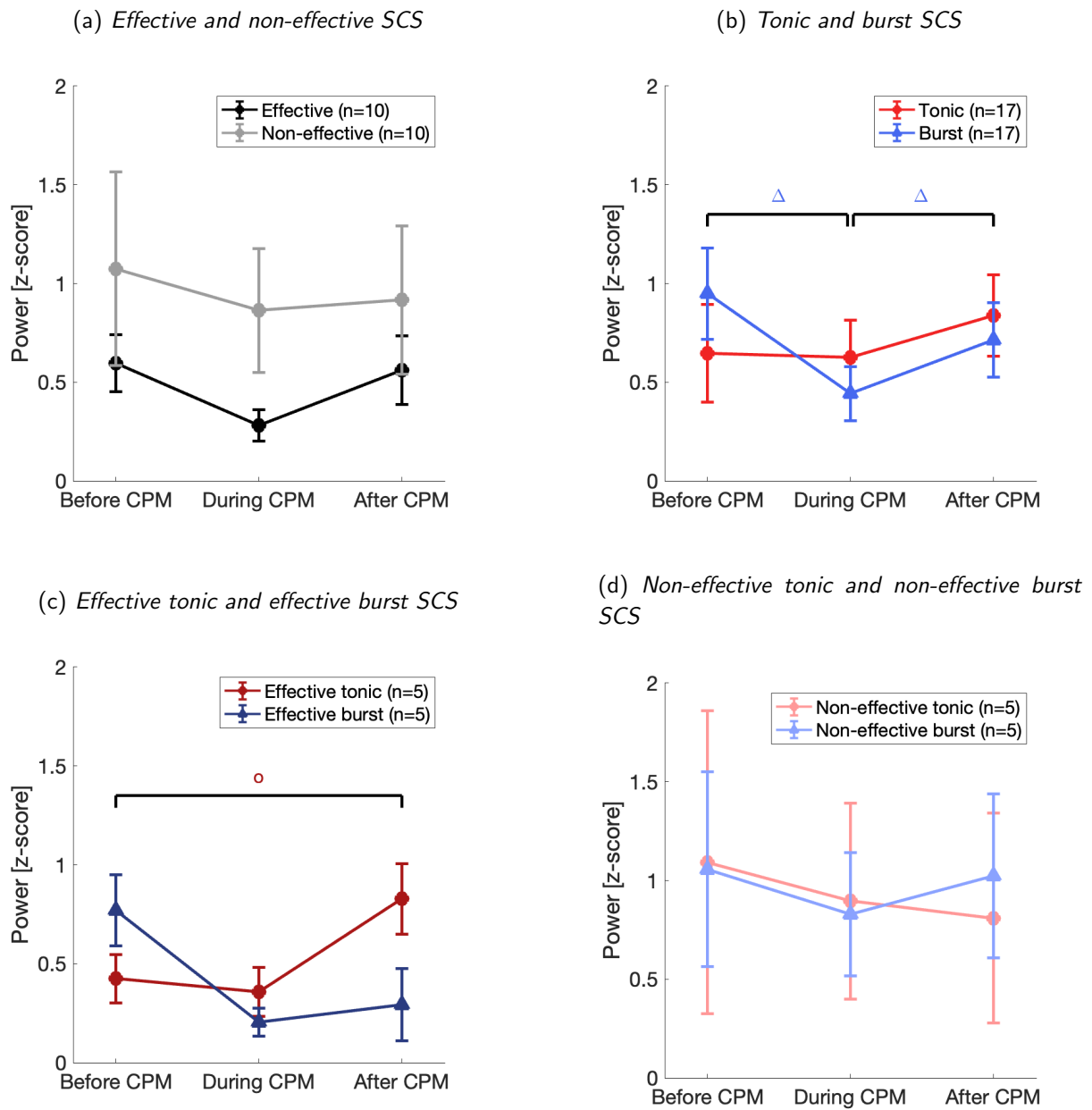
Figure 12: *Mean and standard error of average power [z-score] of beta event related synchronization (ERS) induced by TS before, during and after CPM for the different groups in the bilateral sensorimotor cortices. Difference in power of beta ERS between CPM conditions has a p-value<0.05 for effective tonic (∘) or burst (△) SCS. n is the number of MEG sessions.*

4. Discussion

The main objective of this thesis was to assess how effective spinal cord stimulation affects the supraspinal mechanisms of pain modulation in chronic pain patients. Using magnetoencephalography I assessed the cortical response to a nociceptive stimulus *before*, *during* and *after* conditioned pain modulation.

4.1 Effect of CPM on pain ratings

During CPM the subjective pain ratings of TS were significantly decreased. The decrease was seen in all groups, except for the group non-effective tonic SCS. Although the decrease was observed on a group level, not every subject displayed an inhibitory effect of CPM on the pain ratings. The variability of the response *during* CPM has been observed in previous studies as well [53].

Our observations show on average an efficient inhibitory effect by CPM on the pain ratings, whereas CPM is impaired in chronic pain patients [49, 54]. Therefore, it is suggested that SCS treatment improves CPM on a group-level based on subjective pain ratings. This finding is in line with previous studies that reported improved CPM based on the subjective pain ratings during SCS *on* in comparison with SCS *off* [55, 56]. Ramaswamy et al. [57] and Goudman et al. [58] reported an improved CPM after SCS implantation in FBSS patients, however Kriek et al. [59] did not observe a change in CPM after SCS implantation in CRPS patients. The most common chronic pain condition observed in this study is FBSS (15/17 patients), making it comparable to the patient population of Ramaswamy et al. [57] that showed results in line with our findings.

4.2 Cortical response in the time domain

The source maps displaying the cortical response over time showed that, among other structures, the contralateral primary (S1) and secondary (S2) somatosensory cortices are activated after a nociceptive stimulus. This is in line with previous MEG and fMRI studies that studied the cortical response to nociceptive stimuli [60–67]. The S1 and S2 are both part of the lateral pain pathway and are thought to play a role in the sensory-discriminative aspect of pain processing. We observed activation in S1 accompanied by activation in the S2 around 50 ms later, suggesting a serial activation of the areas which was also observed in other (MEG) studies [66, 67].

It seems that *during* CPM the amplitude of the response is lower in the left S2, bilateral ACC and right insula when compared to the *before* and *after* CPM conditions (Appendix C.2), although this was not confirmed by statistical analysis. Further exploration of the evoked response by TS in the time domain was beyond the scope of this thesis. However, since we did observe a clear response with relatively high z-scores (in comparison to the response observed in the TF domain) it is recommended to further research the cortical response in the time domain and to compare the response between effective and non-effective SCS for tonic and burst stimulation modes.

4.3 Cortical response in the time-frequency domain

The cortical response to TS in the bilateral sensorimotor cortices was evaluated. TS induced alpha ERD (345 - 660 ms post stimulus) and beta ERD (190 - 470 ms post stimulus) followed by alpha ERS (893 - 5020 ms post stimulus) and beta ERS (554 - 2963 ms post stimulus). The ERD might represent the activation of the bilateral sensorimotor cortices and the ERS the following inhibition of the same area which can be described as the off-response to a somatosensory stimulus [45,47,48,68]. The observation of ERD followed by ERS in the alpha and beta frequency ranges is in line with previous studies that reported ERD and ERS in the sensorimotor cortices [46,48,68].

During CPM beta ERS was decreased for some of the evaluated groups. Beta ERS might reflect top-down modulation of nociceptive stimuli, with less beta ERS representing more top-down modulation [48]. Our observation of a decreased beta ERS *during* CPM suggests that the cortical response to TS was inhibited by applying CS and that the subjects were experiencing top-down modulation. Only a limited number of studies reported the cortical effects of CPM in the time-frequency domain. Rustamov et al. [69] observed a decrease in high gamma-ERS (60-100 Hz) 100-300 ms post stimulus. We also investigated the high gamma frequencies by computing TF maps for the frequency range from 60 till 100 Hz, however no clear response in this frequency range was observed, see Appendix H. Two studies observed a decrease in power of delta ERS (1-4 Hz) [70,71], we did not compare the power of ERS in this frequency band due to the low temporal resolution of the TF analysis for the lower frequencies and the influence of stimulus artifact. Jin [49] reported a decrease in the power of beta ERS *during* CPM for the healthy controls, whereas for the chronic pain patients the power of beta ERS did not decrease *during* CPM. Based on the findings by Diers et al. [48] and Jin [49] it is suggested that beta ERS reflects the supraspinal mechanisms of modulation of pain (top-down modulation).

The inhibition of beta ERS was observed on a group-level and was not always observed on subject-level, Appendix G displays the inter-subject variability observed in cortical response to TS in the bilateral sensorimotor cortices for burst SCS during all conditions.

4.3.1 Effective and non-effective SCS

A trend towards a decrease in power of beta ERS was observed *during* CPM for the effective SCS group. The relative observed decrease was 53%. No decrease in power of beta ERS was observed for the non-effective SCS group. The data suggests that when SCS is effective, subjects exhibit a stronger inhibitory effect of CPM on the power of beta ERS in the bilateral sensorimotor cortices than when SCS is non-effective. This finding indicates that during effective SCS more top-down modulation takes place *during* CPM.

Furthermore, a trend was observed towards a higher power of beta ERS for the non-effective SCS group in comparison to the effective SCS group *during* CPM. Also during the other conditions the values of the power of beta ERS seemed to be higher for the non-effective SCS group in comparison with the effective SCS group. Next to the power of beta ERS, also the perceived pain intensity of TS was higher in the non-effective group (Figure 8a). The perceived pain intensity might be caused

by a higher stimulus intensity, which is associated with a higher power of ERSP [72]. Although we aimed for an amplitude of the TS that caused a pain intensity of 5 on a 0 to 10 NRS scale, this was not achieved in every subject. Accordingly, a possible explanation for the observed higher beta ERS power for the non-effective SCS group might be that the pain intensity was higher in this group.

Another possible explanation for the higher power of beta ERS is that when SCS is non-effective I expect that subjects are more bothered by nociceptive stimuli and therefore give more attention to the TS. This is in line with other studies that reported a higher power of beta ERS or increased cortical activity when subjects had to direct their attention to the nociceptive stimulus [48, 73, 74].

4.3.2 Tonic and burst SCS

During burst SCS a significant decrease was observed in power of beta ERS in the bilateral sensorimotor cortices. During tonic SCS no decrease was observed in power of beta ERS. This suggests that burst SCS has a stronger effect on the supraspinal mechanisms of the modulation of pain than tonic SCS.

The power of beta ERS was higher *before* CPM during burst SCS in comparison with tonic SCS. This might be due to the hypothesized higher baseline during tonic SCS than during burst SCS. The baselines were not compared between tonic and burst SCS, it is recommended to further analyze whether the baselines indeed differ between the different SCS stimulation modes.

After CPM the power of beta ERS increased in comparison to the *during* CPM condition for burst stimulation, but it does not statistically differ from the *before* CPM condition suggesting the power of cortical response returned to the *before* CPM condition. For tonic SCS the power of beta ERS also increased *after* CPM and the power was significantly higher than the *before* CPM condition. If regarding the power of beta ERS as a measure for the attention given to the TS, this suggests that in the *after* CPM condition the subjects' attention to the nociceptive stimulus increased during tonic stimulation.

4.3.3 Effective and non-effective SCS per stimulation mode

For the effective SCS group a trend was observed towards a decrease in power of beta ERS *during* CPM during burst SCS. For the same subjects no decrease in power of beta ERS *during* CPM was observed during tonic SCS, despite the treatment being successful. This suggests that only effective burst SCS is capable of improving the inhibitory effect of CPM. Possibly the MOA of burst SCS includes improvement of the supraspinal mechanisms of modulation of pain, whereas tonic SCS is not capable of doing this. This suggests that tonic and burst SCS have a (partly) different MOA which was suggested previously [10, 20, 75].

For the non-effective SCS group, both stimulation modes did not show a clear inhibitory effect of CPM on the power of beta ERS. Suggesting that only effective burst SCS is capable of improving the inhibitory effect of CPM on the power of beta ERS and thereby of improving the top-down modulation of subjects.

The subjects in the effective SCS group were responders to both tonic and burst SCS and the non-

effective SCS group consisted of non-responder to both tonic and burst SCS. One subject in this study was a responder to burst, but a non-responder to tonic SCS (PTN05). Appendix G (Figures 34j, 34k and 34l) display the response in TF domain in the bilateral sensorimotor cortices *before, during* and *after* CPM for PTN05. For this subject a clear decrease in power of beta ERS is observed during burst SCS, whereas this was not observed during tonic SCS. Again suggesting that burst SCS is capable of improving the supraspinal mechanisms of modulation of pain, which possibly explains why this subject experienced effective treatment by burst SCS but lacked effective treatment by tonic SCS.

4.4   Response in other cortical areas

Time-frequency analysis was performed in multiple ROIs, including cortical areas related to the medial pathway of pain (ACC, MCC, PCC, insula, DLPFC and OFC). The cortical response in the bilateral sensorimotor cortices was displayed in this report. For the other ROIs no large differences were observed between the investigated groups of subjects and for many ROIs a low power of response was observed. Two possible explanations for the lower power of the responses observed in these areas are that: 1) these areas are less activated in comparison with the bilateral sensorimotor cortices and 2) these areas are further away from the MEG sensors resulting in a higher signal-to-noise (SNR) ratio.

The same method that was used for the bilateral sensorimotor cortices to calculate the start and end times of the ERD and ERS was applied to all other ROIs, including the same threshold of a z-score of 0.4 (section 2.7). Due to the lower power of response this sometimes resulted in very short time ranges (see Appendix E) used to calculate the average power for that ERSP, making the average power dependent on a smaller time window. I decided to use the same method for consistency, however this might not have been the most optimal threshold for all ROIs.

4.5   Limitations

4.5.1   Number of subjects

One of the main limitations of this study was the limited number of subjects. We collected MEG recordings of 26 subjects, unfortunately, 9 subjects had to be excluded due to contamination of the data by (dental) implants or missing data. The subjects had to be divided into an effective SCS and a non-effective SCS group. Since not every subject was a very clear responder or non-responder to SCS treatment, we could not include every subject in the effective vs. non-effective SCS comparison. This left us with small group sizes of only 5 subjects per group. To increase the power for the effective and non-effective groups, tonic and burst SCS were combined resulting in 10 recordings for each group. However, to specifically analyze the differences between effective tonic and burst SCS the group size was limited to 5. For future research comparing effective and non-effective SCS, it is recommended to select clear responders and non-responder to SCS treatment.

4.5.2 Computation of time-frequency analysis

I computed TF decomposition on the ROI averaged signal instead of computing the TF decomposition on the signal of each vertex of the ROI separately and then averaging the TF maps. The second method is preferred, since computing TF decomposition on an averaged signal might result in information loss, especially for the higher frequencies [76]. The first method was chosen due to limited computational power. To minimize information loss, I divided the bigger ROIs into smaller sub-ROIs. However, computing the TF on the averaged signal may have influenced the results. Computing a TF decomposition per vertex might increase the SNR, which might result in a clearer response which is useful, especially for the ROIs that are currently showing little to no response to the nociceptive stimuli.

4.5.3 Influence of experiment- and subject-related factors on CPM

During the CPM experiment it is almost inevitable that other pain modulating factors influence the pain perception, such as habituation and psychological-cognitive factors [69, 71, 77–83]. We tried to correct for these factors by for example randomizing the inter-stimulus interval and not giving an expectation of the effect of CPM. However applying the CS could potentially act as a distraction, which is a factor with a pain inhibiting effect. Moont et al. [81] investigated the effect of distraction with and without CPM and concluded that CPM has an additive effect. Thus, although distraction may add to pain inhibition, it cannot alone explain the observed pain inhibiting effect of CPM. It could be debated whether the supra-spinal mechanisms of CPM are distinct from the other pain modulating factors. Or that those factors are part of the supra-spinal mechanisms of CPM.

A systematic review by Herman et al. [53] evaluated subject-related factors that influence CPM. They reported an increased pain inhibitory effect by CPM for subjects with male gender, younger age, ovulatory phase and carrier of the 5-HTTLPR long allele. The average age of the subjects in the effective SCS group was 48 years, whereas the average age for the non-effective SCS group was 58 years. The higher inhibitory effect on the power of beta ERS in the effective SCS group in comparison with the non-effective SCS group, might not only be attributed to the SCS being effective but the higher age might also play a role. The subject-related factors might have contributed to the inter-subject variability observed in the cortical response to TS (Appendix G).

Next to the inter-subject variability, the intra-subject variability should also be taken into account. Other studies that investigated CPM on separate days, reported a poor agreement in the classification of a subject as CPM responder or non-responder. therefore they suggested a considerable intra-subject variation in CPM [84, 85]. Future research should further investigate the intra-subject variation in CPM, possibly the variability might be an indication of the top-down modulation capacity of an individual.

Given the influence of experiment-related factors and subject-related factors, which introduce inter- and intra-subject variability it is recommended to evaluate CPM data on a group-level instead of subject-level.

4.5.4 Multiple comparisons

We decided due to the exploratory nature of this research, not to compensate for the multiple comparisons made. Making multiple comparisons increases the risk of finding false statistically significant differences.

4.5.5 Stimulus and linear interpolation artefact

Around t = 0 a clear artifact was visible in the averaged TF maps. The stimulus artifact was removed from the raw recordings using linear interpolation, however there still may be some remaining stimulus activity. The artifact visible in the TF maps probably was caused by the remaining stimulus activity, but also the application of linear interpolation caused an artifact. See Appendix I for an evaluation of the effect of stimulus activity and linear interpolation on the TF analysis.

4.6 Future directions

4.6.1 SCS and the supraspinal mechanisms of modulation of pain

This data suggests that effective burst SCS is capable of improving the supraspinal mechanisms of modulation of pain in a chronic pain patient, whereas effective tonic SCS was not. Future research, using larger subject groups, should further clarify whether burst SCS indeed is capable of improving the supraspinal mechanisms of modulation of pain and if tonic SCS indeed does not improve these mechanisms.

If tonic SCS is not capable of improving the top-down modulation despite being effective, this could clarify the 'chicken or egg' question regarding CPM and chronic pain. If tonic SCS abolishes the ongoing chronic pain but does not improve CPM, then chronic pain is not the only cause of a deficit CPM. In that case, a deficit CPM might be related to the development of chronic pain, although a deficit CPM does not necessarily lead to chronic pain. Regarding a deficit CPM as a risk factor for the development of chronic pain is in accordance with findings by Yarnitsky et al. [37] who investigated CPM in patients (without a chronic pain condition) before they underwent surgery. During follow-up the patients were monitored to see if they developed chronic pain as a result of the surgery. They showed that people with a less efficient CPM had a higher risk of developing chronic pain, also suggesting that a deficit CPM may be a risk factor for the development of chronic pain. Although this does not rule out that experiencing an ongoing chronic pain state also contributes to a less efficient CPM, due to the chronic CPM state these patients may experience a flooring effect on the experimental CPM. Therefore, I suggest that having a less efficient CPM is a risk factor for the development of chronic pain and that having chronic pain further enhances a less efficient CPM due to the flooring effect.

In addition, further research focusing on how SCS improves the supraspinal mechanisms of pain modulation should explore CPM in patients before undergoing SCS implantation and after SCS implantation. The (intra-subject consistency of) CPM efficiency of an individual before SCS implantation could perhaps be a predictor for the success of SCS implantation, which thereby could improve the selection process of individuals suitable for SCS treatment. MEG recordings *during*

CPM before SCS implantation were available for two subjects of this study. Appendix J displays the TF maps and power of beta ERS *before, during* and *after* CPM of both subjects before and after SCS implantation. One of the subjects expressed no inhibitory effect by CPM on the cortical response in the time domain before SCS implantation and during tonic SCS, however during burst SCS a strong inhibitory effect of CPM was observed on the power of alpha and beta ERS.

4.6.2 Thalamus

The thalamus is an important structure involved in the processing of pain, the thalamus is part of both the lateral and medial pathways. The thalamus acts as a relay station that the somatosensory inputs pass on their way to the cerebral cortex [86]. Accordingly, the thalamus is one of the areas that is very consistently activated by nociceptive stimuli as observed in human brain imaging studies [87–90]. The thalamic response to a nociceptive stimulus is limitedly investigated [91].

The thalamus is a deeper brain structure making it hard if not impossible to image using EEG, MEG however offers the potential to reach the deeper structures and to image activity in the thalamus. Several other studies have shown to be able to image deeper structures such as the hippocampus and the amygdala [92–94].

For future research I recommend to further investigate the role of the thalamus in the processing of pain. The same dataset as used in this thesis can be used to evaluate the thalamic response to a nociceptive stimulus in patients receiving SCS. A volume model should be used instead of a cortical model. The response can be regarded in time and TF domain. The 22 stimuli of each CPM condition can be averaged to evaluate the thalamic response to a nociceptive stimulus during SCS. The thalamic response can also be compared between the three CPM conditions to evaluate how the thalamic response is affected by CPM and whether this is different during (effective and non-effective) tonic or burst SCS.
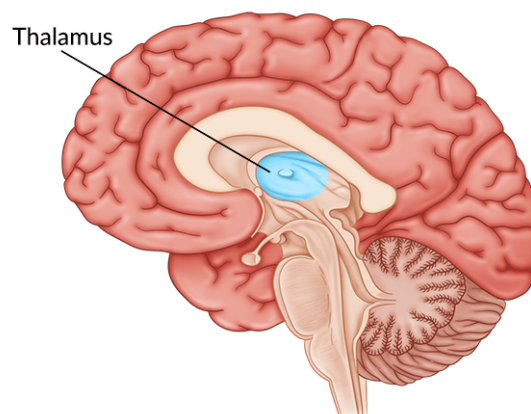
Figure 13: *The thalamus: a deep brain structure that acts as an important relay station in the processing of nociceptive stimuli. The thalamus is an interesting structure to image using MEG in future research focusing on the processing of pain. Figure from Rehab [95].*

4.6.3 Dynamic functional connectivity analysis

It is clear that pain is not processed by one specific area of the brain, but that the processing encompasses a lot of different brain areas. All these brain areas communicate with one another through a complex network. Functional connectivity (FC) analysis can contribute to unraveling the connections within this network. Dynamic functional connectivity (dFC) methods extend this analysis by measuring the changes over time and thereby unraveling the dynamics within the network [96]. Since MEG offers a brain imaging modality with a good spatial and temporal resolution, this is a very suitable technique to apply dFC analysis and can be performed using the *Brainstorm* software [97]. Therefore, I recommend for future research not only to review the brain response to a nociceptive stimulus in a specific ROI, but also to unravel the dynamics of the complex pain network in the brain using dFC analysis.

5. Conclusion

In this thesis project I investigated the effect of spinal cord stimulation (SCS) on the supraspinal mechanisms of pain modulation in chronic pain patients. To evaluate the supraspinal mechanisms of pain modulation I used magnetoencephalography (MEG) to assess the cortical response in the time and time-frequency domain during conditioned pain modulation (CPM). I compared effective and non-effective SCS for tonic and burst SCS stimulation modes. Despite a lot of inter-individual variabilities, we observed that the effective burst SCS group displayed, on a group-level, a decrease in power of beta event-related synchronization (ERS) in the bilateral sensorimotor area *during* CPM in comparison with the *before* CPM condition. Beta ERS might be a measure for the modulation of pain through supraspinal mechanisms. Therefore, this observation suggests that effective burst SCS is capable of improving the supraspinal mechanisms of pain modulation of chronic pain patients, whereas effective tonic SCS is not capable of doing so. This suggestion indicates that tonic and burst SCS have a different mechanism of action (MOA), next to other shared spinal and possibly additional supraspinal MOAs.

Future research should focus on: 1) validating that effective burst SCS improves the supraspinal mechanisms of pain modulation, using larger group sizes and evaluating the cortical response during CPM before and after SCS implantation; 2) exploring the thalamic response to nociceptive stimuli in the time and time-frequency domain and 3) exploring the dynamic functional connectivity between the complex network of brain structures involved in the processing of pain.

6. References

(1) S. N. Raja, D. B. Carr *et al.*, "The revised international association for the study of pain definition of pain: concepts, challenges, and compromises," *Pain*, vol. 161, p. 1976–1982, 2020.

(2) R. D. Treede, W. Rief *et al.*, "Chronic pain as a symptom or a disease: The iasp classification of chronic pain for the international classification of diseases (icd-11)," *Pain*, vol. 160, 2019.

(3) D. S. Goldberg and S. J. McGee, "Pain as a global public health priority," *BMC Public Health*, vol. 11, 2011.

(4) T. Vos, A. A. Abajobir *et al.*, "Global, regional, and national incidence, prevalence, and years lived with disability for 328 diseases and injuries for 195 countries, 1990-2016: A systematic analysis for the global burden of disease study 2016," *The Lancet*, vol. 390, 2017.

(5) brigthbraincentre, "Chronic pain in the brain," Bright Brain Centre – London's EEG, Neurofeedback And Brain Stimulation Centre, 2017. [Online]. Available: https://www.brightbraincentre.co.uk/chronic-pain-brain/

(6) M. F. Yam, Y. C. Loh *et al.*, "General pathways of pain sensation and the major neurotransmitters involved in pain regulation," *International Journal of Molecular Sciences*, vol. 19, 2018.

(7) D. D. Price, "Psychological and neural mechanisms of the affective dimension of pain," *Science*, vol. 288, 2000.

(8) M. C. Bushnell, M. Čeko, and L. A. Low, "Cognitive and emotional control of pain and its disruption in chronic pain," *Nature Reviews Neuroscience*, vol. 14, 2013.

(9) B. A. Vogt and R. W. Sikes, "The medial pain system, cingulate cortex, and parallel processing of nociceptive information," *Progress in Brain Research*, vol. 122, 2000.

(10) D. D. Ridder and S. Vanneste, "Burst and tonic spinal cord stimulation: Different and common brain mechanisms," *Neuromodulation*, vol. 19, 2016.

(11) M. Hauck, C. Domnick *et al.*, "Top-down and bottom-up modulation of pain-induced oscillations," *Frontiers in human neuroscience*, vol. 9, pp. 375–375, 2015.

(12) C. Urch, "Normal pain transmission," *Reviews in Pain*, vol. 1, 2007.

(13) A. K. Compton, B. Shah, and S. M. Hayek, "Spinal cord stimulation: A review," *Current Pain and Headache Reports*, vol. 16, 2012.

(14) K. Garcia, J. Wray, and S. Kumar, "Spinal cord stimulation," StatPearls, 2022. [Online]. Available: https://www.ncbi.nlm.nih.gov/books/NBK553154/

(15) T. Cameron, "Safety and efficacy of spinal cord stimulation for the treatment of chronic pain: A 20-year literature review," *Journal of Neurosurgery*, vol. 100, 2004.

(16) K. Kumar, G. Hunter, and D. Demeria, "Spinal cord stimulation in treatment of chronic benign pain: Challenges in treatment planning and present status, a 22-year experience," *Neurosurgery*, vol. 58, 2006.

(17) K. J. Burchiel, V. C. Anderson *et al.*, "Prospective, multicenter study of spinal cord stimulation for relief of chronic back and extremity pain," *Spine*, vol. 21, 1996.

(18) R. Melzack and D. Wall Patrick, "Pain mechanisms: A new theory," *Science*, vol. 150, no. 3699, pp. 971–979, 1965.

(19) J. C. Oakley and J. P. Prager, "Spinal cord stimulation: Mechanisms of action," *Spine*, vol. 27, 2002.

(20) E. Sivanesan, D. P. Maher *et al.*, "Supraspinal mechanisms of spinal cord stimulation for modulation of pain," *Anesthesiology*, vol. 130, 2019.

(21) H. A. Swadlow and A. G. Gusev, "The impact of 'bursting' thalamic impulses at a neocortical synapse," *Nature Neuroscience*, vol. 4, 2001.

(22) S. M. Sherman, "Tonic and burst firing: Dual modes of thalamocortical relay," *Trends in Neurosciences*, vol. 24, 2001.

(23) T. Kirketeig, C. Schultheis *et al.*, "Burst spinal cord stimulation: A clinical review," *Pain Medicine (United States)*, vol. 20, 2019.

(24) D. D. Ridder, M. W. Lenders *et al.*, "A 2-center comparative study on tonic versus burst spinal cord stimulation: Amount of responders and amount of pain suppression," *Clinical Journal of Pain*, vol. 31, 2015.

(25) J. B. Peeters and C. Raftopoulos, "Tonic, burst, high-density, and 10-khz high-frequency spinal cord stimulation: Efficiency and patients' preferences in a failed back surgery syndrome predominant population. review of literature," *World Neurosurgery*, vol. 144, 2020.

(26) C. C. D. Vos, M. J. Bom *et al.*, "Burst spinal cord stimulation evaluated in patients with failed back surgery syndrome and painful diabetic neuropathy," *Neuromodulation*, vol. 17, 2014.

(27) P. Courtney, A. Espinet *et al.*, "Improved pain relief with burst spinal cord stimulation for two weeks in patients using tonic stimulation: Results from a small clinical study," *Neuromodulation*, vol. 18, 2015.

(28) T. Deer, K. V. Slavin *et al.*, "Success using neuromodulation with burst (sunburst) study: Results from a prospective, randomized controlled trial using a novel burst waveform," *Neuromodulation*, vol. 21, 2018.

(29) G. Niso, M. C. Tjepkema-Cloostermans *et al.*, "Modulation of the somatosensory evoked potential by attention and spinal cord stimulation," *Frontiers in Neurology*, vol. 12, 2021.

(30) S. Ramaswamy and T. Wodehouse, "Conditioned pain modulation-a comprehensive review," *Neurophysiol. Clin.-Clin. Neurophysiol.*, vol. 51, no. 3, pp. 197–208, 2021.

(31) D. L. Kennedy, H. I. Kemp *et al.*, "Reliability of conditioned pain modulation: a systematic review," *Pain*, vol. 157, no. 11, p. 2410–2419, 2016.

(32) R. R. Nir and D. Yarnitsky, "Conditioned pain modulation," no. 1751-4266 (Electronic), 2015.

(33) L. Yarnitsky D Fau Arendt-Nielsen, D. Arendt-Nielsen L Fau Bouhassira *et al.*, "Recommendations on terminology and practice of psychophysical dnic testing," *European journal of pain (London, England)*, vol. 14, no. 4, p. 339, 2010.

(34) D. Le Bars, J.-M. Dickenson Ah Fau Besson, and J. M. Besson, "Diffuse noxious inhibitory controls (dnic). i. effects on dorsal horn convergent neurones in the rat," *Pain*, vol. 6, no. 3, p. 283–304, 1979.

(35) M. A.-O. Kucharczyk, D. A.-O. Valiente, and K. A.-O. Bannister, "Developments in understanding diffuse noxious inhibitory controls: Pharmacological evidence from pre-clinical research," *Journal of pain research*, vol. 14, p. 1083–1095, 2021.

(36) G. Pickering, B. Pereira *et al.*, "Impaired modulation of pain in patients with postherpetic neuralgia," *Pain Res Manage*, vol. 19, no. 1, pp. e19–e23, 2014.

(37) B. Yarnitsky, C. Crispel *et al.*, "Prediction of chronic post-operative pain: pre-operative dnic testing identifies patients at risk," *Pain*, vol. 138, no. 1, pp. 22–29, 2008.

(38) S. P. Singh, "Magnetoencephalography: Basic principles," *Annals of Indian Academy of Neurology*, vol. 17, no. suppl 1, p. S107–S112, 2014.

(39) P. Volegov, M. A. Matlachov An Fau Espy *et al.*, "Simultaneous magnetoencephalography and squid detected nuclear mr in microtesla magnetic fields," *Magnetic resonance in medicine*, vol. 52, no. 3, p. 467–470, 2004.

(40) M. Ploner and E. S. May, "Electroencephalography and magnetoencephalography in pain research—current state and future perspectives." *PAIN*, vol. 159, pp. 206–211, 2018.

(41) R. Hari, S. Baillet *et al.*, "Ifcn-endorsed practical guidelines for clinical magnetoencephalography (meg)," *Clinical neurophysiology : official journal of the International Federation of Clinical Neurophysiology*, vol. 129, no. 8, p. 1720–1747, 2018.

(42) B. J. Baars and N. M. Gage, "Chapter 4 - the tools: Imaging the living brain," in *Cognition, Brain, and Consciousness (Second Edition)*, second edition ed., B. J. Baars and N. M. Gage, Eds. London: Academic Press, 2010, pp. 94–125. [Online]. Available: https://www.sciencedirect.com/science/article/pii/B9780123750709000048

(43) N. Vukovic, "Illustration of a piece of cortex showing the cross-section of a gyrus and upper layer of nerve cells," figshare, 2014. [Online]. Avail-

able: https://figshare.com/articles/figure/Illustration_of_a_piece_of_cortex_showing_the_cross_section_of_a_gyrus_and_upper_layer_of_nerve_cells/1217586

(44) O. David, J. M. Kilner, and K. J. Friston, "Mechanisms of evoked and induced responses in meg/eeg," *NeuroImage*, vol. 31, 2006.

(45) G. Pfurtscheller and F. H. L. D. Silva, "Event-related eeg/meg synchronization and desynchronization: Basic principles," *Clinical Neurophysiology*, vol. 110, 1999.

(46) C. Neuper and G. Pfurtscheller, "Event-related dynamics of cortical rhythms: Frequency-specific features and functional correlates," *International Journal of Psychophysiology*, vol. 43, 2001.

(47) M. Ploner, J. Gross *et al.*, "Pain suppresses spontaneous brain rhythms," *Cerebral Cortex*, vol. 16, 2006.

(48) M. Diers, C. C. de Vos *et al.*, "Induced oscillatory signaling in the beta frequency of top-down pain modulation," *Pain Reports*, vol. 5, 2020.

(49) H. Jin, "Conditioned pain modulation analgesia reduces beta oscillations in the sensorimotor cortex." MSc Thesis, 2021.

(50) F. Tadel, S. Baillet *et al.*, "Brainstorm: A user-friendly application for meg/eeg analysis," p. 13, 2011.

(51) Francois Tadel and Elizabeth Bock and John C Mosher and Richard Leahy and Sylvain Baillet, "Head modeling," Brainstorm. [Online]. Available: https://neuroimage.usc.edu/brainstorm/Tutorials/HeadModel#Forward_model

(52) C. Destrieux, "Destrieux atlas changes," 2009.

(53) L. Hermans, J. V. Oosterwijck *et al.*, "Inventory of personal factors influencing conditioned pain modulation in healthy people: A systematic literature review," *Pain Practice*, vol. 16, 2016.

(54) G. N. Lewis, D. A. Rice, and P. J. McNair, "Conditioned pain modulation in populations with chronic pain: A systematic review and meta-analysis," *Journal of Pain*, vol. 13, 2012.

(55) S. Schuh-Hofer, J. Fischer *et al.*, "Spinal cord stimulation modulates descending pain inhibition and temporal summation of pricking pain in patients with neuropathic pain," *Acta Neurochirurgica*, vol. 160, 2018.

(56) C. H. Meyer-Frießem, T. Wiegand *et al.*, "Effects of spinal cord and peripheral nerve stimulation reflected in sensory profiles and endogenous pain modulation," *Clinical Journal of Pain*, vol. 35, 2019.

(57) S. Ramaswamy, T. Wodehouse *et al.*, "Characterizing the somatosensory profile of patients with failed back surgery syndrome with unilateral lumbar radiculopathy undergoing spinal cord stimulation: A single center prospective pilot study," *Neuromodulation*, vol. 22, 2019.

(58) L. Goudman, R. Brouns *et al.*, "Association between spinal cord stimulation and top-down nociceptive inhibition in people with failed back surgery syndrome: A cohort study," *Physical Therapy*, vol. 99, 2019.

(59) N. Kriek, C. C. de Vos *et al.*, "Allodynia, hyperalgesia, (quantitative) sensory testing and conditioned pain modulation in patients with complex regional pain syndrome before and after spinal cord stimulation therapy," *Neuromodulation: Technology at the Neural Interface*, 2022.

(60) M. Ploner, F. Schmitz *et al.*, "Parallel activation of primary and secondary somatosensory cortices in human pain processing," *Journal of Neurophysiology*, vol. 81, 1999.

(61) R. C. Coghill, J. D. Talbot *et al.*, "Distributed processing of pain and vibration by the human brain," *Journal of Neuroscience*, vol. 14, 1994.

(62) K. L. Casey, S. Minoshima *et al.*, "Comparison of human cerebral activation patterns during cutaneous warmth, heat pain, and deep cold pain," *Journal of Neurophysiology*, vol. 76, 1996.

(63) J. D. Talbot, S. Marret *et al.*, "Multiple representations of pain in human cerebral cortex," *Science*, vol. 251, 1991.

(64) S. F. Worthen, A. R. Hobson *et al.*, "Primary and secondary somatosensory cortex responses to anticipation and pain: A magnetoencephalography study," *European Journal of Neuroscience*, vol. 33, 2011.

(65) A. R. Hobson, P. L. Furlong *et al.*, "Real-time imaging of human cortical activity evoked by painful esophageal stimulation," *Gastroenterology*, vol. 128, 2005.

(66) "Functional organization of the human first and second somatosensory cortices: a neuromagnetic study," *European Journal of Neuroscience*, vol. 5, 1993.

(67) T. Allison, G. McCarthy *et al.*, "Human cortical potentials evoked by stimulation of the median nerve. ii. cytoarchitectonic areas generating long-latency activity," *Journal of Neurophysiology*, vol. 62, 1989.

(68) W. Gaetz and D. Cheyne, "Localization of sensorimotor cortical rhythms induced by tactile stimulation using spatially filtered meg," *NeuroImage*, vol. 30, 2006.

(69) N. Rustamov, A. Wagenaar-Tison *et al.*, "Electrophysiological investigation of the contribution of attention to altered pain inhibition processes in patients with irritable bowel syndrome," *J Physiol Sci*, vol. 70, no. 1, p. 46, 2020.

(70) S. Albu and M. W. Meagher, "Divergent effects of conditioned pain modulation on subjective pain and nociceptive-related brain activity," *Exp Brain Res*, vol. 237, no. 7, pp. 1735–1744, 2019.

(71) L. Plaghki, D. Delisle, and J. M. Godfraind, "Heterotopic nociceptive conditioning stimuli and mental task modulate differently the perception and physiological correlates of short co2 laser stimuli," *PAIN*, vol. 57, no. 2, pp. 181–192, 1994.

(72) L. Tiemann, E. S. May *et al.*, "Differential neurophysiological correlates of bottom-up and top-down modulations of pain," *Pain*, vol. 156, 2015.

(73) M. Hauck, J. Lorenz, and A. K. Engel, "Attention to painful stimulation enhances gamma-band activity and synchronization in human sensorimotor cortex," *The Journal of neuroscience : the official journal of the Society for Neuroscience*, vol. 27, no. 35, pp. 9270–9277, 2007.

(74) S. Ohara, N. E. Crone *et al.*, "Attention to a painful cutaneous laser stimulus modulates electrocorticographic event-related desynchronization in humans," *Clinical Neurophysiology*, vol. 115, 2004.

(75) D. D. Ridder, M. Plazier *et al.*, "Burst spinal cord stimulation for limb and back pain," *World Neurosurgery*, vol. 80, 2013.

(76) F. Tadel, *et al.*, "Tutorial 24: Time-frequency," Brainstorm, 2018, accessed 4 November 2020. [Online]. Available: https://neuroimage.usc.edu/brainstorm/Tutorials/TimeFrequency

(77) L. Eitner, S. Özgül *et al.*, "Conditioned pain modulation using painful cutaneous electrical stimulation or simply habituation?" *Eur J Pain*, vol. 22, no. 7, pp. 1281–1290, 2018.

(78) P. Goffaux, W. J. Redmond *et al.*, "Descending analgesia - when the spine echoes what the brain expects," *Pain*, vol. 130, no. 1-2, pp. 137–143, 2007.

(79) A. Reinert, R. D. Treede, and B. Bromm, "The pain inhibiting pain effect: an electrophysiological study in humans," *Brain Res*, vol. 862, no. 1-2, pp. 103–110, 2000.

(80) R. Dowman, "Pain-evoked anterior cingulate activity generating the negative difference potential may reflect response selection processes," *Psychophysiology*, vol. 39, no. 3, pp. 369–379, 2002.

(81) R. Moont, Y. Crispel *et al.*, "Temporal changes in cortical activation during distraction from pain: A comparative loreta study with conditioned pain modulation," *Brain Res*, vol. 1435, pp. 105–117, 2012.

(82) A. Ladouceur, N. Rustamov *et al.*, "Inhibition of pain and pain-related brain activity by heterotopic noxious counter-stimulation and selective attention in chronic non-specific low back pain," *Neuroscience*, vol. 387, pp. 201–213, 2018.

(83) A. T. L. Do, E. K. Enax-Krumova *et al.*, "Distraction by a cognitive task has a higher impact on electrophysiological measures compared with conditioned pain modulation," *BMC Neurosci*, vol. 21, no. 1, 2020.

(84) Y. Oono, H. Nie *et al.*, "The inter- and intra-individual variance in descending pain modulation evoked by different conditioning stimuli in healthy men," *Scandinavian Journal of Pain*, vol. 2, 2011.

(85) H. B. Vaegter, K. K. Petersen *et al.*, "Assessment of cpm reliability: Quantification of the within-subject reliability of 10 different protocols," *Scandinavian Journal of Pain*, vol. 18, 2018.

(86) C. T. Yen and P. L. Lu, "Thalamus and pain," *Acta Anaesthesiologica Taiwanica*, vol. 51, 2013.

(87) D. G. Owen, Y. Bureau *et al.*, "Quantification of pain-induced changes in cerebral blood flow by perfusion mri," *Pain*, vol. 136, 2008.

(88) G. Wagner, M. Koschke *et al.*, "Reduced heat pain thresholds after sad-mood induction are associated with changes in thalamic activity," *Neuropsychologia*, vol. 47, 2009.

(89) C. M. Cahill and P. W. Stroman, "Mapping of neural activity produced by thermal pain in the healthy human spinal cord and brain stem: A functional magnetic resonance imaging study," *Magnetic Resonance Imaging*, vol. 29, 2011.

(90) U. Friebel, S. B. Eickhoff, and M. Lotze, "Coordinate-based meta-analysis of experimentally induced and chronic persistent neuropathic pain," *NeuroImage*, vol. 58, 2011.

(91) H. Bastuji, M. Frot *et al.*, "Thalamic responses to nociceptive-specific input in humans: Functional dichotomies and thalamo-cortical connectivity," *Cerebral Cortex*, vol. 26, 2016.

(92) F. Pizzo, N. Roehri *et al.*, "Deep brain activities can be detected with magnetoencephalography," *Nature Communications*, vol. 10, 2019.

(93) Y. Attal and D. Schwartz, "Assessment of subcortical source localization using deep brain activity imaging model with minimum norm operators: A meg study," *PLoS ONE*, vol. 8, 2013.

(94) "Meg evidence for dynamic amygdala modulations by gaze and facial emotions," *PLoS ONE*, vol. 8, 2013.

(95) F. Rehab and A. Tran, "Damage to the thalamus: Understanding the side effects and recovery process," Flint Rehab, tools to spark recovery, 2021, accessed 17 November 2022. [Online]. Available: https://www.flintrehab.com/thalamus-damage/

(96) E. A. Necka, I. S. Lee *et al.*, "Applications of dynamic functional connectivity to pain and its modulation," *Pain Reports*, vol. 4, 2019.

(97) H. Shahabi, R. Cassani *et al.*, "Connectivity," Brainstorm, 2022, accessed 17 November 2022. [Online]. Available: https://neuroimage.usc.edu/brainstorm/Tutorials/Connectivity

Appendices

A. Pre-processing of MEG recordings
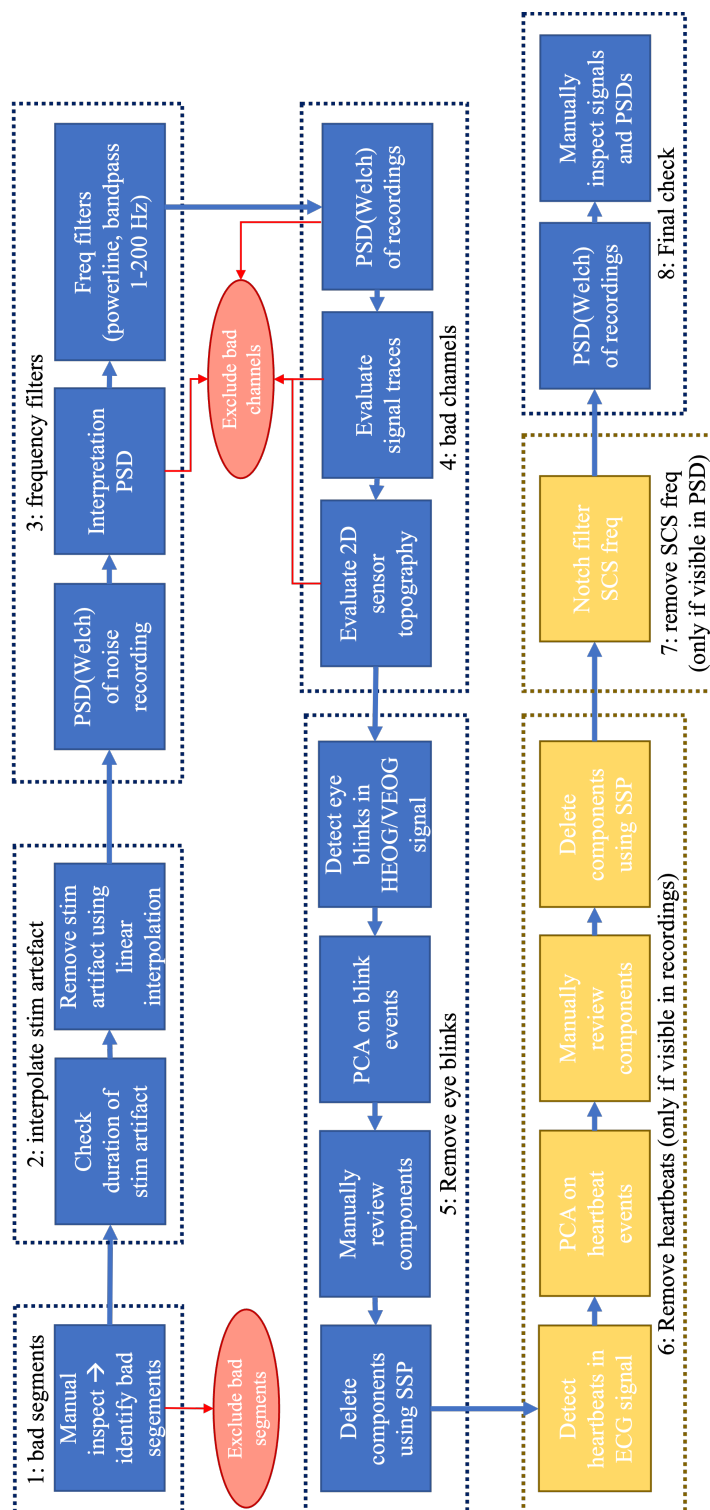
Figure 14: *Steps of pre-processing the raw MEG recordings*

B. Region of interests

The response in multiple ROIs was evaluated. Figure 15 displays an overview of the projections of all ROIs on the source map.

(a) *S1 left hemisphere, view from above*

(b) *S1 left hemisphere, view from side*

(c) *S1 right hemisphere, view from above*

(d) *S1 right hemisphere, view from side*
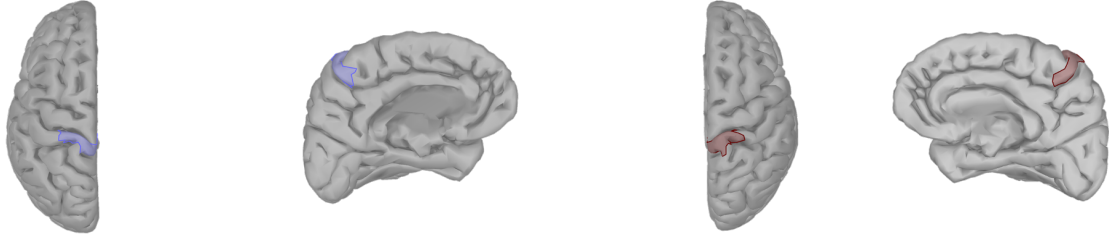
(e) *M1 left hemisphere, view from above*

(f) *M1 left hemisphere, view from side*

(g) *M1 right hemisphere, view from above*

(h) *M1 right hemisphere, view from side*
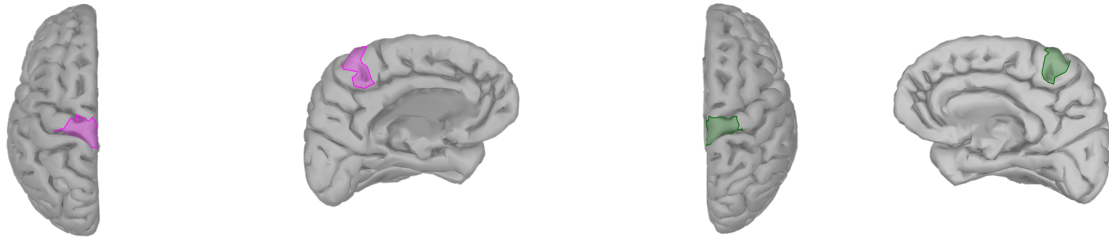
(i) *SMA left hemisphere, view from above*

(j) *SMA left hemisphere, view from side*

(k) *SMA right hemisphere, view from above*

(l) *SMA right hemisphere, view from side*
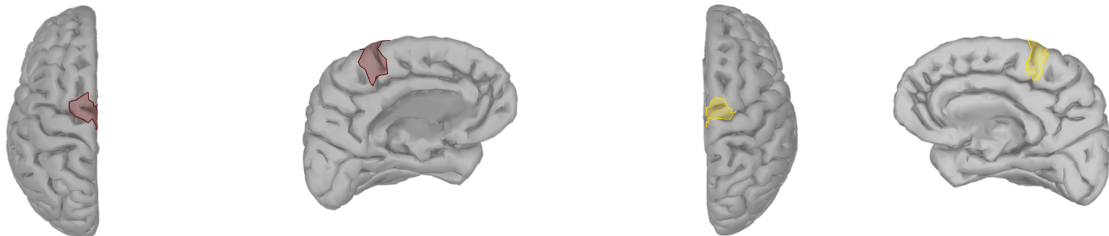
(m) *S2 left hemisphere*

(n) *S2 right hemisphere*

(o) *Superior parietal lobule left hemisphere*

(p) *Superior parietal lobule right hemisphere*

(q) *ACC left hemisphere* (r) *ACC right hemisphere* (s) *MCC left hemisphere* (t) *MCC right hemisphere*

(u) *PCC left hemisphere* (v) *PCC right hemisphere* (w) *DLPFC left hemisphere* (x) *DLPFC right hemisphere*

(y) *OFC left hemisphere* (z) *OFC right hemisphere* () *Insula left hemisphere* () *Insula right hemisphere*
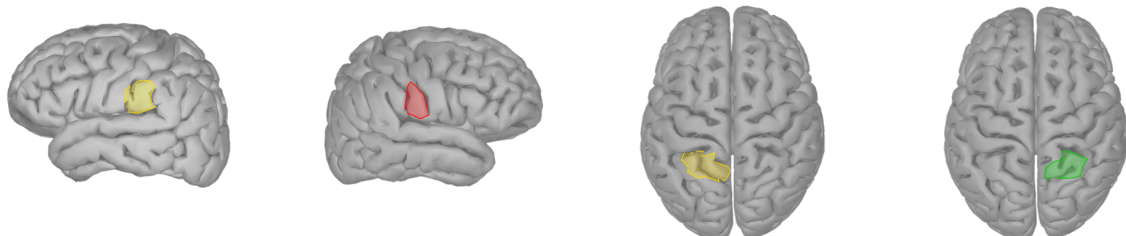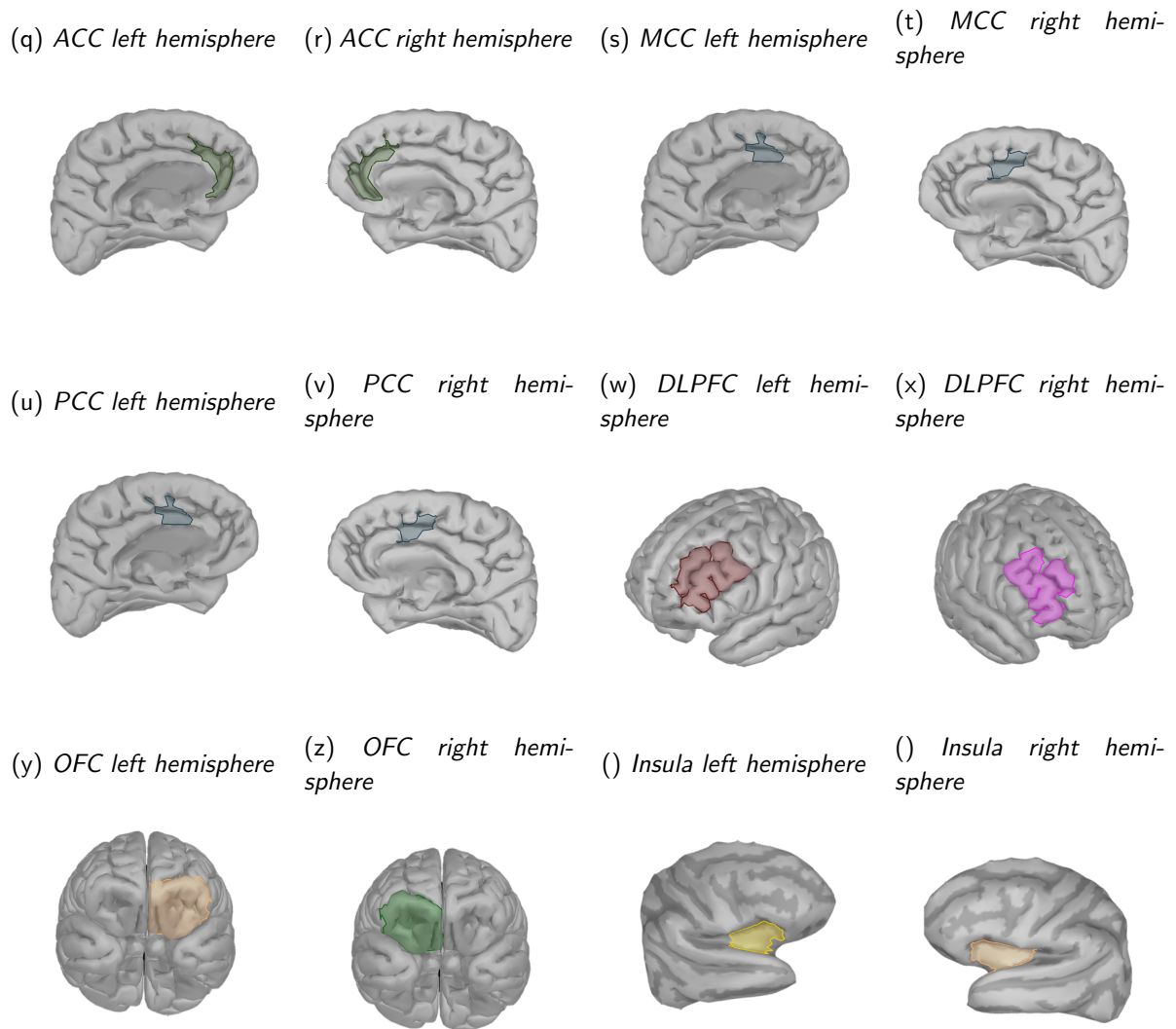
Figure 15: *All regions of interest (ROIs), projected on the source map, in which the response to TS was evaluated.*

C. Cortical response in the time domain

C.1 Cortical activation patterns

Figure 16 shows the cortical activation pattern evoked by TS on a source map *before, during* and *after* CPM. During all conditions first activity is observed in the S1, M1 and SMA in mainly the left hemisphere. Around 120 ms post stimulus activity is observed in the S2. No statistical analysis was performed to compare the different CPM conditions.
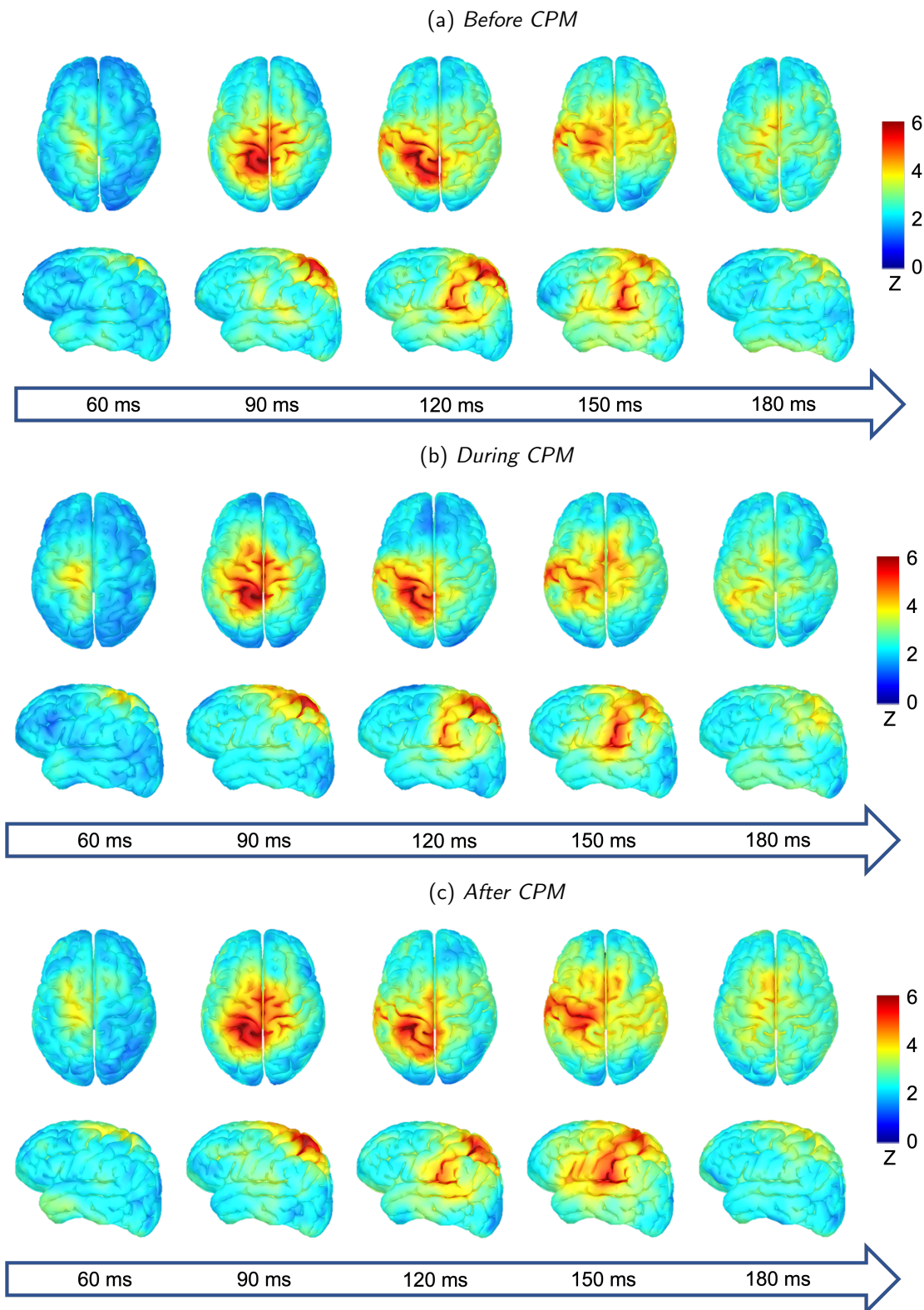
Figure 16: *Source map showing the cortical response in the time domain to a nociceptive stimulus (TS) applied at the right sural nerve, expressed in z-scores relative to the baseline. The response is displayed per CPM condition, averaged over all subjects and stimulation modes. At t = 0 TS is applied, the primary somatosensory cortices (S1, S2), primary motor cortex (M1) and supplementary motor area (SMA) show increased activity between 60 till 180 ms post stimulus. View from above and view on the left hemisphere.*

C.2   Extracted time series per ROI

Figure 17 shows the extracted time series of several ROIs *before, during* and *after* CPM. The amplitude seems to be lower *during* CPM in the left S2, the bilateral ACC and the right insula, although this was not confirmed by statistical analysis.

(a) *Bilateral sensorimotor cortices*
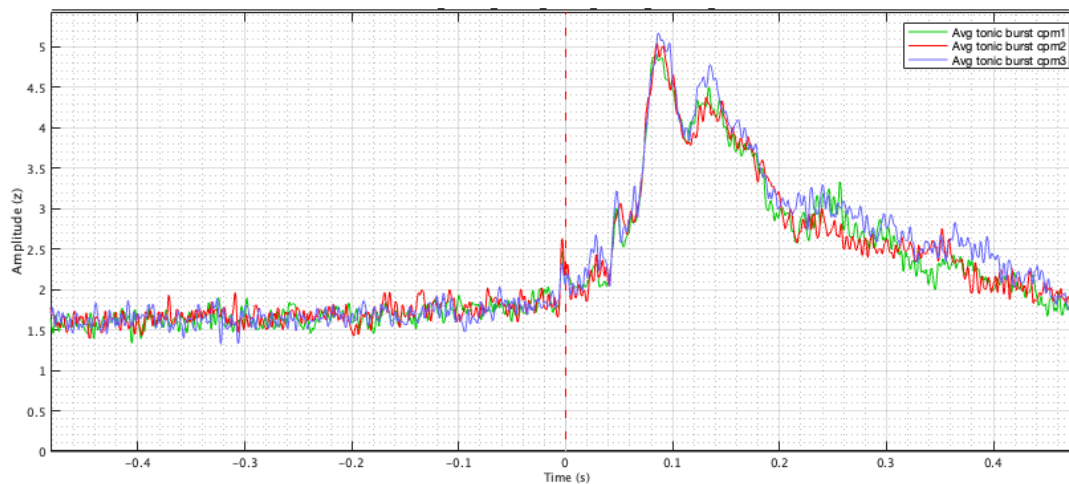
(b) *Left S2*
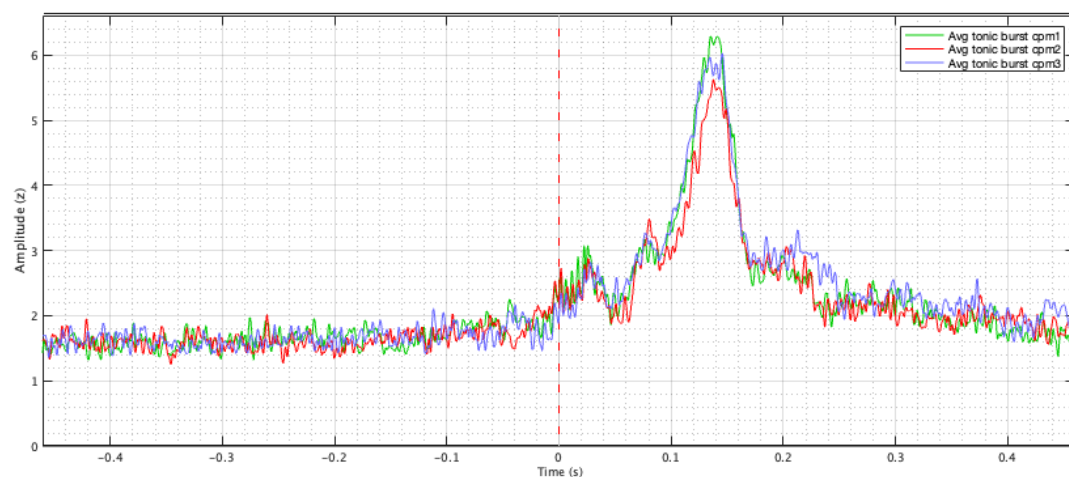
(c) *Bilateral ACC*
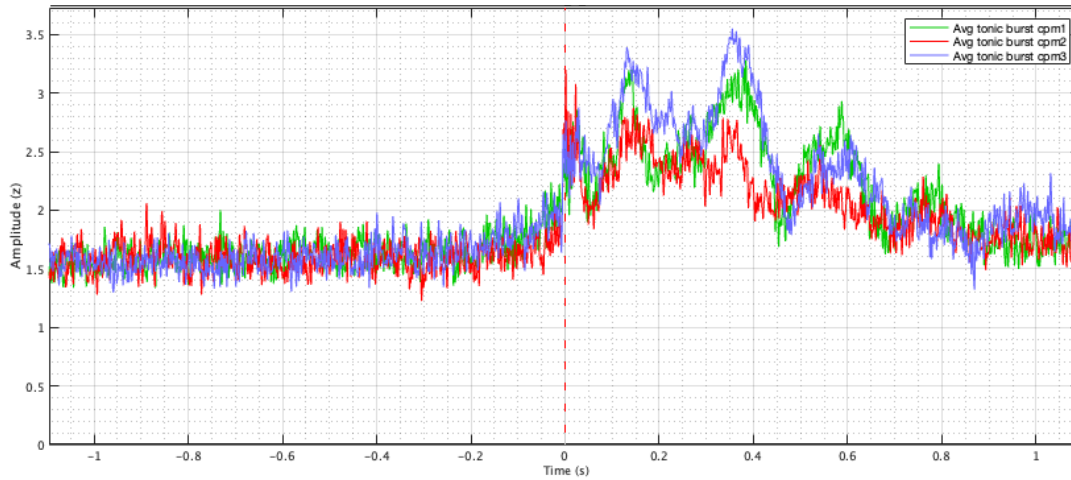
(d) *Right insula*
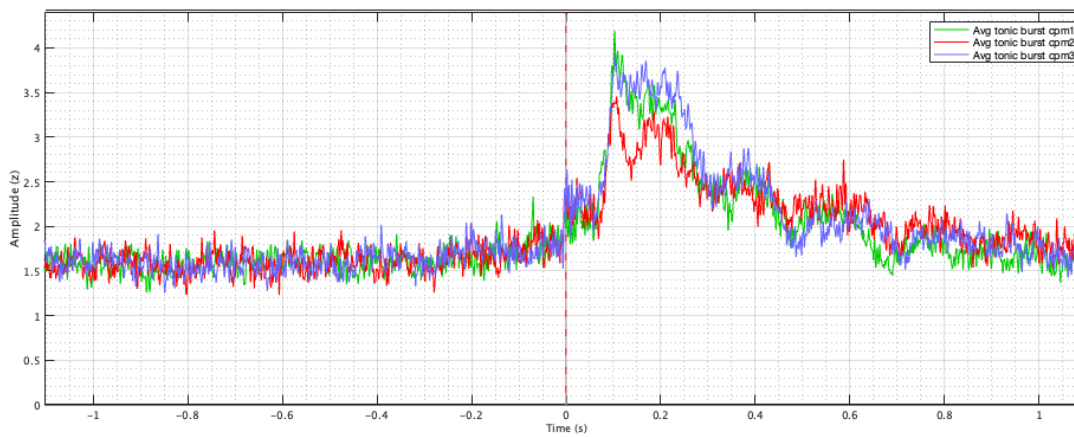
Figure 17: *Extracted time series before (cpm1, green line), during (cpm2, red line) and after (cpm3, blue line) CPM for ROIs: the bilateral sensorimotor cortices (S1, M1, SMA), the left secondary somatosensory cortex (S2), the bilateral anterior cingulate cortices (ACC) and the right insula. At t=0 the nociceptive test stimulus (TS) is applied. Note the different time and amplitude ranges on the x- and y-axes. Also note that the response is the norm of three orientations, resulting in only positive values for the amplitude, meaning that negative deflections of the evoked response are expressed as positive values.*

D. Determine start and end time ERSP

The start and end times of each ERSP were calculated using the averaged TF map of all subjects and conditions per ROI. From this averaged TF the time series was extracted per ROI. The time range of the ERD was marked when the z-score was smaller than 0.4. The time range of the ERS was marked when the z-score was larger than 0.4. Figure 18 displays the time series of the beta frequency range for the ROI of the S1, M1 and SMA of both hemispheres. The time range for the ERD was defined where the power was below the threshold of 0.4. The time range for the ERS was defined where the power was above the threshold of 0.4.
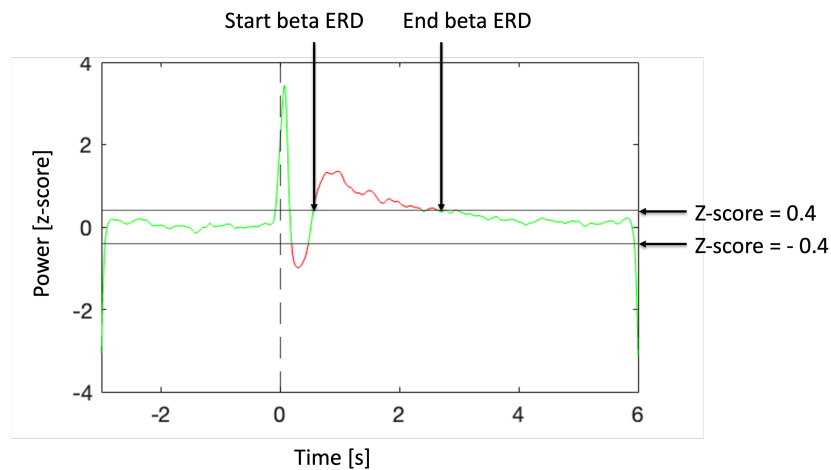
Figure 18: *Averaged time series of the power in the beta frequency range of all subjects and conditions in the bilateral sensorimotor cortices. At t = 0 the nociceptive stimulus is given. First event related desynchronization (ERD) is observed, followed by event related synchronization (ERS). The time range for ERD and ERS are defined where the power is respectively below or above the threshold for the z-score of +/- 0.4.*

E. Overview start and end times per ERSP per ROI

Table 5 displays the start and end times of each ERSP per ROI.

ROI	Alpha ERD Start time [s]	Alpha ERD End time [s]	Alpha ERS Start time [s]	Alpha ERS End time [s]	Beta ERD Start time [s]	Beta ERD End time [s]	Beta ERS Start time [s]	Beta ERS End time [s]
S1, M1, SMA bilateral	0.34	0.66	0.89	5.02	0.19	0.47	0.55	2.96
S1, M1, SMA left	0.34	0.65	0.84	3.34	0.18	0.47	0.54	3.03
S1, M1, SMA right	0.35	0.67	0.93	5.04	0.20	0.47	0.57	2.35
S1 left	0.32	0.69	0.91	3.26	0.18	0.48	0.55	3.02
S1 right	0.32	0.72	0.99	5.06	0.19	0.49	0.58	2.95
M1 left	0.33	0.66	0.82	5.05	0.18	0.47	0.54	3.08
M1 right	0.35	0.69	0.90	5.06	0.20	0.48	0.58	2.35
SMA left	0.37	0.58	0.73	3.40	0.19	0.44	0.53	3.02
SMA right	0.41	0.60	0.88	3.72	0.20	0.45	0.55	2.26
S2 left	0.34	0.59	0.72	2.33	0.17	0.48	0.62	1.95
S2 right	0.39	0.54	0.79	1.77	0.20	0.46	0.60	1.88
Superior parietal lobule left	0.29	0.74	1.00	3.02	0.17	0.50	0.59	2.99
Superior parietal lobule right	0.33	0.78	1.11	5.00	0.19	0.51	0.69	1.77
Insula left	-	-	0.61	1.94	0.25	0.32	0.57	1.24
Insula right	0.37	0.55	1.36	2.23	0.23	0.34	0.60	1.84
ACC bilateral	0.42	0.52	1.04	2.60	-	-	0.62	1.16
MCC bilateral	0.38	0.58	0.92	2.48	0.21	0.39	0.56	1.87
PCC bilateral	0.35	0.62	0.95	5.12	0.19	0.46	0.56	2.23
ACC, MCC bilateral	0.40	0.55	0.99	2.57	0.26	0.31	0.60	1.58
ACC, MCC, PCC bilateral	0.38	0.57	0.97	2.64	0.22	0.37	0.58	1.61
DLPFC left	-	-	0.68	2.21	-	-	0.59	1.57
DLPFC rigth	0.45	0.52	1.36	1.57	0.27	0.35	0.62	1.11
OFC left	-	-	-	-	-	-	-	-
OFC right	0.41	0.48	2.03	2.16	-	-	-	-

Table 5: *The start and end times of each ERSP per ROI. - = no z-score above or below the ERSP threshold of 0.4 is detected.*

F. Power of event related spectral perturbations for all regions of interest

The following pages contain an overview of the average power of each ERSP (alpha ERD, alpha ERS, beta ERD, beta ERS) for each investigated ROI *before, during* and *after* CPM. The frequency ranges used to determine the average power are 8 till 12 Hz for alpha activity and 13 till 30 Hz for beta activity. The time ranges, used to determine the average power, are defined by applying a threshold of 0.4 to the response in the ROI averaged over all subjects, stimulation modes and conditions (Appendix D). If the threshold of 0.4 was not passed by the averaged response, no ERSP was detected and therefore no graph is displayed. None of the four ERSPs was detected in the ROI OFC of the left hemisphere, therefore no graphs are displayed for this ROI. The cortical response in the TF domain in the S1, M1 and SMA showed quite similar results, therefor in this appendix only the results of the combined ROIs (left, right and bilateral sensorimotor cortices) are displayed. The results of the S1, M1 and SMA separately can be provided by the author.
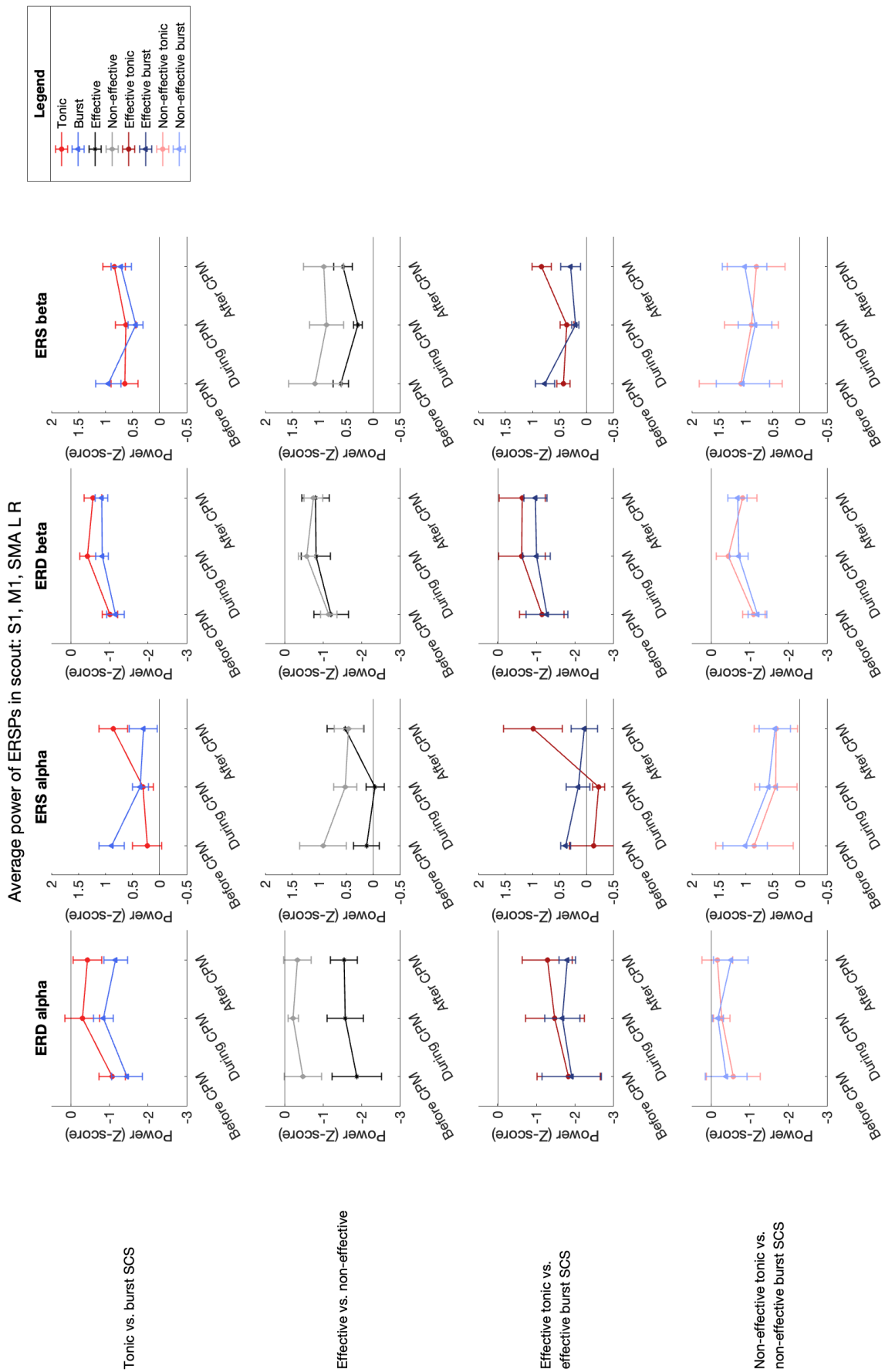
Figure 19: *Mean and standard error of average power [z-score] of alpha ERD, alpha ERS, beta ERD and beta ERS before, during and after CPM for the different groups in the ROI consisting of the S1, M1 and SMA of both hemispheres.*
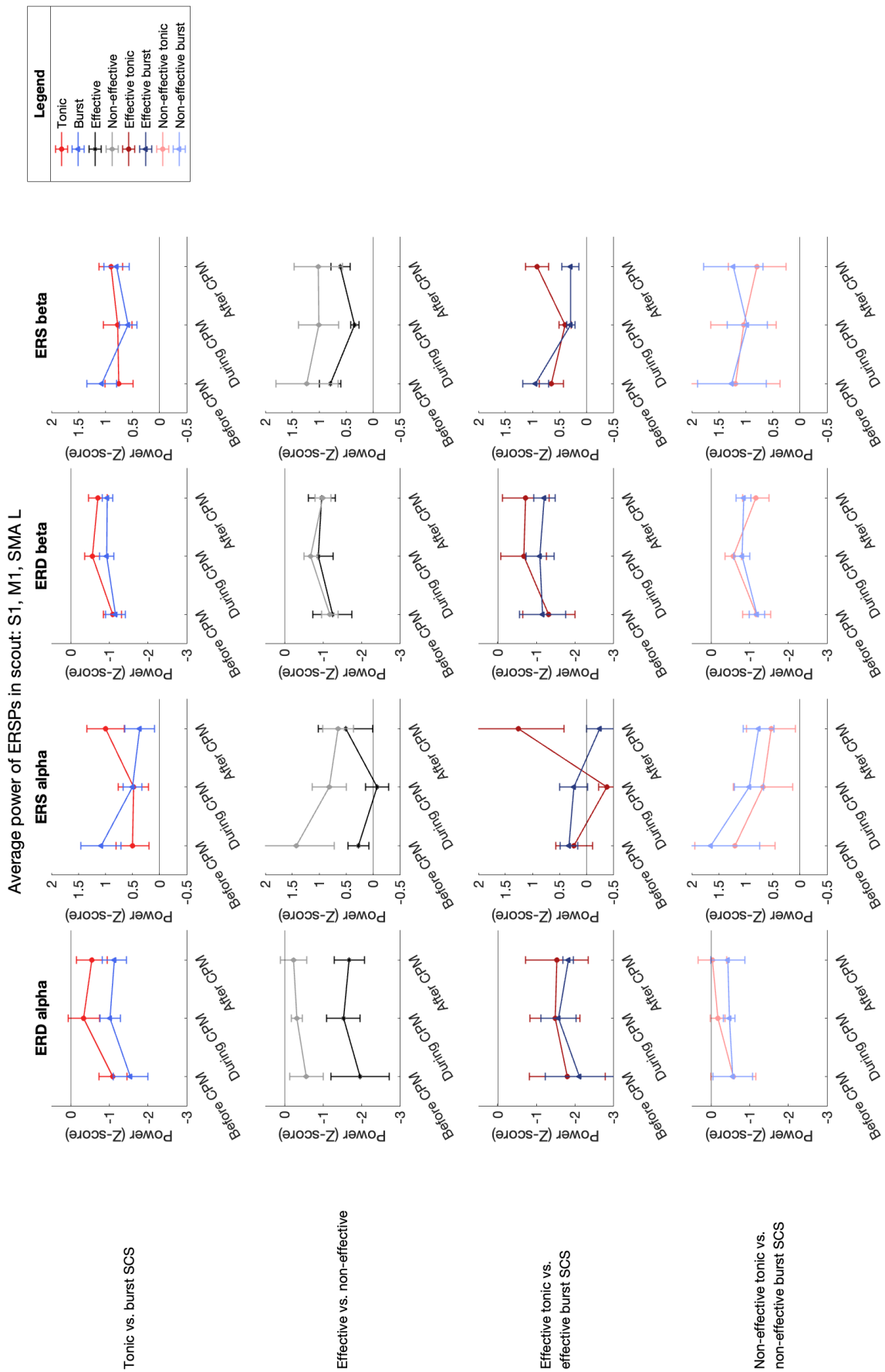
Figure 20: *Mean and standard error of average power [z-score] of alpha ERD, alpha ERS, beta ERD and beta ERS before, during and after CPM for the different groups in the ROI consisting of the S1, M1 and SMA of the left hemisphere.*
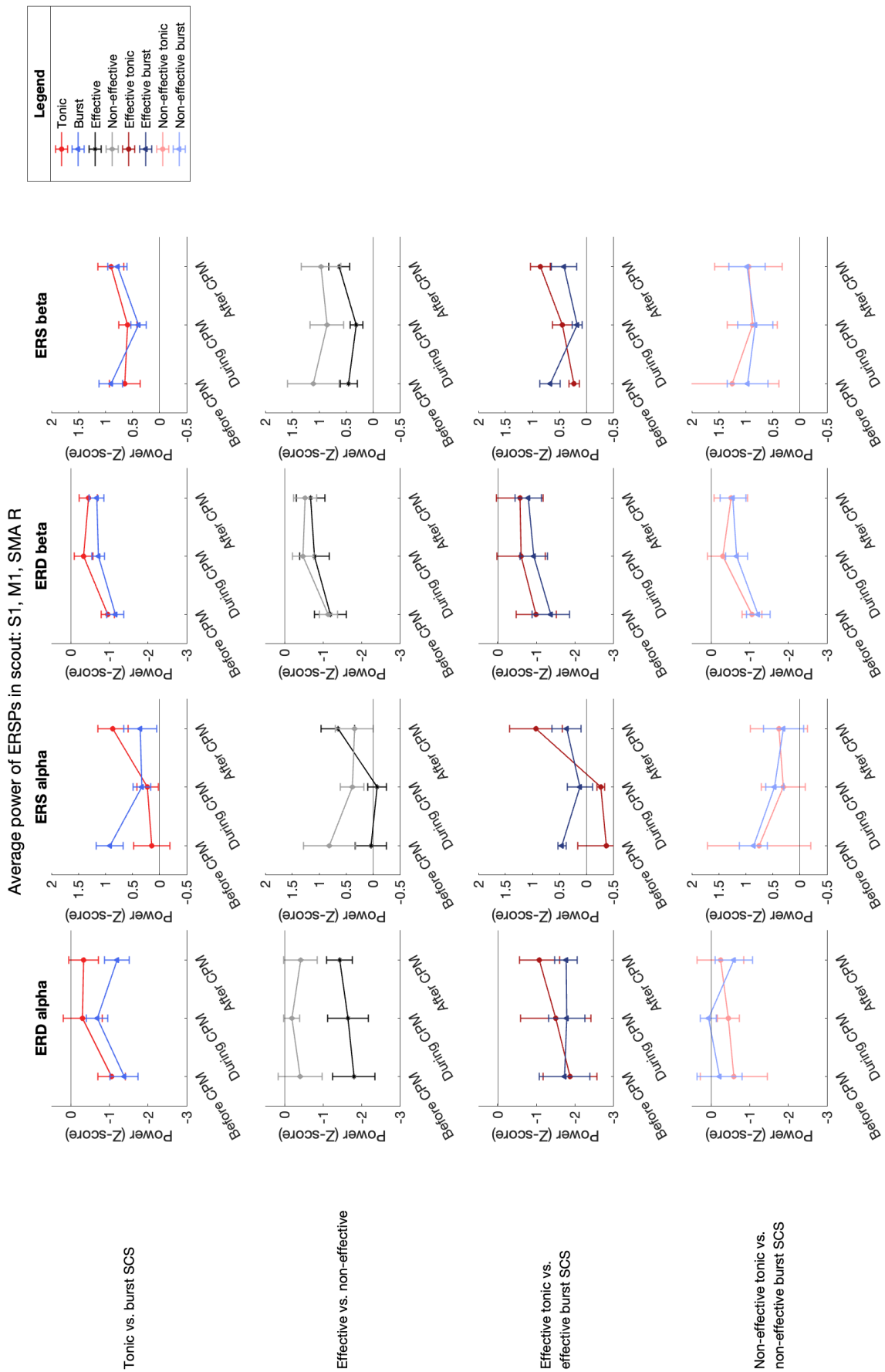
Figure 21: *Mean and standard error of average power [z-score] of alpha ERD, alpha ERS, beta ERD and beta ERS before, during and after CPM for the different groups in the ROI consisting of the S1, M1 and SMA of the right hemisphere.*
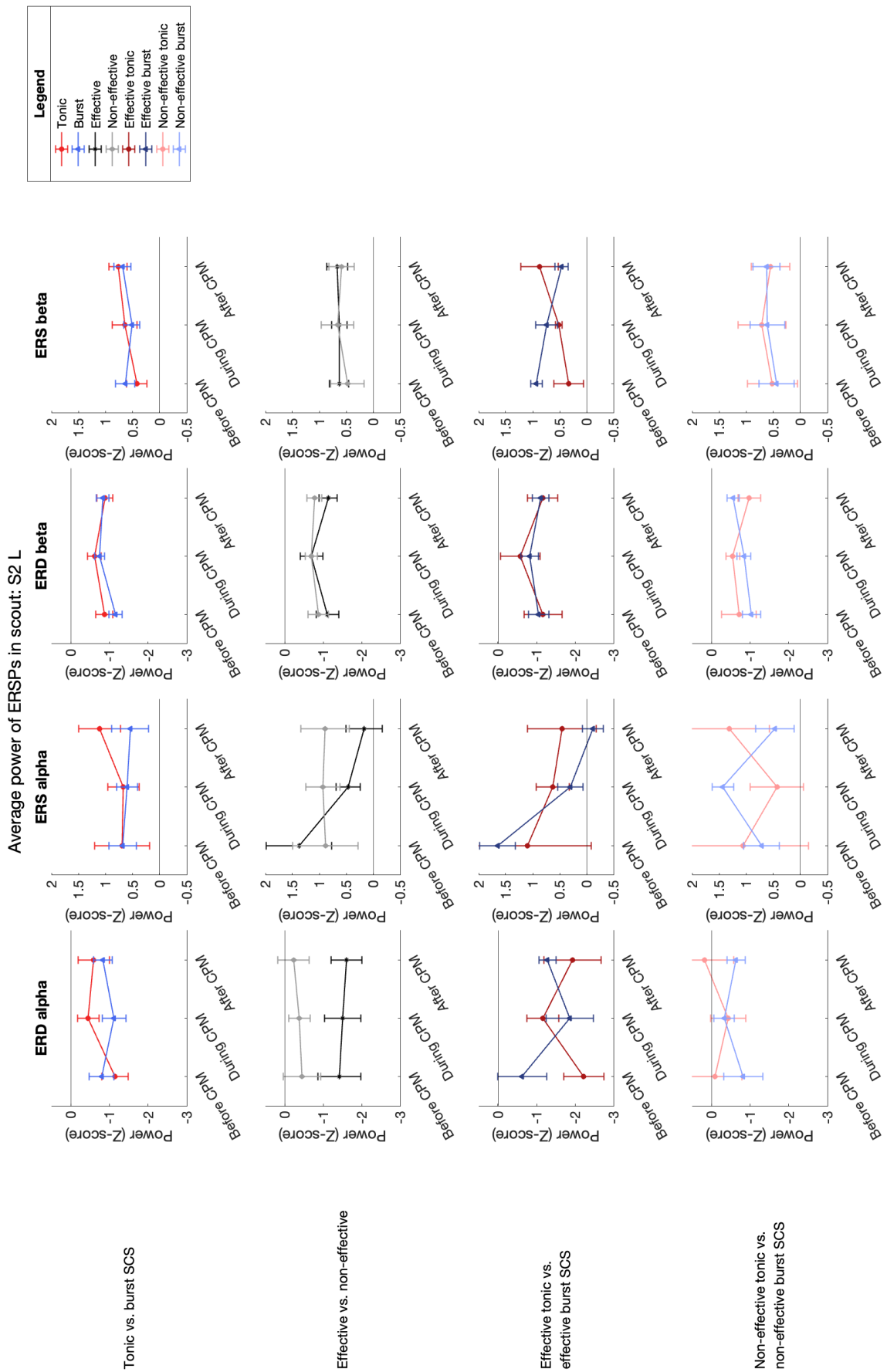
Figure 22: *Mean and standard error of average power [z-score] of alpha ERD, alpha ERS, beta ERD and beta ERS before, during and after CPM for the different groups in the ROI consisting of the S2 of the left hemisphere.*
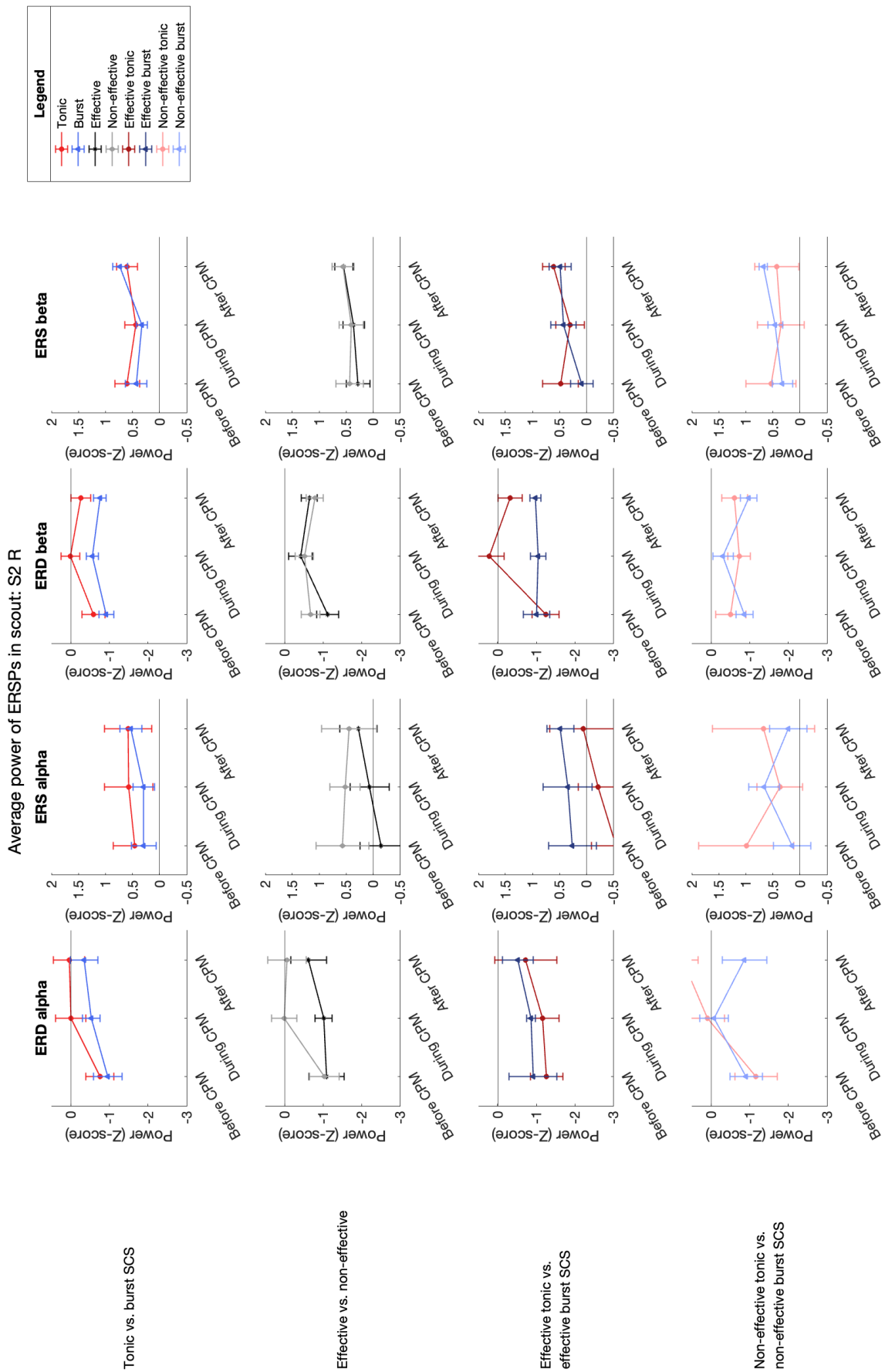
Figure 23: *Mean and standard error of average power [z-score] of alpha ERD, alpha ERS, beta ERD and beta ERS before, during and after CPM for the different groups in the ROI consisting of the S2 of the right hemisphere.*
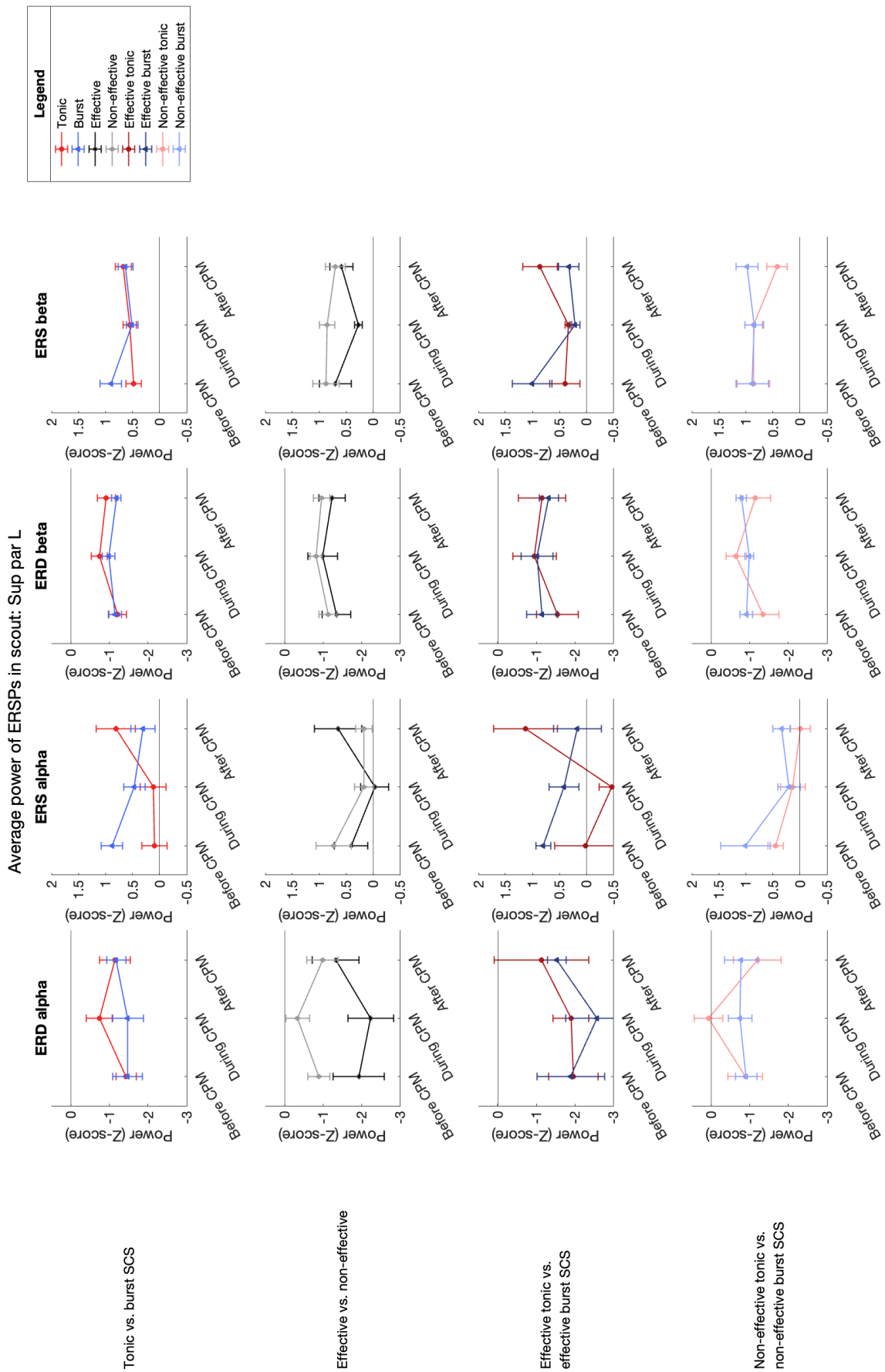
Figure 24: *Mean and standard error of average power [z-score] of alpha ERD, alpha ERS, beta ERD and beta ERS before, during and after CPM for the different groups in the ROI consisting of the superior parietal lobule of the left hemisphere.*
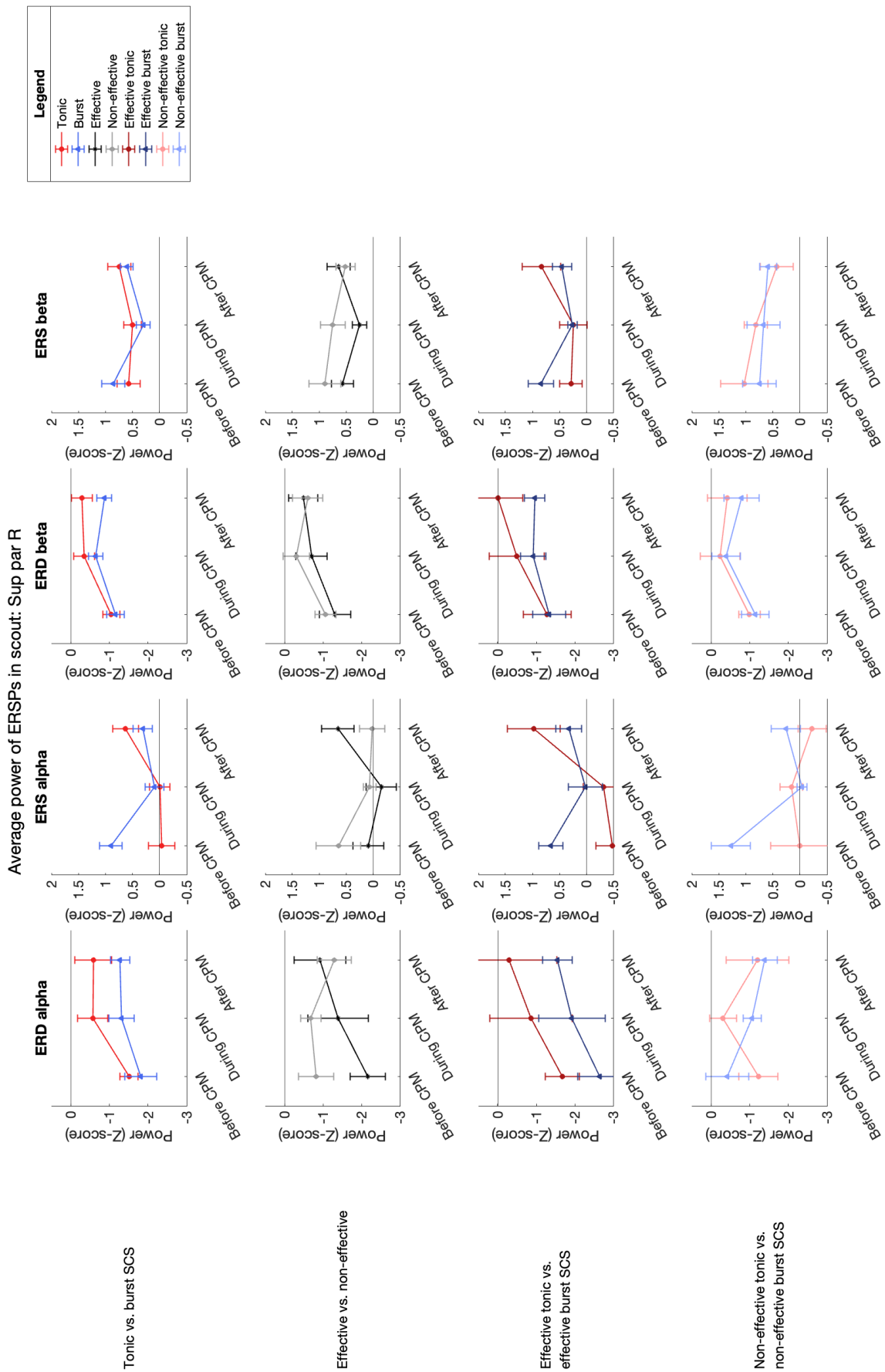
Figure 25: *Mean and standard error of average power [z-score] of alpha ERD, alpha ERS, beta ERD and beta ERS before, during and after CPM for the different groups in the ROI consisting of the superior parietal lobule of the right hemisphere.*
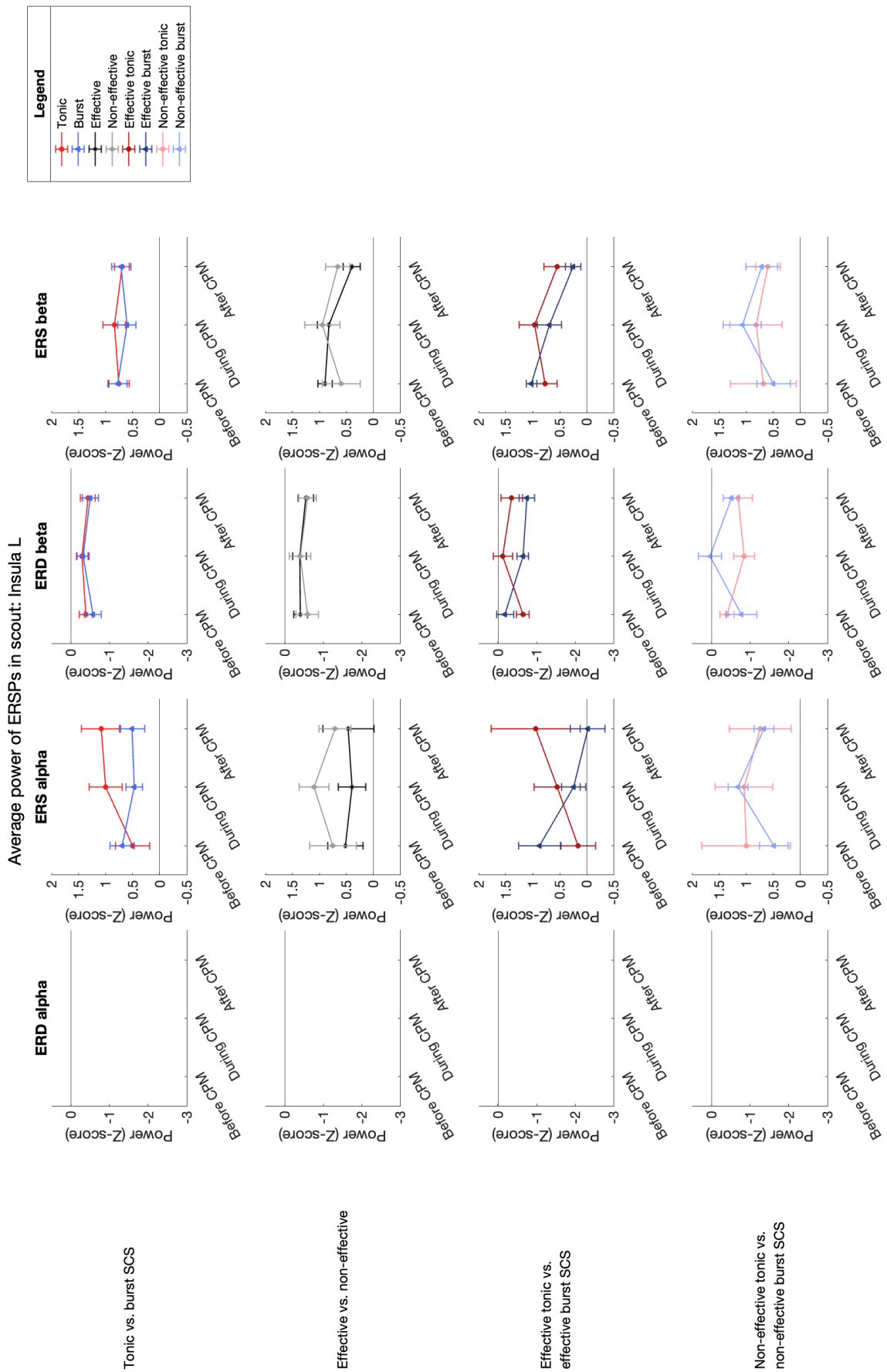
Figure 26: *Mean and standard error of average power [z-score] of alpha ERD, alpha ERS, beta ERD and beta ERS before, during and after CPM for the different groups in the ROI consisting of the insula of the left hemisphere.*
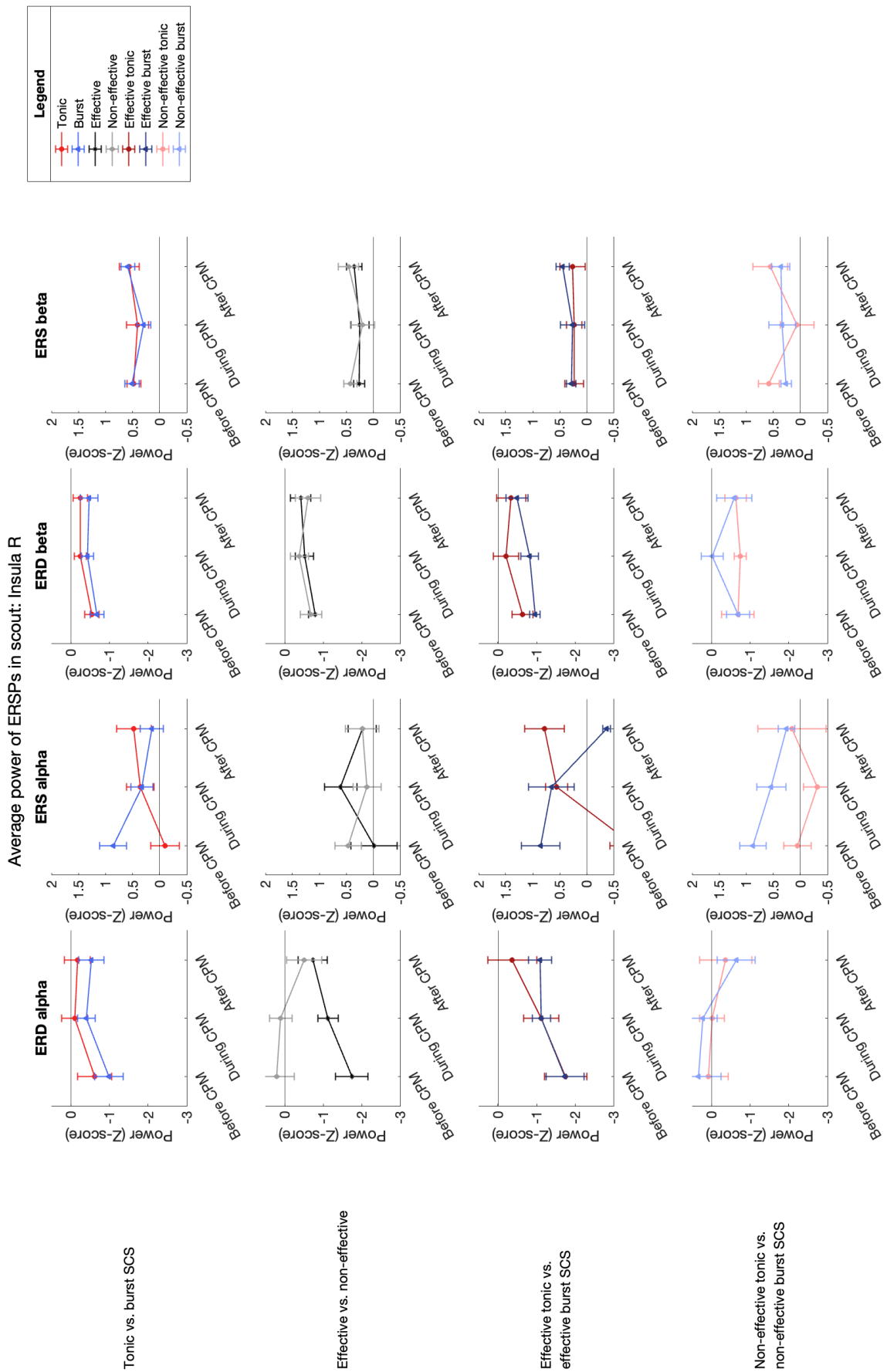
Figure 27: *Mean and standard error of average power [z-score] of alpha ERD, alpha ERS, beta ERD and beta ERS before, during and after CPM for the different groups in the ROI consisting of the insula of the right hemisphere.*
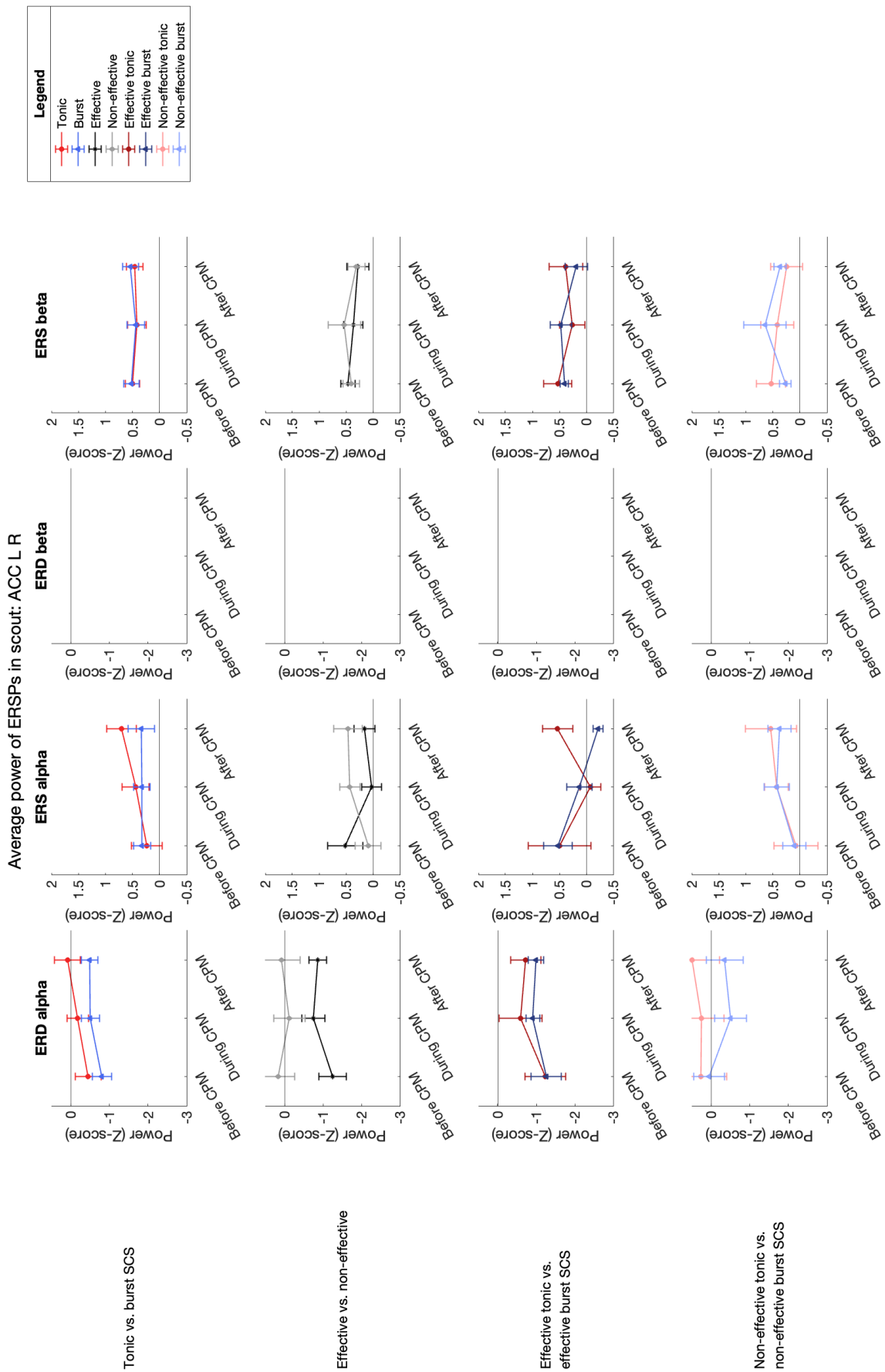
Figure 28: *Mean and standard error of average power [z-score] of alpha ERD, alpha ERS, beta ERD and beta ERS before, during and after CPM for the different groups in the ROI consisting of the ACC of both hemispheres.*
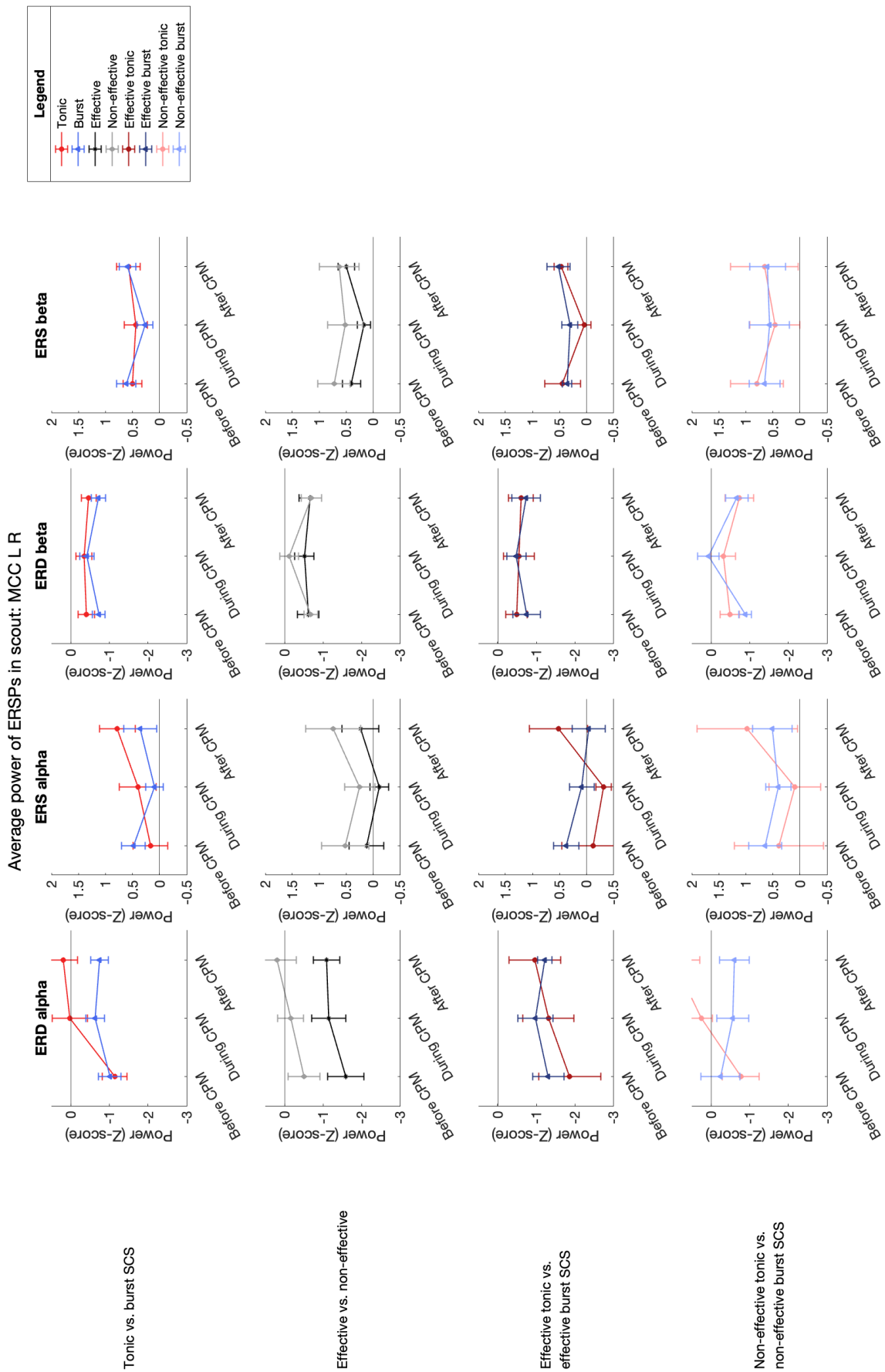
Figure 29: *Mean and standard error of average power [z-score] of alpha ERD, alpha ERS, beta ERD and beta ERS before, during and after CPM for the different groups in the ROI consisting of the MCC of both hemispheres.*
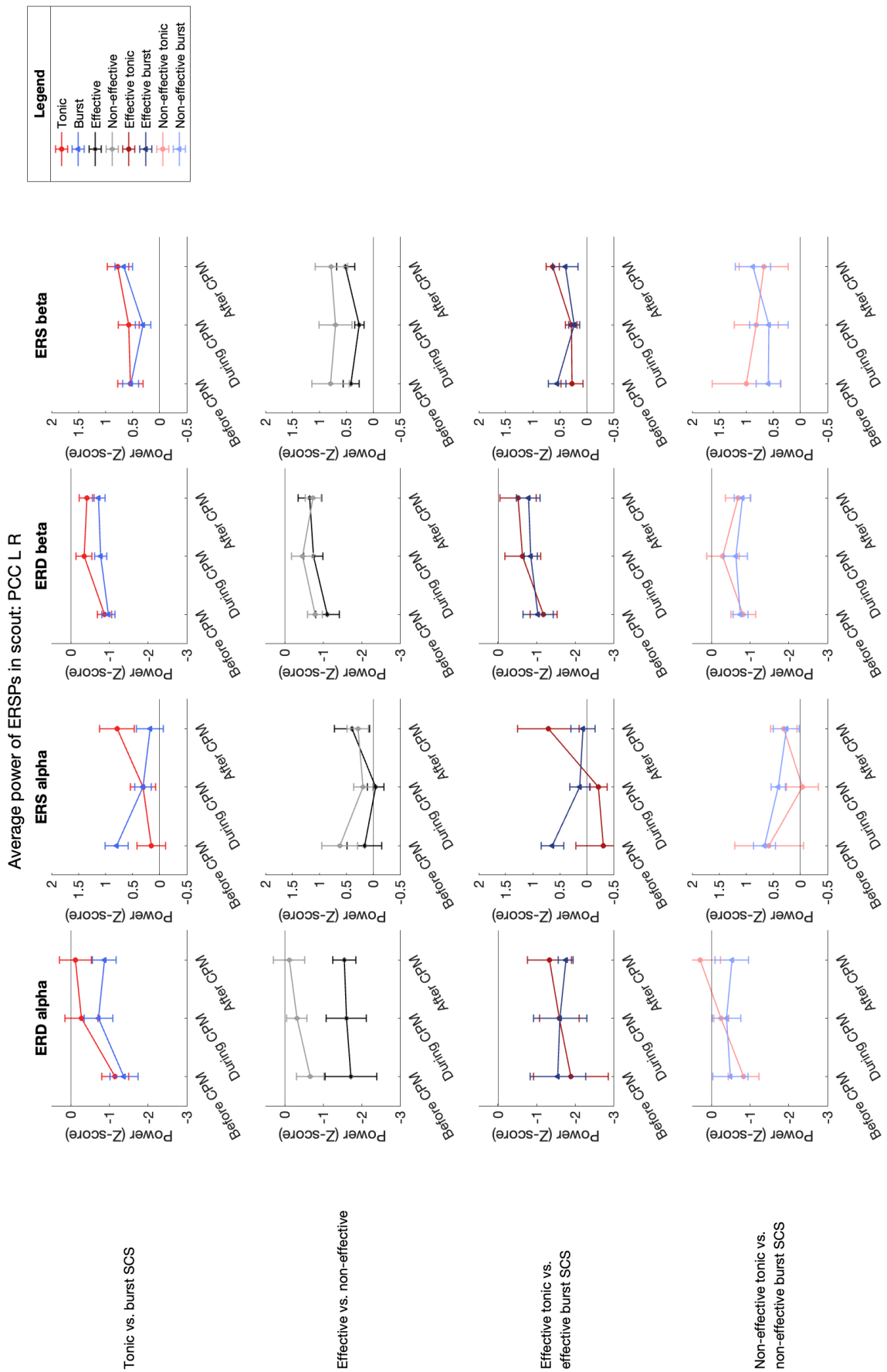
Figure 30: *Mean and standard error of average power [z-score] of alpha ERD, alpha ERS, beta ERD and beta ERS before, during and after CPM for the different groups in the ROI consisting of the PCC of both hemispheres.*
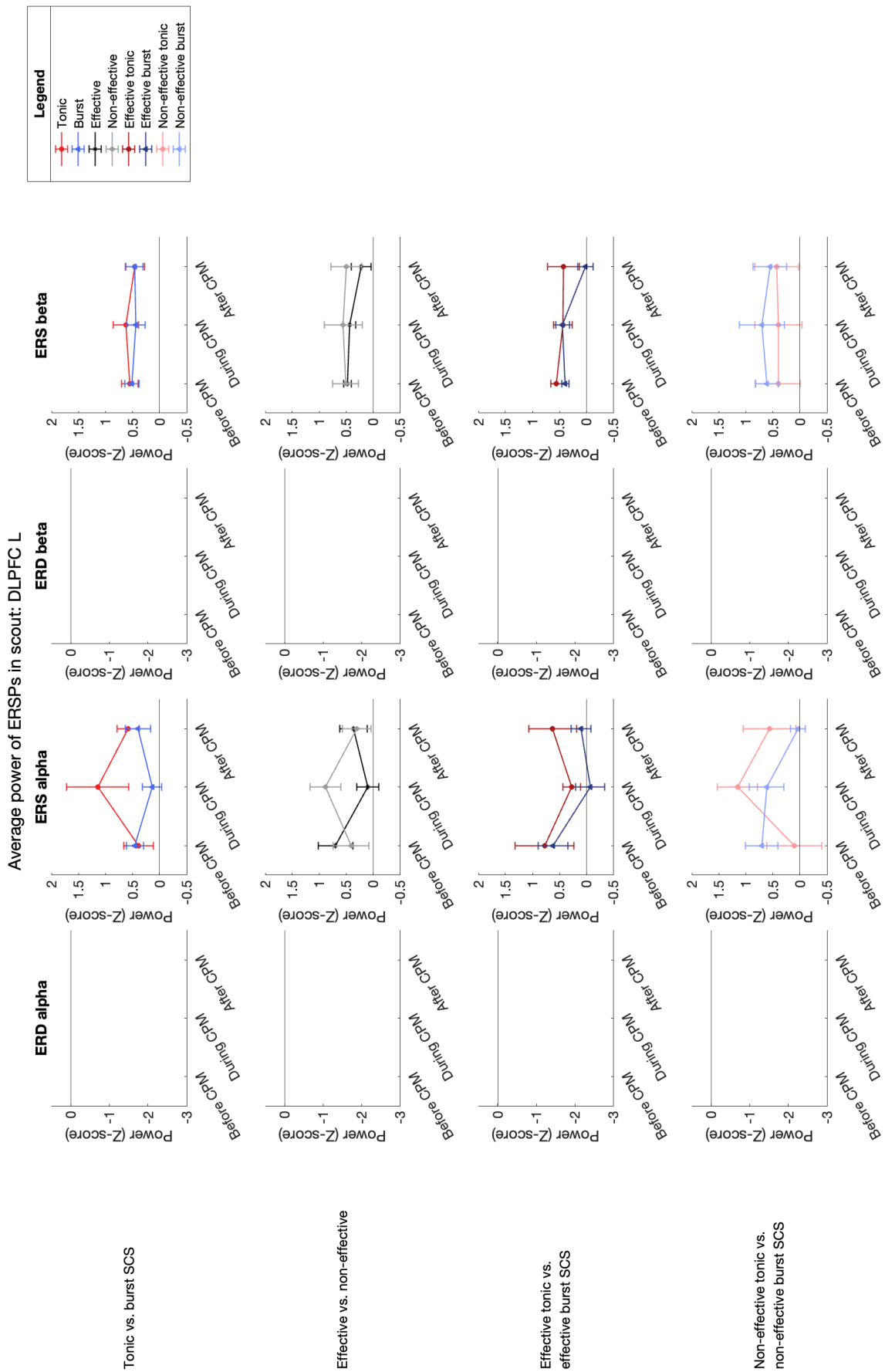
Figure 31: *Mean and standard error of average power [z-score] of alpha ERD, alpha ERS, beta ERD and beta ERS before, during and after CPM for the different groups in the ROI consisting of the DLPFC of the left hemisphere.*
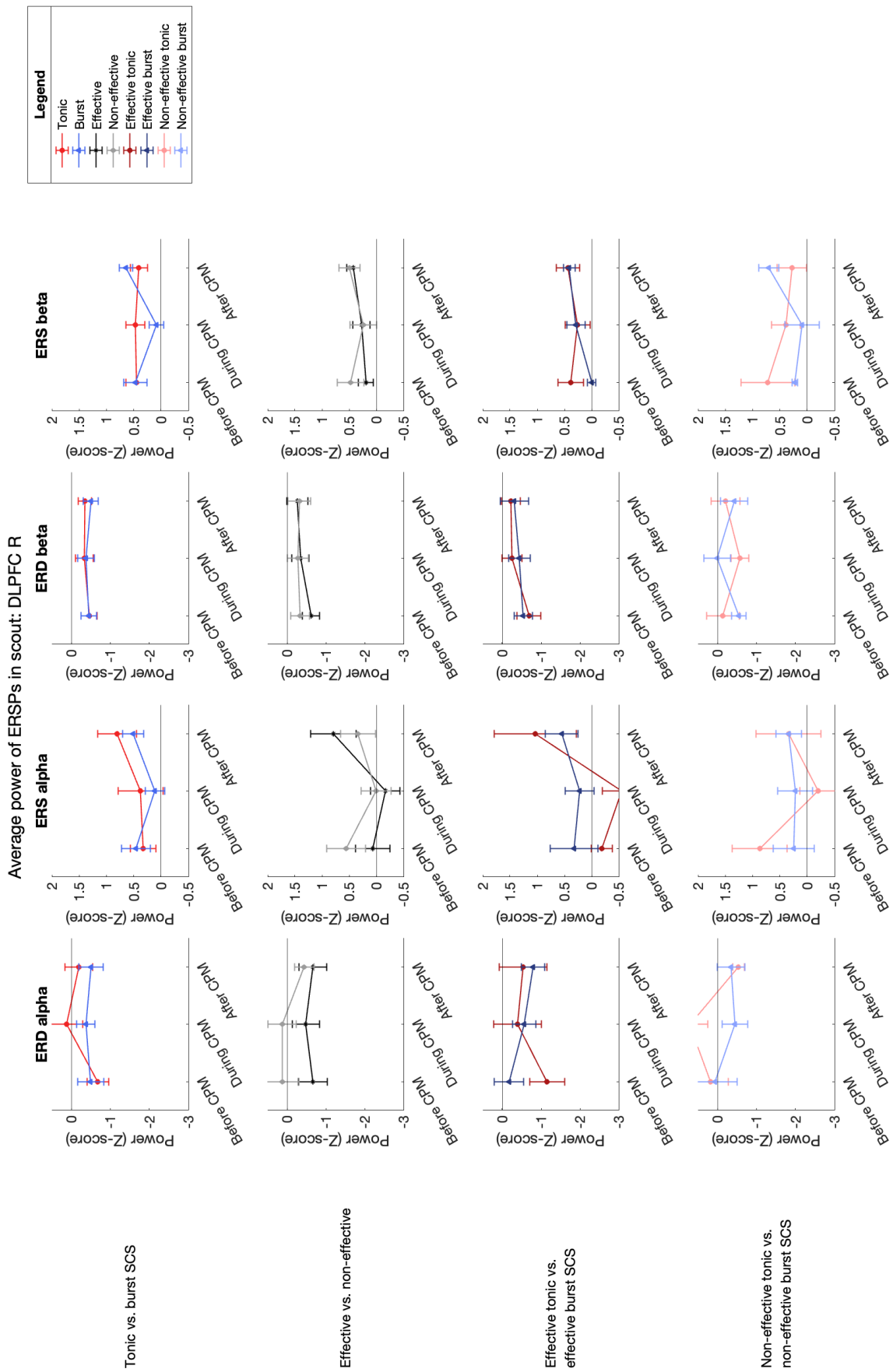
Figure 32: *Mean and standard error of average power [z-score] of alpha ERD, alpha ERS, beta ERD and beta ERS before, during and after CPM for the different groups in the ROI consisting of the DLPFC of the right hemisphere.*
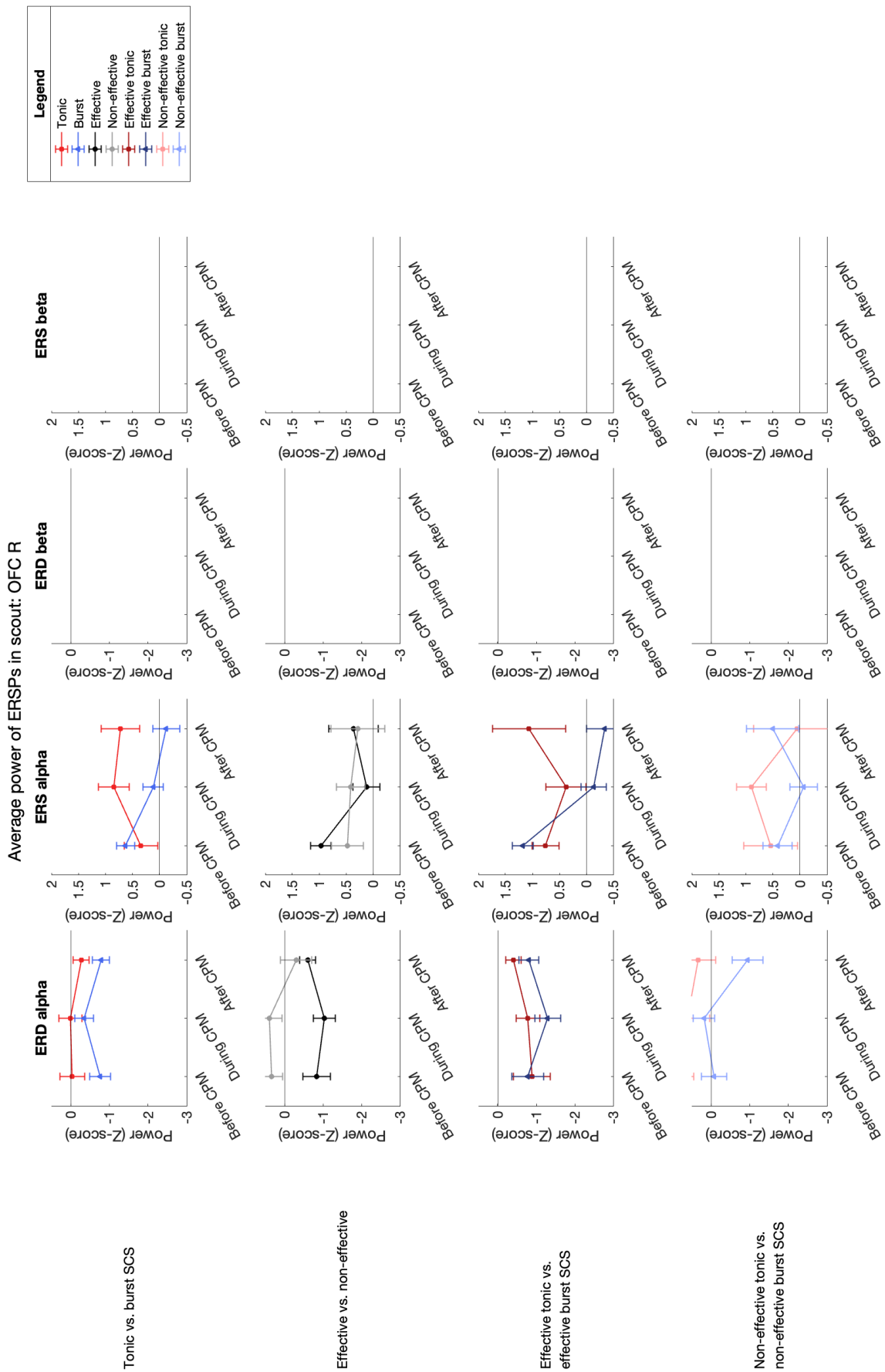
Figure 33: *Mean and standard error of average power [z-score] of alpha ERD, alpha ERS, beta ERD and beta ERS before, during and after CPM for the different groups in the ROI consisting of the OFC of the right hemisphere.*

G. Inter-subject variability of cortical response in bilateral sensorimotor cortices

We observed a large inter-subject variability in cortical response in the bilateral sensorimotor cortices to the TS. Figure 34 displays the TF maps of the subjects PT02 (non-responder SCS), PTN05 (responder burst SCS, non-responder tonic SCS) and PTN09 (responder SCS) during tonic and burst SCS for all CPM conditions.

(a) *PT02 tonic SCS before CPM*   (b) *PT02 tonic SCS during CPM*   (c) *PT02 tonic SCS after CPM*
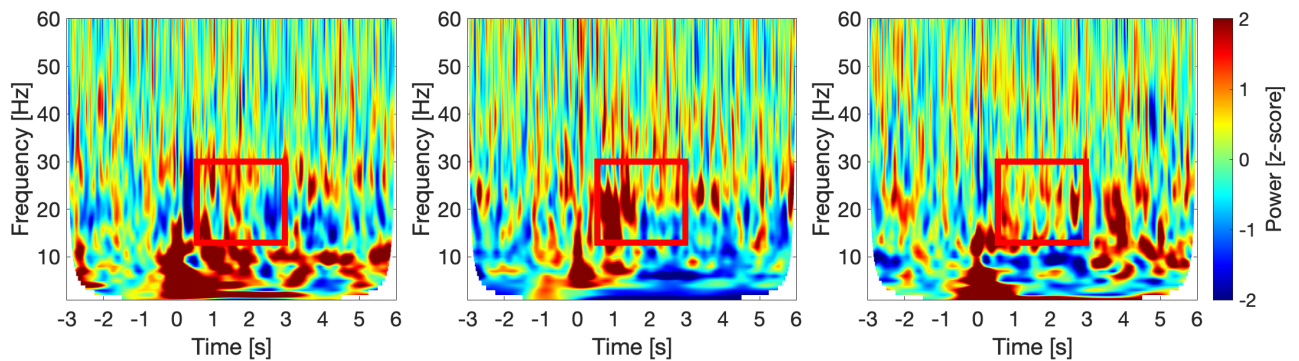
(d) *PT02 burst SCS before CPM*   (e) *PT02 burst SCS during CPM*   (f) *PT02 burst SCS after CPM*
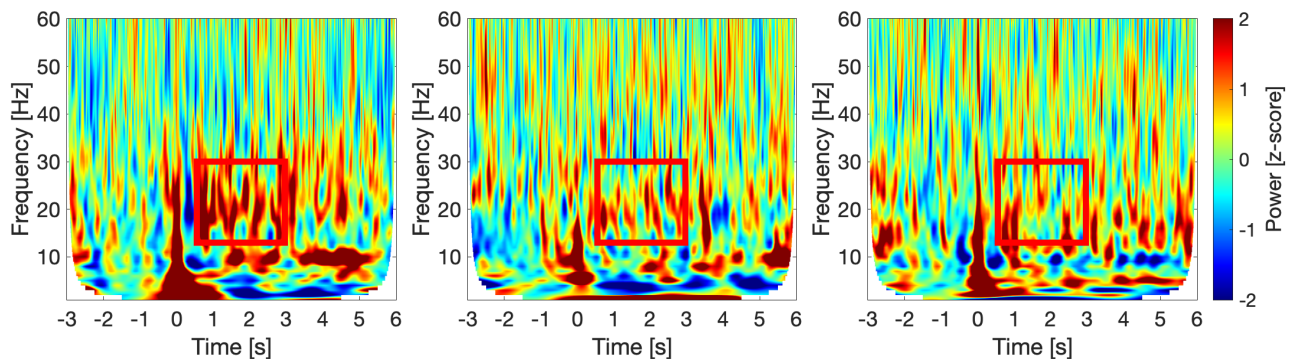
(g) *PTN05 tonic SCS before CPM* (h) *PTN05 tonic SCS during CPM* (i) *PTN05 tonic SCS after CPM*
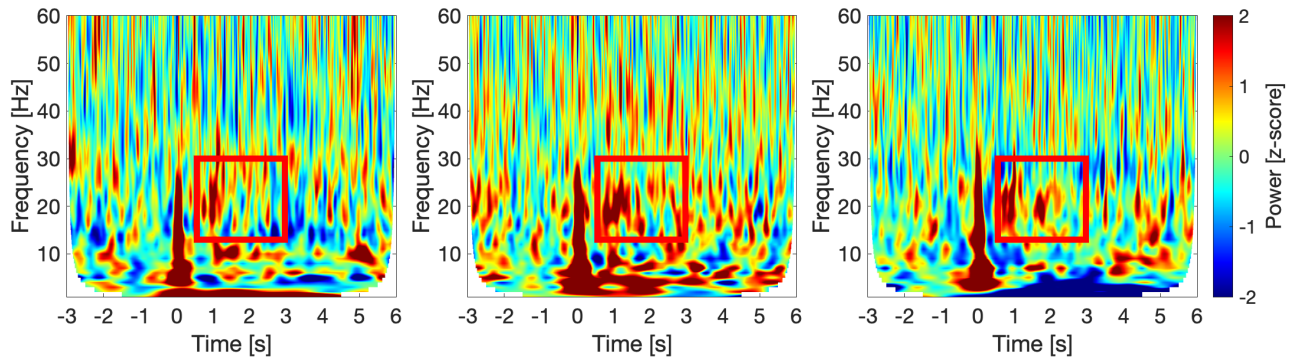
(j) *PTN05 burst SCS before CPM* (k) *PTN05 burst SCS during CPM* (l) *PTN05 burst SCS after CPM*
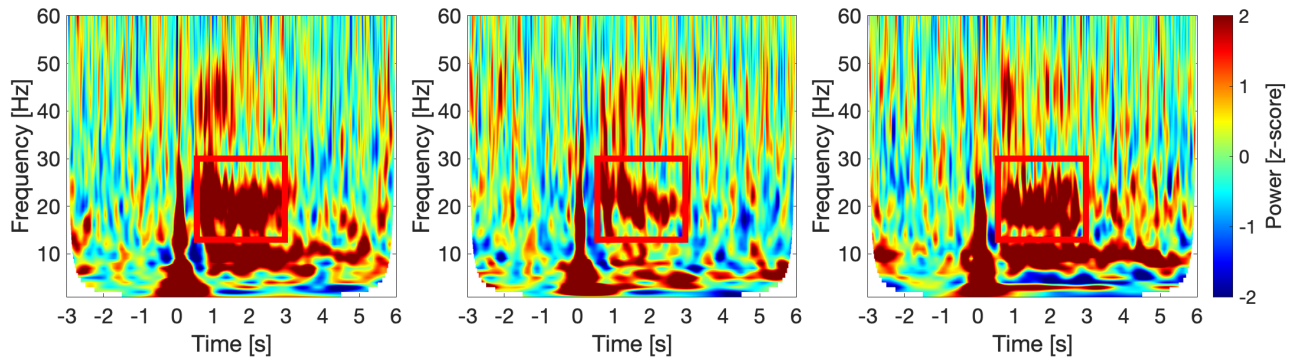
(m) *PTN09 tonic SCS before CPM* (n) *PTN09 tonic SCS during CPM* (o) *PTN09 tonic SCS after CPM*
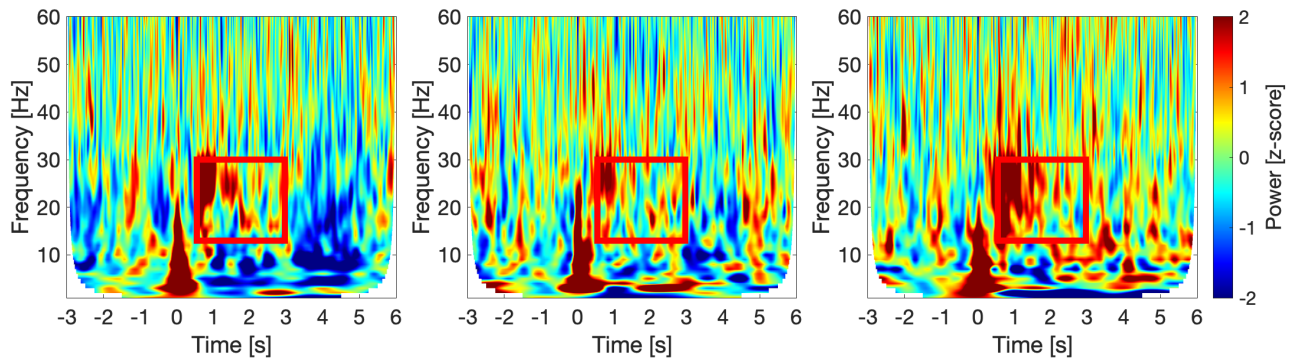
(p) *PTN09 burst SCS before CPM* (q) *PTN09 burst SCS during CPM* (r) *PTN09 burst SCS after CPM*
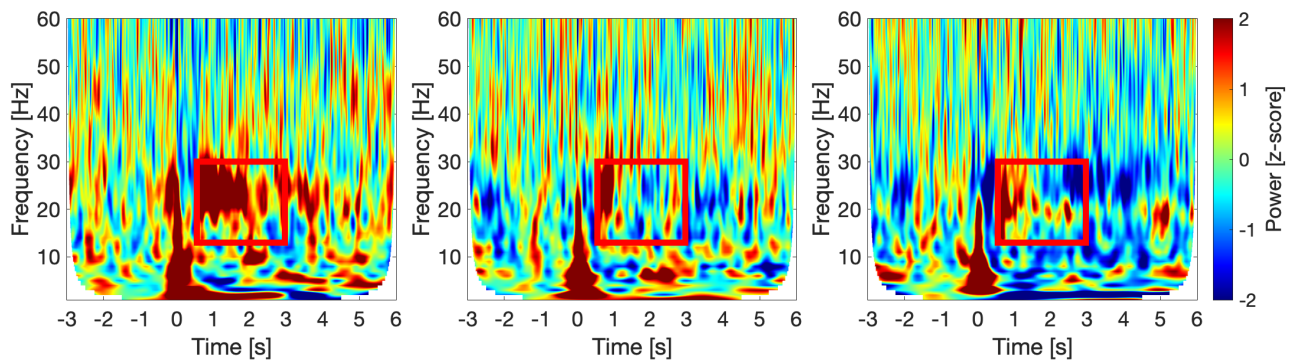
Figure 34: *Time frequency (TF) maps, z-scored with respect to baseline, for three subjects during burst SCS per CPM condition in the bilateral sensorimotor cortices. At $t = 0$ the nociceptive stimulus is given. The red box indicates the time and frequency range used to determine the average power of beta ERS.*

H. Time frequency analysis high gamma (60-100 Hz)

Time-frequency analysis was also performed for the high gamma frequencies (60-100 Hz). No gamma ERSPs were observed following a nociceptive stimulus in the time-frequency response. Also when z-scoring the time-frequency map with respect to the baseline no ERSPs became visible, as can be seen in Figure 35. Only the stimulus artifact is noted around t = 0.

(a) *Non z-scored power*
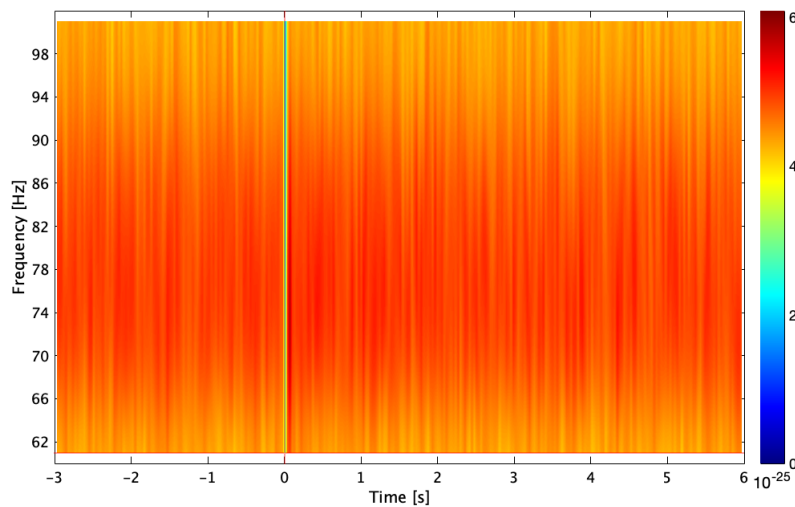
(b) *Z-scored power with respect to baseline*
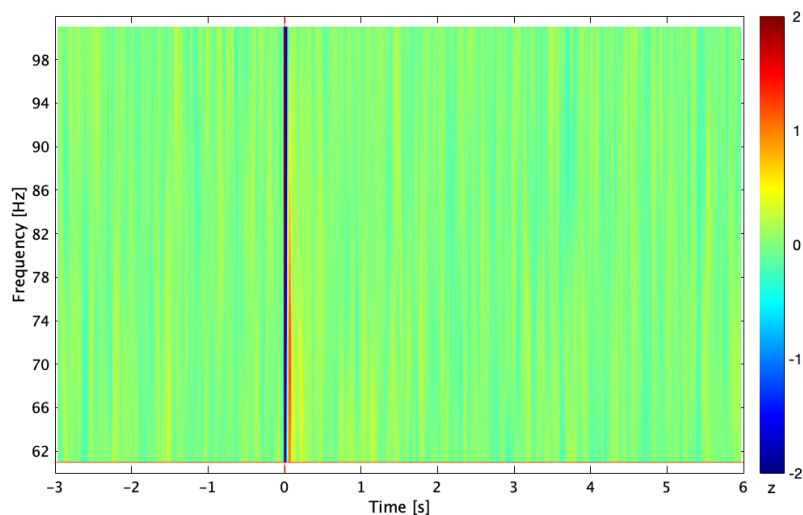
Figure 35: *Averaged time frequency response for the frequency range 60-100 Hz in the left primary somatosensory cortex for all subjects and conditions.*

I. Stimulus and linear interpolation artefact

Figure 36a displays the effect of linear interpolation on the TF decomposition. The TF map shows a TF decomposition of a noise recording with at t = 0 linear interpolation applied. Figure 36b displays the effect of stimulation activity on the TF decomposition. The TF map shows a TF decomposition of 22 trials before CPM of subject PTN04, without removing the stimulation artifact using linear interpolation. The noise recording and the recording of PTN04 are both pre-processed following the same steps as described in the methods.

Figures 36c and 36d show the TF maps with the color range set to the local maximum. As can be seen from the color bar the artifact caused by the stimulation activity has a much higher power (z-score of +/- 2000) in comparison to the artifact caused by linear interpolation(z-score of +/- 25). Therefore I recommend to always cut out the stimulation artifact by for example using linear interpolation. Using the linear interpolation method it should always be kept in mind that this also introduces an artifact and therefore it is not possible to draw reliable conclusions about the first hundreds of ms in the time-frequency domain, especially for the lower frequencies.

(a) *Linear interpolation artifact, colormap range [-2, 2]*
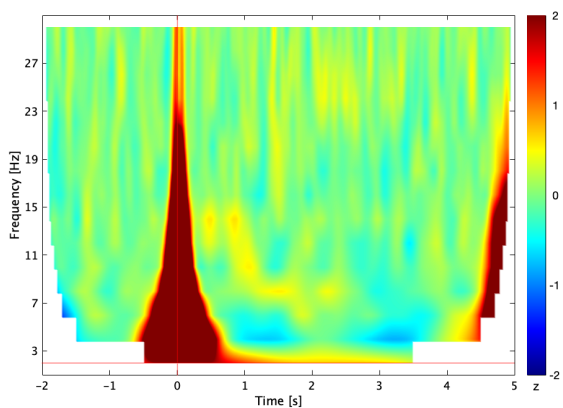
(b) *Stimulation artifact, colormap range [-2, 2]*
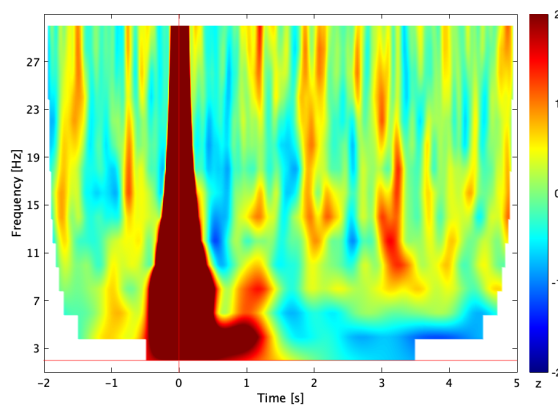
(c) *Linear interpolation artifact, colormap range [-25, 25]*
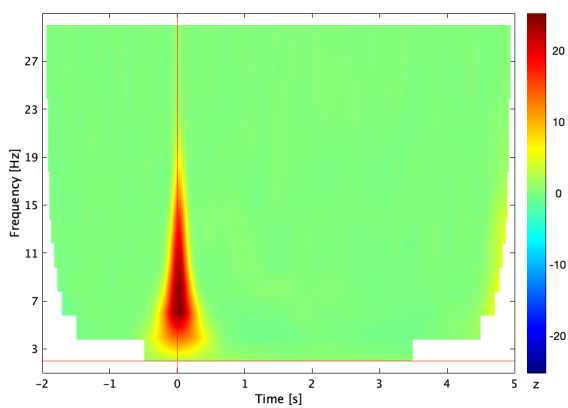
(d) *Stimulation artifact, colormap range [-2500, 2500]*
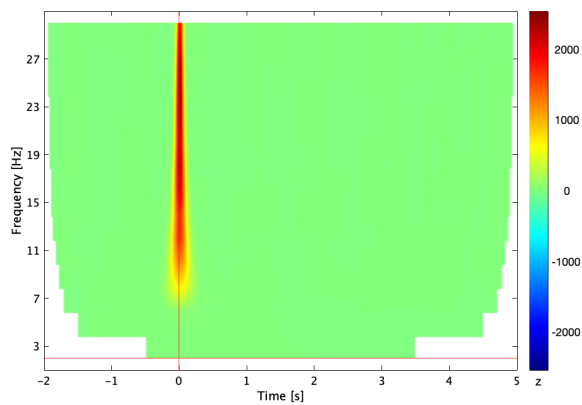
Figure 36: *Time frequency maps displaying the effects of linear interpolation and stimulation activity on the TF decompositions.*

J.   CPM before and after SCS implantation

Two subjects of this study underwent another MEG session with CPM measurements before SCS implantation. Figure 37 displays the TF maps of the two subjects before and after SCS implantation *before, during* and *after* CPM. Subject PT08 was a SCS responder and PTN11 was a tonic SCS responder and experienced some pain relief during burst SCS although she reported a NRS $\geq$ 4 and was therefore not included in the effective SCS group. PT08 seems to express a small inhibitory effect by CPM on the cortical response for all sessions. PTN11 seemed to express no inhibitory effect by CPM on the cortical response before SCS implantation and during tonic SCS, however during burst SCS a strong inhibitory effect by CPM is observed on the power of alpha and beta ERS.

(a) *PT08 before SCS implantation before CPM*

(b) *PT08 before SCS implantation during CPM*

(c) *PT08 before SCS implantation after CPM*
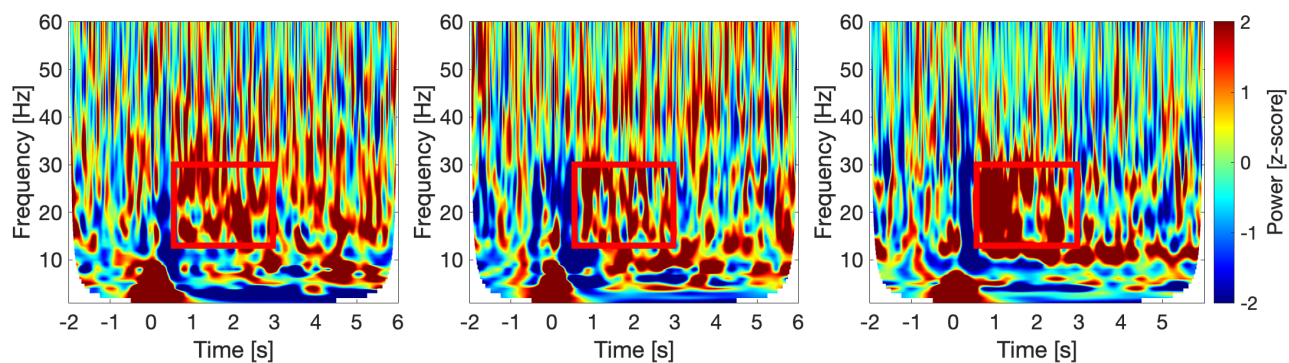
(d) *PT08 tonic SCS before CPM*

(e) *PT08 tonic SCS during CPM*

(f) *PT08 tonic SCS after CPM*
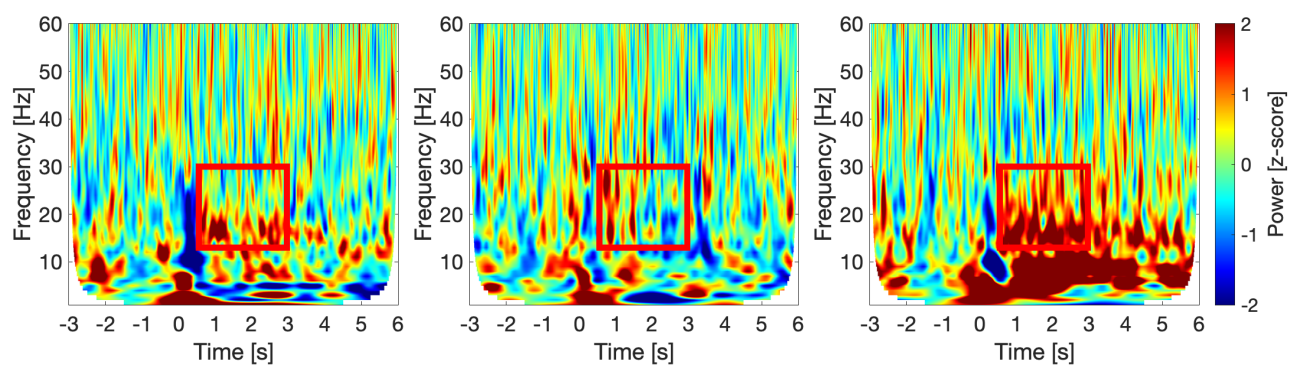
(g) *PT08 burst SCS before CPM*

(h) *PT08 burst SCS during CPM*

(i) *PT08 burst SCS after CPM*
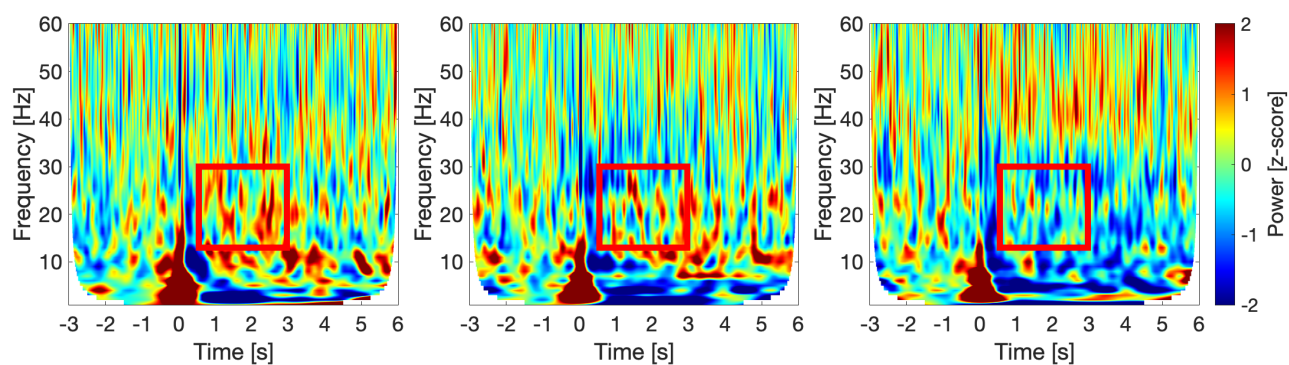
(j) *PTN11 before SCS implantation before CPM* (k) *PTN11 before SCS implantation during CPM* (l) *PTN11 before SCS implantation after CPM*
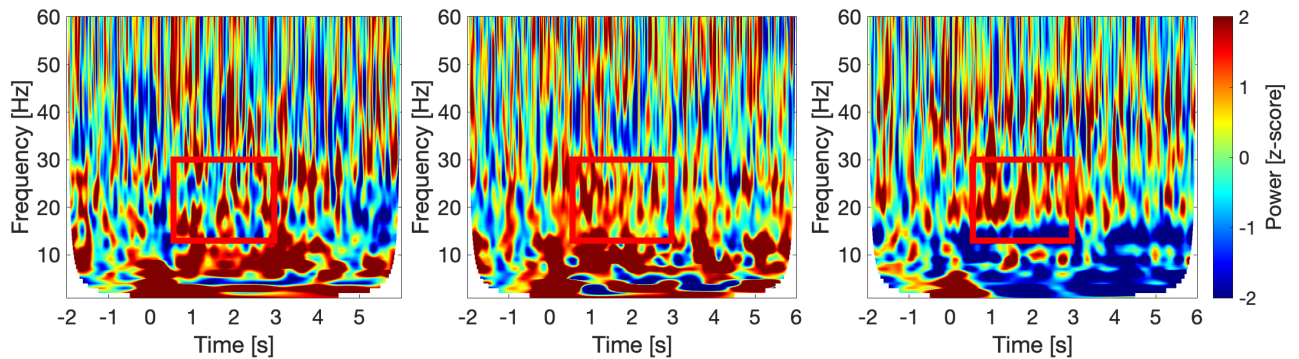
(m) *PTN11 tonic SCS before CPM* (n) *PTN11 tonic SCS during CPM* (o) *PTN11 tonic SCS after CPM*
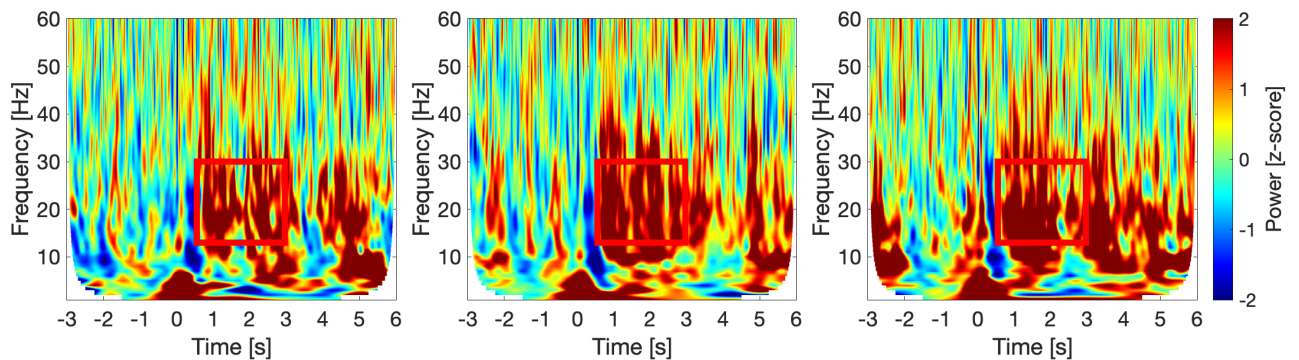
(p) *PTN11 burst SCS before CPM* (q) *PTN11 burst SCS during CPM* (r) *PTN11 burst SCS after CPM*
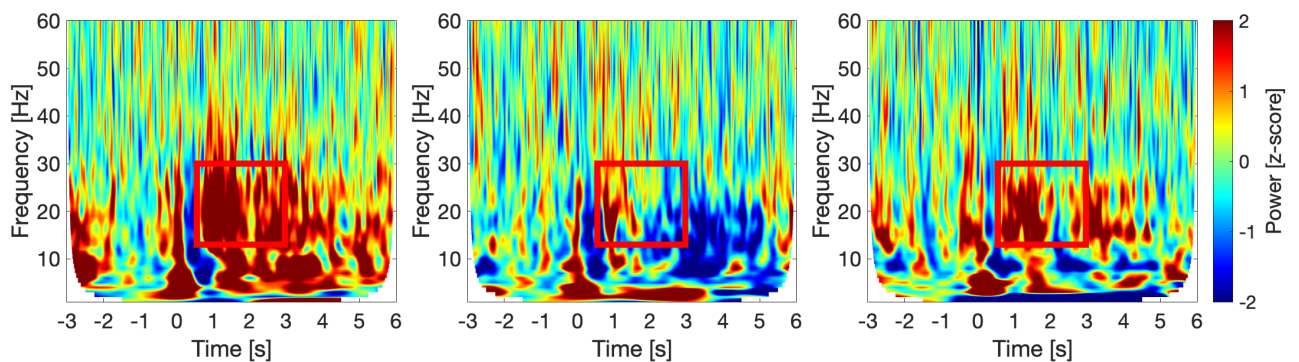
Figure 37: *Time frequency (TF) maps, z-scored with respect to baseline, for two subjects that underwent three MEG CPM sessions (before SCS implantation, during tonic SCS and burst SCS) in the bilateral sensorimotor cortices. At t = 0 the nociceptive stimulus is given. The red box indicates the time and frequency range used to determine the average power of beta ER*